Université de Paris

Université de Paris

École doctorale 474
"Frontières de l'Innovation en Recherche et Éducation"

Laboratoires : Equipe Danijela Vignjevic, Migration et Invasion Cellulaire, UMR144, CNRS – Biologie Cellulaire et Cancer; Equipe Ana-Maria Lennon-Duménil, Dynamique spatio-temporelle des cellulles du système immunitaire, U932, Inserm – Immunite et Cancer

Role of macrophages in colon homeostasis

Par Aleksandra Chikina

Thèse de doctorat de Biologie cellulaire et biologie du développement

Dirigée par Danijela Matic Vignjevic
Et par Ana-Maria Lennon-Duménil

Présentée et soutenue publiquement le 22 octobre 2020

Devant un jury composé de :

Mme Molly Ingersoll, PhD HDR, Universite Paris 6, rapportrice
M Florent Ginhoux, PhD, group leader, Singapore Immunology Network, rapporteur
M Eduardo Villablanca, PhD, group leader, Karolinska Institute, examinateur
Mme Silvia Fre, PhD HDR, UPMC, examinatrice

Except where otherwise noted, this is work licensed under
https://creativecommons.org/licenses/by-nc-nd/3.0/fr/

Titre : Les rôles des macropahges dans l'homéostasie du côlon.

Résumé : Une des principales fonctions du côlon est d'abriter la plus large proportion de microorganismes du corps humain, ainsi que d'absorber les fluides issus de la digestion. Ainsi, la muqueuse du côlon doit constamment affronter l'arrivée de produits potentiellement dangereux. Un des objectifs de mon étude est de déterminer comment le système immunitaire périphérique du côlon assure la surveillance des fluides absorbés. Il a été montré que les macrophages ont des spécificités distinctes dans les différentes portions de l'intestin et représentent l'un des acteurs majeurs du système immunitaire intestinal. Nous proposons que ces différents types de macrophages associés à la muqueuse épithéliale participent au maintien des fonctions des régions proximales et distales du côlon. J'ai observé que les macrophages des régions distales possèdent des protrusions trans-épithéliales uniques – que nous appelons « baloon-like protrusions », ou BLP, qui traversent la lame basale et contactent les cellules épithéliales. J'ai montré que la formation des BLP est fortement dépendante de la quantité d'eau absorbée au niveau du côlon, ainsi que de la présence des microorganismes intestinaux. La prolifération fongique non-contrôlée libère des métabolites qui provoquent l'apoptose des cellules intestinales. En rejoignant la circulation sanguine, ces métabolites sont responsables d'une septicémie létale chez l'Homme. Notre hypothèse de travail propose que les BLPs des macrophages servent de senseurs évaluant les fluides absorbés et contrôlant le niveau d'absorption de l'épithelium intestinal, afin d'éviter que des métabolites fongiques potentiellement dangereux puissent atteindre la circulation.

Mots clefs : macrophages, intestin, intégrité de l'épithélium, champignons, microbiote, absorption de liquide, protrusions

Title : Role of macrophages in colon homeostasis

Abstract : The colon is primarily responsible for absorbing fluids. It contains a large number of microorganisms including fungi, which are enriched in its distal segment. The colonic mucosa must therefore tightly regulate fluid influx to control absorption of fungal metabolites, which can be toxic to epithelial cells and lead to barrier dysfunction. How this is achieved remains unknown. Here, we describe a mechanism by which the innate immune system allows rapid quality-check of absorbed fluids to avoid intoxication of colonocytes. This mechanism relies on a population of distal colon macrophages that are equipped with "balloon-like" protrusions (BLPs) inserted in the epithelium, which sample absorbed fluids. In the absence of macrophages or BLPs, epithelial cells keep absorbing fluids containing fungal products, leading to their death and subsequent loss of epithelial barrier integrity. These results reveal an unexpected and essential role of macrophages in the maintenance of colon-microbiota interactions in homeostasis.

Keywords : macrophages, gut, epithelium integrity, fungi, microbiota, fluid absorption, protrusions

Résumé

Le tractus intestinal présente un environnement unique car il est continuellement exposé aux antigènes alimentaires ainsi qu'au microbiote commensal. Pour permettre une absorption efficace des nutriments et des électrolytes, la barrière intestinale est relativement mince. Mais ceci peut créer des difficultés pour l'hôte car des substances toxiques qui se trouvent dans la cavité luminale peuvent également atteindre la circulation sanguine [1]. Une perturbation de la barrière intestinale est donc impliquée dans de multiples situations pathologiques allant de la privation de nutriments [2] à des maladies intestinales inflammatoires [3,4], la septicémie [5] ou encore des défaillances au niveau de différents plusieurs organes [1,6,7].

Selon la région de l'intestin, la barrière épithéliale du côlon distal est confrontée à des défisimportants. D'une part, l'épithélium du côlon distal est exposé à l'extrême pression osmotique de 10 atm nécessaire pour absorber l'eau et solidifier les fèces [8]. D'autre part, le microbiote, y compris les bactéries, les champignons, les archées et les virus, sont présents à leur niveau le plus élevédans cette région de l'intestin [9–12]. Les champignons,particulièrement abondants dans le côlon distal [13], peuvent produire des métabolites qui déclenchent l'apoptose des cellules épithéliales intestinales [14]. En conséquence, la barrière intestinale est la principale cible de nombreuses toxines fongiques, telles que la gliotoxine [14], l'aflatoxine [15], les trichothécènes [16] et la candidalysine [17].

Ainsi, la muqueuse du côlon régule étroitement l'absorption des fluides pour éviter l'entréede métabolites fongiques toxiques dans les cellules épithéliales voir au niveau de la circulation sanguine. Les mécanismes impliquaient dans cette régulation restent inconnus.

Dans des conditions homéostatiques, les macrophages font partis des cellules immunitaires intestinales les plus abondantes. Il se différencient principalement en monocytes en réponse à des signaux locaux. Les macrophages intestinaux résident soit dans la lamina propria, soit dans la couche musculaire où ils participent à divers processus biologiques notamment la dégradation des micro-organismes [18], l'élimination silencieuse des corps apoptotiques [19,20], la réparation des tissus [21] et la motilité gastro-intestinale [22]. Les macrophages intestinaux limitent également l'inflammation [23–25], facilitent la survie des cellules locales de régulation FOXP3+ T et la

tolérance à la nourriture [26,27]. Leur fonction étroitement régulée par le microbiote [28] reflète leur nombre plus abondants dans le côlon que dans l'intestin grêle [29,30].

Il est intéressant de noter que dans le côlon, les macrophages peuvent être étroitementassociésaux cellules épithéliales [30,31]. La perturbation de la localisation sous-épithéliale des macrophages participe à la perte de l'intégrité de la barrière intestinale observée dans les maladies inflammatoires de l'intestin telles que la colite ulcéreuse et la maladie de Crohn [32]. Les macrophages sont donc idéalement placés pour orchestrer les interactions entre les cellules épithéliales et le microbiote afin de maintenir l'homéostasie du côlon.

La principale question de ma thèse était d'identifier le rôle des macrophages du côlon dans l'intégrité et la fonction de la barrière épithéliale intestinale dans l'homéostasie.

Ci-dessous, je présente les résultats marquants qui nous permettent d'aborder cette question.

1. Les macrophages contrôlent la survie des cellules épithéliales et l'intégrité de la barrière épithéliale dans le côlon distal

Pour étudier le rôle des macrophages dans la barrière colique, j'ai analysé l'intégrité de la barrière épithéliale intestinale chez des animaux dépourvus de macrophages. Indépendamment, dans deux modèles murins différents déplétés pour les macrophages, j'ai observé une apoptose massive de l'épithélium colique.

Etonnamment, la mort de l'épithélium a été observé dans le côlon distal mais pas dans le côlon proximal malgré une efficacité de déplétion des macrophages identique dans les deux régions. La mort de l'épithélium a été accompagnée par une augmentation de l'absorption d'un colorant infusé dans la lumière du côlon indiquant une défaillance de la barrière intestinale.

2. Les macrophages du côlon distal génèrent des protubérances "en forme de ballon" (BLP) entre les cellules épithéliales et présentent un profil transcriptomique distinct

J'ai pu observer que les macrophages sous-épithéliaux du côlon distal sont morphologiquement différents de leurs homologues proximaux. Ils forment des protubérances particulières, en forme de ballons (protubérances "en forme de ballon", ou BLP), qui pénètrent la membrane basale pour interagir physiquement avec l'épithélium. Nous avons ensuite procédé au séquençage de l'ARN

monoclonal des macrophages isolés du côlon proximal et distal. Nous avons constaté que les macrophages BLP+ présentent un profil transcriptomique distinct enrichi pour les gènes de détection des microbiotes.

3. Les métabolites fongiques absorbés avec les fluides stimulent la formation de BLP dans le côlon distal

Les résultats du séquençage nous ont conduit à émettre l'hypothèse que les macrophages forment des BLP pour détecter les membres du microbiome. Pour y répondre, j'ai traité des animaux avec des antibiotiques ou des antimycotiques et j'ai observé que les BLP se formaient en réponse aux champignons locaux mais pas aux bactéries. L'inverse était également vrai. Les macrophages des souris sans germes formaient un nombre accru de BLP après la recolonisation fongique, tandis que la reconstitution bactérienne n'avait aucun effet. Mais comment les macrophages détectent-ils les champignons présents dans la lumière du côlon à travers une couche de mucus épaisse et stérile en utilisant des protubérances qui ne pénètrent pas l'épithélium? En effet, nous avons découvert que les macrophages du côlon distal ne sur-expriment pas les récepteurs habituellement associés à la détection des champignons, tels que la dectine 1 et la dectine 2. L'élimination de la dectine 1 n'a pas affecté le nombre de BLP. Comme le rôle physiologique principal du côlon distal est d'absorber l'eau dans un environnement riche en microbes et particulièrement en champignons, il est possible que les BLP en prélèvent une partie et réagissent à la présence de métabolites dérivés de champignons.

J'ai recueilli plusieurs éléments pour étayer cette hypothèse : (1) le nombre de BLP augmente lorsqu'on stimule l'absorption d'eau et cet effet est réduit si les souris ont été prétraitées avec des antimycotiques ; (2) les BLP prélèvent directement les fluides absorbés, comme le montre le traceur d'eau à faible poids moléculaire ; (3) le nombre de BLP augmente fortement en réponse aux toxines fongiques, telles que la gliotoxine, la candidalysine et la toxine T-2. Sur la base de ces éléments, nous avons conclu que les macrophages coliques distaux forment des BLP en réponse aux toxines fongiques, présentes dans les liquides absorbés au niveau de l'épithélium intestinal.

4. Les macrophages protègent les cellules épithéliales contre l'empoisonnement par des toxines fongiques

Des expériences de perfusion de toxines ont montré que dans l'homéostasie, les cellules épithéliales du côlon distal peuvent arrêter l'absorption des liquides contaminés par des toxines de champignons. Il est intéressant de noter que ce phénomène n'a pas été observé chez les souris dépourvues de macrophages où l'absorption incontrôlée de produits fongiques a entraîné la mort de l'épithélium intestinal. Ces résultats suggèrent donc un rôle majeur des macrophages dans le contrôle de l'absorption épithéliale. En revanche, le rôle des BLP reste à étudier.

Il est important de souligner la fonction essentielle de la protéine CD74 dans l'échantillonnage des fluides par les BLP. En effet, chez les animaux CD74KO, les BLP n'ont pas absorbé le fluide aussi efficacement que leurs congénères CD74WT mettant en évidence des souris avec des BLP "déficientes" dans leur capacité d'échantillonnage. Il est aussi important de constater que l'épithélium colique des animaux CD74KO ne pouvait pas distinguer les fluides infusés sains de ceux contenant des toxines conduisant à une apoptose de l'épithélium peu de temps après l'infusion. Ces résultats suggèrent fortement que les BLP orchestrent le prélèvement de fluides par les macrophages coloniaux distaux, processus essentiel à la protection des cellules épithéliales lors l'absorption de liquides enrichis en toxines/métabolites fongiques.

En résumer, je décris ici un mécanisme par lequel le système immunitaire inné permet un contrôle rapide et efficace de la qualité des fluides absorbés afin d'éviter l'intoxication des colocytes. Ce mécanisme repose sur une population de macrophages du côlon distal équipés de protubérances en forme de "ballons" (BLP) insérées dans l'épithélium pour prélèver les fluides absorbés. En l'absence de macrophages ou de BLP, les cellules épithéliales continuent d'absorber des fluides contenant des produits fongiques, ce qui entraîne leur mort et la perte ultérieure de l'intégrité de la barrière épithéliale.

Ces résultats révèlent un rôle inattendu et essentiel des macrophages dans le maintien des interactions côlon-microbiote dans l'homéostasie.

Acknowledgements

I would like first to thank my wonderful supervisors for their endless support and trust. For believing in me and teaching me so much over the course of the last 5 years, which helped me to grow not only professionally, but also personally. For showing me how joyful the science can be and how to overcome periods, when the joy is limited. I am honored to be a member of the two teams, which dynamics is quite different but they share the same values – the value of the collective effort, support and help. Thus, secondly, I would like to thank each member, former and current, of Cell Migration and Invasion and STRAP teams for welcoming me 5 years ago, and with time, for sharing their experience and also for becoming my friends. I would also like to thank some members of Pasteur Institute, Livia Lacerda Mariano and Elisa Gomez Perdiguero, for helpful discussions that led to multiple breakthrough during the project. I am thankful to my doctoral school, FIRE, for the great learning environment and atmosphere. Overall, if we return in time and I have to choose PhD-labs again, I would do exactly the same choice.

Avertissement

This document is the result of a long work and is the subject of the intellectual property of the author: this implies an obligation of quotation and referencing when use of this document.

On the other hand, any counterfeiting, plagiarism, illegal reproduction of this work leads to criminal prosecution.

Abbreviations

MNPs Mononuclear Phagocytes

Mϕ Macrophages

BLPs Balloon-Like Protrusions

DCs Dendritic Cells

Tregs T regulatory cells

GALTs Gut-Associated Lymphoid Tissues

TLRs Toll-Like Receptors

SCFAs Short-Chain Fatty Acids

PAMPs Pathogen Associated Molecular Patterns

CSF1 Colony Stimulating Factor 1

DT Diphtheria Toxin

DSS Dextran Sodium Sulfate

IHC Immunohistochemistry

Table of contents

RESUME EN FRANÇAIS 1-4

ACKNOWLEDGEMENTS 5

AVERTISSEMENT 6

ABBREVIATIONS 7

INTRODUCTION 9-60

CHAPTER 1. GASTRO-INTESTINAL SYSTEM 9-18
CHAPTER 2. SPECIALIZED SEGMENTS OF THE GASTRO-INTESTINAL SYSTEM ... 19-25
CHAPTER 3. LUMINAL GRADIENTS ALONG THE GUT 26-36
CHAPTER 4. MICROBIOTA 36-47
CHAPTER 5. INTESTINAL MACROPHAGES 47-57
CHAPTER 6. SUMMARY 57-60

RESULTS 61-86

DISCUSSION 87-95

MATERIALS AND METHODS 96-108

BIBLIOGRAPHY 108-134

Introduction

Chapter 1. Gastro-intestinal tract

The anatomical structure of the gastro-intestinal tract has been known since ancient times. Medieval anatomists recognized how important digestion is for other organs. Galen described the intestines as the “thinking agent” in the body, who “feels its own emptiness and generates the sensation of hunger”. At that time, however, the only function of the gastro-intestinal system was considered to be digestion. Even the anatomical localization of intestines was justified as such: “The stomach is lowest and has a hidden place in the body because of its uncleanness, as though nature had spared the principal members and had relegated the stomach or bowels further away from the site of reason’’. - Alessandro Benedetti, 1497.

Nowadays, it is well-accepted that the gut possesses multiple functions, ranging from the electrolyte balance homeostasis to the control of brain neuronal activity, and new physiological roles for this incredible organ being continuously discovered.

General structure

The structure of the gut conforms to a general plan that is preserved from the esophagus to the anus. It consists of four distinct functional layers: mucosa, submucosa, muscularis propria and adventitia briefly described below and illustrated on Figure 1.

• **Mucosa.** The mucosa is made up of three components: (1) epithelial lining, which creates the first barrier between external environment and interstitial milieu; (2) lamina propria rich in blood and lymphatic capillaries necessary to support the secretory and absorptive functions of the mucosa [33]; (3) muscularis mucosae, thin smooth muscle layer, which produces local movement and folding of the mucosa, increasing the abortive surface in the small intestine by the formation of folds and allowing the mucosa to stretch and flatten when the solid content is passing through the colon [34]

• **Submucosa.** The submucosa contains denser connective tissue with larger blood and lymph vessels and the submucosal (Meissner) plexus of autonomic nerves. It may also contain glands and significant lymphoid tissue [33].

• **Muscularis propria (externa).** The muscular wall proper consists of smooth muscle that is usually arranged as an inner circular layer and an outer longitudinal layer. In the stomach only, there is an inner oblique layer of muscle. The action of the two layers, at right angles to one another, is the basis of peristaltic contraction [34].

• **Adventitia.** This layer is exposed to the abdominal cavity and often referred to as the serosa. It contains major blood vessels, nerves and variable adipose tissue.

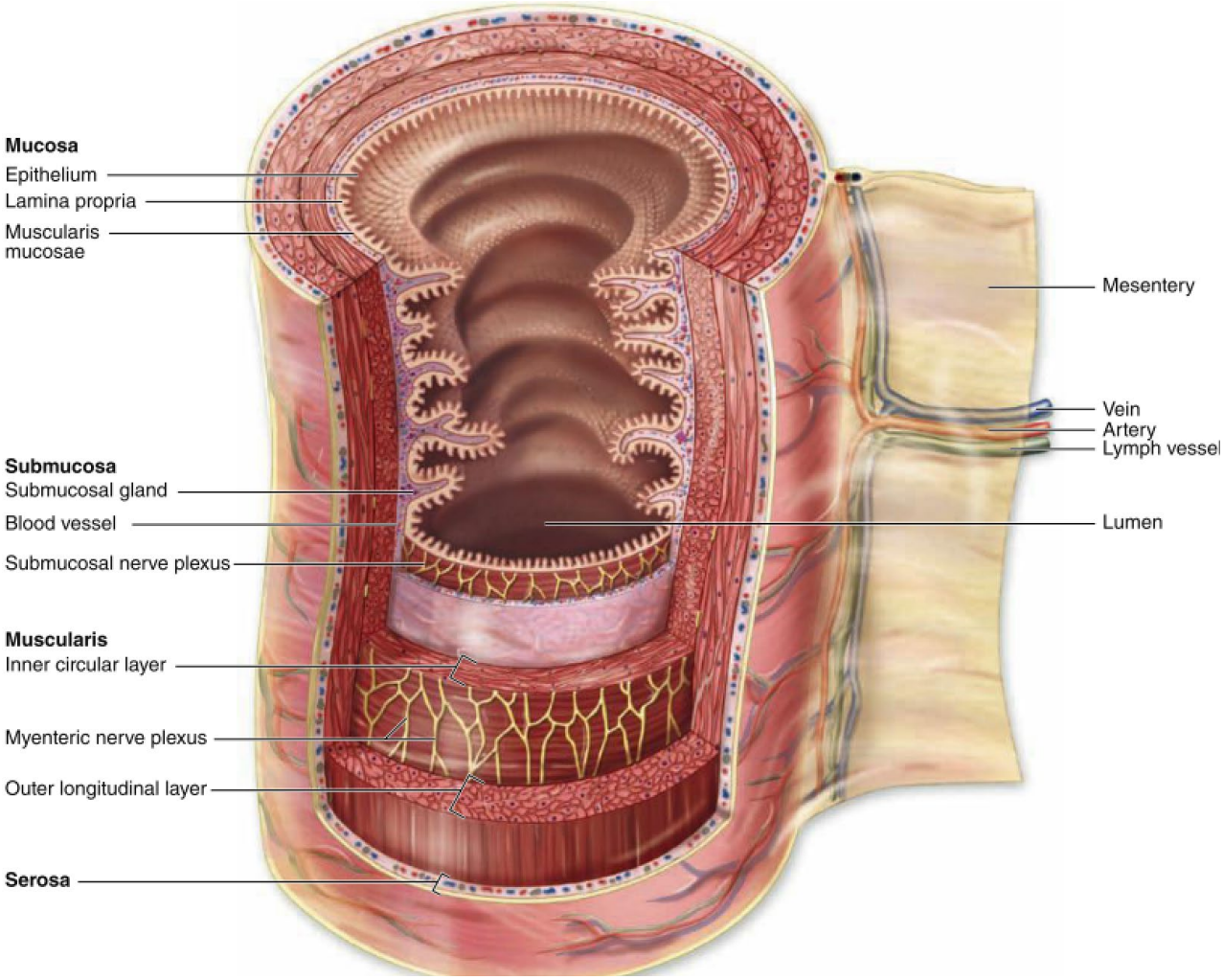


Figure 1. General scheme of the intestinal wall. Some segments, such as mucosa and muscularis undergo through major changes along intestinal length, while the others, mesentery and serosa remain relatively constant. *Adapted from Junqueira`s Basic Histology Atlas, Mescher, 2016*

The organization of mucosal layer undergoes pronounced changes throughout the intestine, adapting to distinct physiological roles performed in its segments. In contrast, the structure of the other layers is preserved or slightly changed (muscularis externa).

Four histological types of mucosa are found lining the gut can be classified according to their main function [34]:

- Protective. This type is found in the oral cavity, pharynx, esophagus and anal canal. The surface epithelium is of stratified squamous type and, although not keratinized in humans, it may be keratinized in some animals that have a coarse diet (e.g. rodents, herbivores). A stratified mucosal lining of this type is a physiological adaptation to potential frictional trauma, such as that associated with the passage of food during chewing and swallowing, or during the passage of feces through the anal canal.
- Secretory. This type of mucosa occurs only in the stomach. It consists of long, closely packed tubular glands that are simple or branched, depending on the region of the stomach. These glands act to produce various combinations of acid and digestive enzymes to facilitate the digestion of food and also secreting mucus to avoid self-digestion.
- Absorptive. This mucosa covers the entire small intestine. It is arranged into finger-like projections called villi, which serve to dramatically increase the surface area of the mucosa, with intervening short glands called crypts, where epithelial stem cells reside.
- Absorptive/protective. This form lines the entire large intestine. The mucosa is arranged into tightly packed, straight tubular glands, called crypts, consisting of cells specialized in water/electrolyte absorption, as well as mucus-secreting goblet cells.

Functions of the gastro-intestinal system

Digestive. The primary function of the gastro-intestinal system is digestive – proteins, carbohydrates and fats from the ingested food are broken down into small molecules that are absorbed through the intestinal wall into the circulation. This process occurs in five main phases: ingestion, fragmentation, digestion, absorption and elimination of waste products.

Electrolyte balance. Together with the kidney, the intestine participates in the maintenance of electrolyte balance and

The gastro-intestinal tract performs multiple physiological roles beyond digestion, that include:

- secretion of more than 15 hormones,
- hosting and establishing symbiotic relations with bacteria, fungi, archea, viruses;
- regulation of peripheral and systemic immune responses
- regulation of mental processes, such as learning and memory
- regulation of limbic system, stress and anxiety levels

body fluid homeostasis. The human intestinal tract is responsible for the absorption of 8-10L of fluid every day, usually highly-loaded with electrolytes (0.8 mol of sodium, 0.7 mol of chloride and 0.1 mol of potassium)[35]. While most nutrient transport occurs in the small intestine, the colon is primarily responsible for water and electrolyte transport (1.5L per day). Under homeostatic conditions, the small bowel has a limited capacity to conserve sodium [36]. In contrast, the colon absorbs most of the sodium and water and secretes potassium and bicarbonate into the lumen [37]. Impairment of the colon's ability to absorb water and salt may, under a variety of circumstances, lead to the loss of fluid and electrolytes from the body and life-threatening conditions.

Endocrine. With more than thirty different hormones identified as being produced in the gastro-intestinal tract, the gut has been described as 'the largest endocrine organ in the body' (reviewed in [38]). There are more than 20 types of entero-endocrine cells (EECs) in the intestine [39], secreting more than 15 hormones [40]. They are the main chemical sensors of the luminal nutrient status [41,42], regulate gut motility, insulin sensitivity and energy storage [43]. EECs, therefore, have a key role in regulating energy homeostasis and represent the first link that connects the dietary nutrient status to systemic metabolic processes.

Ecological niche/Commensalism. The gastro-intestinal system is highly populated by microorganisms that include all three domains of the leaving -Archaea, Bacteria and Eukarya- and altogether they form the microbiota. Symbiosis is initiated in contact with maternal microbial communities, dominated by vaginal or skin-communities depending on the delivery mode, as it has been shown that vaginally delivered infants acquired bacterial communities resembling maternal vaginal microbiota, dominated by *Lactobacillus*, *Prevotella* or *Sneathia spp*, and C-section infants harbored bacterial communities similar to those found on the skin surface of their mothers, dominated by *Staphylococcus*, *Corynebacterium* and *Propionibacterium spp* [44]. Those initial communities are further shaped later on by selective pressure imposed by the immune system and environmental factors, such as milk oligosaccharides, immunoglobulins and the diet [45].

For centuries, the physiological role of the microbiota was considered to be limited to the digestion process, including fermentation of dietary fibers and cellulose (more pronounced in herbivores). For the last decade, more and more studies uncovered unexpected roles for the gut microbiota on

the central-nervous system (“gut-brain axis”), in the respiratory tract (“gut-lung axis”), in the skin barrier function (“gut-skin” axis), and in the function of peripheral and central immune system due to systemic dissemination of microbiome-derived components and metabolites.

- Gut-brain axis.

  Studies on germ-free animals have shown that bacterial colonization of the gut is essential for the development and maturation of both enteric (ENS) [46] and central (CNS) [47] nervous systems by regulating the secretion of neurotransmitters such as cortisol, tryptophan, and serotonin (5-HT). Microbiota affects ENS and CNS by various pathways, which include the direct effect of microbial metabolites, secretion of host-recognized neurotransmitters and through the regulation of enteroendocrine cells.

  The gut microbiota directly affects the limbic system - facilitate learning and memory, adaptation to the environmental stress and influence anxiety level, since fecal transplantation from high-anxiety Balb/C mice to low-anxiety GF NIH Swiss mice is anxiogenic for the recipient, and the opposite [48]. Moreover, bacterial metabolites of intestinal origin are found in the murine brain and there, they participate in neuronal metabolism by antagonizing carnitine, thus inhibiting specifically the mitochondria function of neurons in CNS [49]. Additionally, bacteria synthesize their own-host recognized neurotransmitters, such as dopamine and GABA [50], which constitutes a new field of research, called microbial endocrinology [51].

  On the apical side intestinal enteroendocrine cells possess multiple chemosensory receptors that can detect intestinal microbiota and microbial metabolites [52]. On the basal side they form neuropods - specific processes that directly contact mucosal neurons and glial cells located underneath the epithelium of the small intestine, providing a link between the microbiota and ENS [53]. The ENS, in turn, forms synaptic connections with the vagus nerve, which connects the intestine to the brain and constitutes an information transmission pathway that could be described as the gut microbiota-enteric nervous system (ENS)-vagus-brain pathway [54].

- Gut-lung axis

  The first evidence of pulmonary-intestinal cross-talk was reported nearly 40 years ago as the development of severe, a chronic broncho-pulmonary disease, occurs in patients with

inflammatory bowel disease [55]. On the physiological level, it was found that gut-restricted pathogen *Citrobacter rodentium* causes immune protection against pulmonary infection of an unrelated pathogen *Citrobacter neoformans* [56], suggesting inter-communication across gut and lung mucosal sites. Similar cross-protection was observed after the administration of air-born antigen through the milk to the neonatal mice gut which protects them against future development of respiratory allergy [57]. Recently, it has been shown that changes in intestinal fungal communities also exacerbates allergic airways disease in mice [58,59].

Cellular mechanisms of gut-lung communication started to be addressed and the axis appears to be bidirectional: while changes in the gut communities affect mucosal protection in the lung, lung dendritic cells (DCs) in turn program T cells to migrate to the gut by up-regulating the expression of gut-homing molecules (integrin a4b7 and CCR9) and induce protection against intestinal pathogens [60]. In addition, the microbiota of these two organs also depend on each other; modification of newborns' diet influences the composition of their lung microbiota [61] while gut microbiota alterations in rats, achieved by fecal transplantations, induces changes in lung microbial communities [62].

Microbial metabolites, such as short-chain-fatty acids (SCFAs), produced by the dietary fiber fermentation by the majority of bacterial commensals [63], are found to be an important molecular mediator of gut-lung communication [64]. SCFAs may translocate across the intestinal barrier, reach the systemic circulation and act in the lungs as signaling molecules on resident antigen-presenting cells dampening the lung immune response in experimental models of respiratory allergy [65] and influenza infection [66]. In line with these studies, SCFA receptor-deficient mice show increased inflammatory response in experimental models of asthma [67], highlighting the important role of SCFAs as the mediator in lung-gut communication.

- Gut-skin axis. Cumulative evidence have demonstrated a physiological link between the gut and the skin, starting from clinical reports of increased cutaneous manifestations during gastro-intestinal disorders [68,69]. The mechanisms of such connection were shown to be related to modulation of systemic immunity by microbial metabolites, which led to the

accumulation of anti-inflammatory or pro-inflammatory T cells in the skin [70], but also by the direct effect of gut commensals metabolites on skin homeostasis [71].

Thus, the gastro-intestinal tract is currently viewed not only as the digestive tube but more like the interactive platform on which inter-species and inter-kingdom communications occur, leading to the major changes into the immune system homeostasis, the host physiology and mental processes.

Intestinal immune system

The intestine is continually exposed to high loads of dietary and microbial antigens, that must be rapidly analyzed: harmless food antigens and commensal microbiota must be well-tolerated while toxins and pathogenic microorganisms must be recognized and eliminated, as the intestine is an entry point of many clinically important pathogens [72]. Thus it is not surprising, given the size of the organ, that the intestinal immune system contains the largest amount of immune cells in the body. For example, it has been recently calculated that amounts of antibodies, produced by intestinal plasma cells, lay in the range of grams per day[73].

Intestines are surveilled by large and diverse populations of **innate immune cells** that include mononuclear phagocytes (dendritic cells and macrophages), mast cells, eosinophils, and innate lymphoid cells. The function of innate immune cells in homeostasis might be surprisingly different from those known for infections. For example, while eosinophils are most known for their role in allergy and response to helminth infections, in intestinal homeostasis they play an important role in tissue repair[74] and maintenance of plasma cells [75]. Mast cells regulate epithelial barrier integrity, peristalsis, vascular permeability and interactions with the local nervous system [76]. Innate lymphoid cells participate in the synchronization of hematopoiesis with circadian rhythms [77]. As the function of macrophages at homeostasis is the main focus of this work it will be discussed in a dedicated chapter.

The major homeostatic role of the gut conventional dendritic cells ($CD103^+$) is the cross-talk between innate and adaptive immunity, which is essential for the establishment of tolerance to food antigens and commensal microbiota. Dendritic cells, that have acquired an antigen, upregulate the expression of CCR7 which allows them carry it away from the gut mucosa into the draining lymph node, or in the nearest lymphoid structure [78]. In mucosa-draining lymph nodes, a portion of migrating $CD103^+$ dendritic cells becomes conditioned for tolerance induction and drives the expansion of Tregs (T regulatory cells), that later home into the intestinal mucosa [79]. In the lamina propria, Tregs are then expanded by IL-10 derived from macrophages.

Both, innate and adaptive immune system orchestrate immune responses of the intestine, where dietary and commensals antigens are well-tolerated, while protection against invaders is maintained.

Myeloid cells (dendritic cells and macrophage), are responsible for directing the immune response towards tolerance or inflammation.

While relying on the same principal food tolerance and tolerance to intestinal bacteria differ by its effects on the immune system. It has been shown that oral tolerance inhibits autoimmune and inflammatory diseases in rodent experimental models of type 1 diabetes, encephalomyelitis, arthritis, myasthenia, thyroiditis, and other pathologies [80]. Thus, oral tolerance to food protein induced through the small intestine influences both local and systemic immunity, while tolerance to gut bacteria in the colon does not attenuate systemic responses [81].

The initiation of adaptive immune responses relies on dendritic cells, which present antigens that they have found in the intestine to T cells, leading to their activation. This occurs in **draining lymph nodes** and **gut-associated lymphoid tissue (GALT)**. Mesenteric lymph nodes drain the small and large intestine, where distinct nodes are responsible for different intestinal segments, as shown by the injection of the dye into the mouse intestine [82]. GALT is a complex term, which includes all non-encapsulated lymphoid tissue of the gut. They correspond to:

(1) Peyer`s/caecal/colonic/rectal patches, which consist of numerous B cell lymphoid follicles, flanked by T cell areas. They always contain germinal centers, as an indicative of a constant immune stimulation by luminal antigens; (2) solitary isolated lymphoid tissues that can only be detected microscopically and range from small cryptopatches to mature isolated lymphoid follicles,

probably representing a maturation process. Those structures only contain B cell –zones with germinal centers, indicating a primary function in humoral immunity.

Upon antigen presentation, newly primed lymphocytes return to the gut. There, some of them can home to the epithelium to form the intraepithelial lymphocyte pool, while majority of T cells, invariant T cells, B and plasma cells reside within the lamina propria. Of note, new types of adaptive immune cells and associated functions keep being discovered.

Intra-epithelial lymphocytes (IELs) can be found at a frequency of up to 10-15 lymphocytes per 100 epithelial cells [83]. Given the great intestinal epithelia surface area, IELs comprise a considerable fraction of the total body's T cells. IELs belong to both the T-cell receptor (TCR) αβ+ (TCRαβ+) and TCRγδ+ lineages [84], and can be classified as *induced* (conventional, derived from CD4+ or CD8αβ+ TCRαβ+ T cells, shaped by exogenous antigens and that thus increase with age [85]) or *natural* (unconventional, resulting in the functional differentiation of mature CD4 and CD8αβ double-negative, TCRγδ-, or TCRαβ-expressing T cells that directly migrate to the intestinal epithelium[86] and do not rely on exogenous antigens to develop [87]). Most of them exhibit an effector-/memory-like phenotype and have a protective role. While natural IELs protect the epithelium in response to stress antigens, induced IELs protect the epithelium against pathogen-expressed antigens [88]. γδT-cells are ideally suited to provide IL-17 in the very earliest stage of an inflammatory response, i.e. before antigen-specific αβT-cells can do it. They often increase in number at early stages of infection [87]. γδT-cells also regulate the influx of neutrophils at the beginning of this process and regulate the onset of T and B lymphocyte responses [87].

Both $CD4^+$ T cells and $CD8^+$ T cells are found in the lamina propria, at an approximate ratio of 2/1 and are derived from conventional T cells that have been primed in secondary lymphoid organs. They display an effector memory phenotype [89].

The *$CD4^+$ T cell compartment* of the lamina propria is highly diverse, containing IL-2^+, IL-2^+IFNγ^+, IFNγ^+ and IL-17^+ subsets[90], as well as IL-10-producing $FOXP3^+$ and $FOXP3^-$ Treg cells [91,92].

The intestinal lamina propria also contains subsets of T cells that express invariant forms of the TCR and that may have innate immune functions [93]. These subsets include mucosal-associated invariant T cells (*MAIT cells*), as well as invariant natural killer T cells *(iNKT cells*). *MAIT* cells

selectively recognize metabolites from the riboflavin metabolism pathway of bacteria and are absent in germ-free mice. They are activated by cells infected with bacteria and can display a cytolytic activity. *iNKT* cells display an effector memory phenotype, and they produce large amounts of IL-4 and IFNγ within hours of TCR-mediated recognition of conserved glycolipids that are presented by the non-classical MHC class I molecule CD1d. Their natural ligands include both self and bacterial lipids.

B-cell responses are also organized in gut-associated lymphoid tissues and regional lymph nodes [73]. IgA-producing [72]plasma cells predominate throughout the length of the intestine. In the lumen, released antibodies can bind antigens, and thereby mediate immune exclusion and antigen clearance. Secreted IgA bound to antigens can then be taken by epithelial cells through the transferrin receptor, during the process known as retrotranscytosis. This facilitates the uptake of antigens against which there is an already established humoral response across the epithelial barrier. IgA can also bind and neutralize lipopolysaccharide thereby having an anti-inflammatory role.

As a next level of complexity, cells of non-hematopoietic origin, such as epithelial [94–96] and stromal cells [97,98], possess a wide range of immunomodulatory properties, that guide and direct the immune responses, but will not be discussed here. It therefore appears that intestinal mucosal immunity is a highly complex system that includes cells of hematopoietic and non-hematopoietic origin, which act together to orchestrate immune responses whether they are inflammatory or tolerogenic. Failure to do so inevitably leads to inflammatory diseases such as ulcerative colitis, Crohn`s disease, or to food intolerances, allergies or chronic gut infection.

Chapter 2. Specialized segments of the gastro-intestinal system

The gastro-intestinal system is highly compartmentalized where individual segments perform separate tasks to achieve common physiological goals. These distinct gut segments are described below in the context of the digestive function of the gastro-intestinal tract.

The **esophagus** conducts food from the oral cavity to the stomach where fragmentation is completed and digestion begins. Initial digestion, accompanied by the intense muscular action of the stomach wall, converts the stomach contents to a semi-digested liquid called chyme. Chyme is squirted through a muscular sphincter, the pylorus, into the **duodenum**, the short first part of the small intestine (25-30 sm in humans). Digestive enzymes from a large exocrine gland, the pancreas, enter the duodenum together with bile from the gallbladder via the common bile duct. Bile contains excretory products of liver metabolism, some of which act as emulsifying agents necessary for fat digestion. The duodenal content passes along the rest of the small intestine where the process of digestion is completed and most of the absorption occurs. The middle segment of the small intestine is called the **jejunum** (following 2 - 3 m in humans) and the distal segment the **ileum** (4 - 4.5 m in humans). The liquid residue from the small intestine passes through the ileocecal valve into the large intestine. Here, residual fluid is absorbed from the liquid chyme, which becomes progressively more solid as it passes towards the anus.

The first part of the large intestine is called the **caecum,** which is developed in rodents, and is the primary site of fermentation (digestion of dietary fibers). The following part is the **colon,** which is divided anatomically into the proximal and distal regions, with different histological features and physiological roles. The terminal portion of the large intestine, the **rectum**, is a holding chamber for the feces that are expulsed via the anal canal.

Accordingly, the intestinal immune system changes along the length of the intestine (Figure 2). Distinct populations of innate and adaptive immune cells that are present in the small and large intestine are shaped by the local microenvironment, and can adapt to the physiological needs of a given intestinal segment.

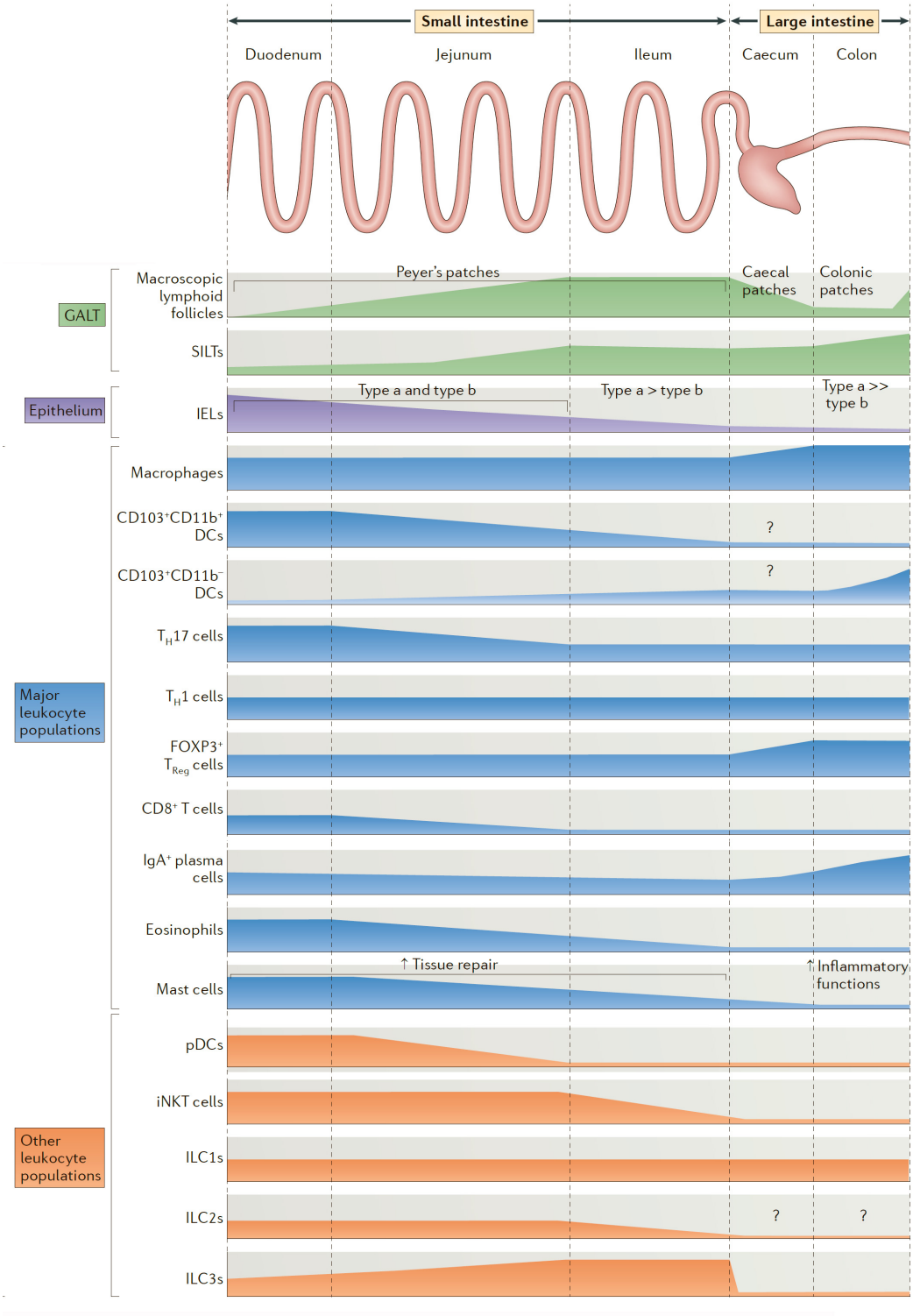


Figure 2. Regional specialization within the intestinal immune system. GALT- gut-associated lymphoid tissue (green graphs, SILTs-solitary isolated lymphoid tissue). Various leukocyte populations are presented in purple, blue and orange graphs, IELs – intra-epithelial lymphocytes, DCs – dendritic cells, iNKT – invariant natural killer cells, ILC – innate lymphoid cells. The question marks indicate regions for which the regional specialization has not been characterized. *Adapted from Mowat and Agace, Nature Reviews Immunology, 2014*

Small intestine

The small intestine is the site where digestive processes are completed and where the nutrients are absorbed through the epithelium into the blood or lymphatics. Viewed macroscopically, the lining of the small intestine shows a series of permanent circular or semilunar folds (*plicae circular*es), consisting of mucosa and submucosa, which are best developed in the jejunum. Lymphoid tissue of the small intestine is organized in the large conglomerates (up to 9 sm in humans [99]), present mostly in terminal jejunum and concentrated in ileum, and called Peyer`s patches.Absorptive type of mucosa with numerous villi and crypts is characteristic of this region of the gut. Villi are covered by a single layer of columnar epithelium, which faces the lumen. Originating from $Lgr5^{+}$ stem-cells in the bottom of the crypt and going through series of divisions in the transient-amplifying zone, epithelial cells differentiate and arrive in the villi, where they operate [100]. Among the differentiated cell types, nutrient absorbing enterocytes make up the majority of cells lining the villi. Other lineages are secretory cell types that include (1) goblet cells that produce mucus to generate a protective barrier; (2) enteroendocrine cells that secrete various hormones and neuromediators; (3) Paneth cells, which constitute the niche for stem-cells at the crypt base [101], secrete antimicrobial peptides and essential factors for stem cell maintenance; (4) Tuft cells that serve as sensors for luminal contents and initiate immune responses to helminth infections [102,103]; (5) M (microfold) cells that reside in specialized epithelium overlying Peyer's patches and deliver antigens to antigen-presenting cells, that are located below [104].

Each villus has a core of connective tissue that extends from the lamina propria and contains fibroblasts, smooth muscle cells, immune cells, fenestrated capillaries, and a central lymphatic called a lacteal [33]. The structure of the different segments of small intestine can be a great example of how mucosal sites adapt to the local microenvironment to perform their physiological roles (Figure 3).

The mucosa of duodenum, jejunum and ileum is subjected to different chemical, microbial and physical environments and changes its structure accordingly.

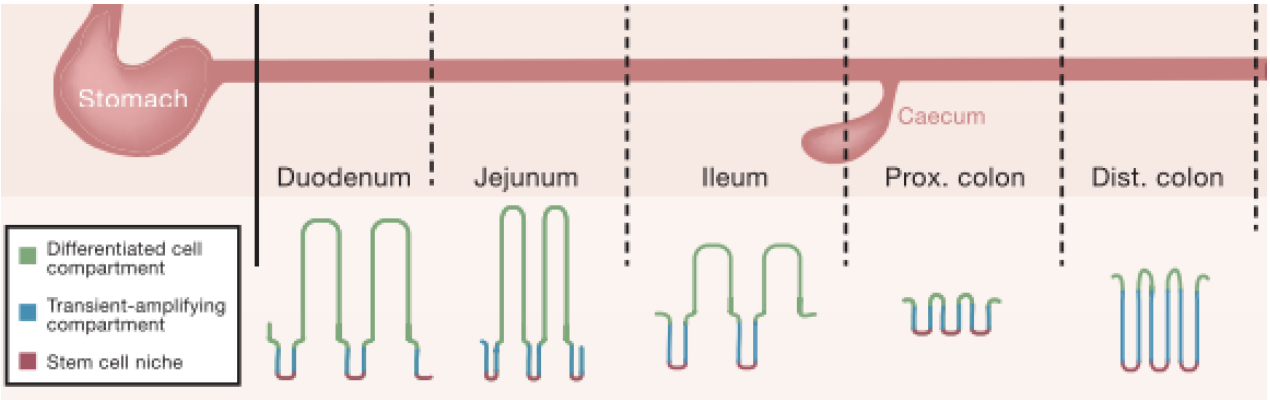


Figure 3. Differences of mucosa organization along the gut. In the small intestine mucosa forms villi – finger-like protrusions that extend into the lumen. Villi change the shape and size along the small intestine.In the large intestine villi are absent and mucosa is organized in crypts – cylindrical invaginations of the epithelium into the stroma. Throughout the intestine epithelial lining contains three similar zones: stem cell niche, transient-amplifying zone and differentiated cell compartment. *Adapted from Clevers and Batlle, SnapShot: The Intestinal Crypt. Cell, 152, 2013. http://dx.doi.org/10.1016/j.cell.2013.02.030*

For example, shape and length of villi changes along the small intestine [105,106] and this phenomenon was referred to as the villus size gradient [106], with the longest villi being present in the duodenum.

Thus, to ensure the synchronization of epithelial renewal in the longer duodenal villi with shorter villi in ileum, production rate of differentiated cells is higher in duodenum vs ileum. Given the fact that mitotic index is unchanged along the length of the small intestine [106], it can be achieved only by the increase in number of crypts, that fuel the individual villus. Indeed, it has been shown that while crypts/villus ratio is 27 for the duodenum, it falls down to 10 in the terminal ileum [107]. Surgical transplantation studies in the 70s led light on the nature of villus size gradient [105,106]. When the ileum, which possesses the shortest villi, was transplanted in place of the jejunum, villi increased in length and reached the size of regular jejunal villi and *vice versa*. The same phenomenon was observed when ileum was attached directly to the pyloris, but not the forestomach, suggesting that duodenum and pyloris are the sources of “villi-enlarging factors”, pancreatic juice and bile, and affect villus length through the factors secreted into in the chyme that pass along the small intestine.

The same phenomenon is also observed in patients with the short-bowel syndrome, when large segments of the small intestine are excised, and the residual parts undergo adaptation,

characterized by increased villi length, wider lumen and higher enzymatic activity [108,109]. These studies highlight the importance of the gradients of physiological factors that create the local microenvironment, which dictates the morphological and physiological adaptations of the intestinal mucosa.

Intestinal mucosa changes its structure along the length of the gut to fulfill local physiological needs.

Villi in the small intestine facilitate the digestion/absorption process by being constantly immersed in the liquid chime, while crypts of the colon allow efficient fluid absorption from solidified feces.

Thus epithelium barrier adjusts its structure along the length of the gut, being more "leaky" in the small intestine and "tight" in the colon, as it faces different environmental challenges.

Large intestine

The large intestine consists of cecum, colon, and rectum. The cecum is an elongated blind sac in the lower abdominal cavity. In contrast to the small intestine, the colon is not coiled and consists of a proximal, traverse and distal regions [110].

As opposed to the small intestinal crypts, colonic crypts contain terminally differentiated cells, which appear in the top third of the crypt and on the luminal side [111].

Proximal and distal colon possess many physiological and morphological differences, as well as a different embryonic origin [112]. In the proximal colon, the mucosa forms stable traverse folds that project into the lumen and are immersed in liquid content [113]. Crypts are shorter [114,115] but more numerous resulting in a 30% larger absorptive surface [116], compared to the distal colon. Epithelial cell migration along the crypt was also shown to be faster compared to the distal colon [114]. In the distal colon, the mucous layer is much thicker due to the greater presence of the larger number of goblet cells in the mucosa and is considered to be a physiological adaptation to the solidified content [117]. Net sodium and water absorption is significantly higher as shown by infusion through the alive proximal and distal segments during surgery [116], as well as different mechanisms of sodium absorption are employed, in proximal colon sodium is absorbed by electroneutral mechanism following osmolarity gradient, while in the distal colon, electrogenic ENaC-sodium pumps are used[118].

As in the small intestine, the content of the colon is different across its length and is changing from the liquid in the proximal region, which contains 95% of water, to solid in the distal region, with

less than 68% of water [8]. The reduction of fecal water content from 95 % to about 80 % is relatively easy, requiring a force of only = 5 kPa. However, to reduce the water content of feces further to < 60 % is much more difficult, requiring ~ 1000 kPa (= 10 atmospheres). Thus, the epithelium barrier of the proximal and distal colons is subjected not only to different mechanical stimuli due to the solidity of its contents but also to different values of osmotic pressure, which reaches its maximum in the distal colon.

Thus, the epithelium of the distal colon faces additional environmental challenges, such as the highest microbiota load, the highest osmotic pressure and solidified content. Thus epithelial barrier of the distal colon must therefore harbor additional mechanisms to ensure: (1) effective initiation of the healing process and elimination of leaked luminal products, if the breakage of the barrier occurred; (2) fast elimination of dead cells; (3) analysis of absorbed fluids to avoid intoxication.

Distinct immunological landscapes in the small and large intestine

The function of the intestinal immune system in the steady state is to ensure intestinal functions in the face of constant influx of foreign materials. There are, however, marked differences in luminal content, function and anatomy along the length of the intestine, which present distinct challenges to the immune system. As a result, although the various segments of the gastro-intestinal tract can employ similar immune functions, the exact balance between individual cell types and mechanisms varies considerably along the length of the intestine.

The small intestinal epithelium contains 10-fold to 20-fold more intra-epithelial lymphocytes compared with the colon [83,119], but proportionally contains less of CD4+ and CD8αβ+type[120]. The relevance of this gradient remains unclear and probably is related to different luminal content and antigens the epithelium is subjected to.

Regarding, effector T-cells subsets, an inverse correlation between the number of T helper 17 (Th 17) and Tregs has been reported, with Th17 cell numbers progressively decreasing from the duodenum to the colon and Treg numbers being the highest in the colon [29]. The beneficial effects of Treg activity in suppressing chronic inflammation in the gut may be partially offset by compromising protective immune responses, which is compensated in the upper intestine by

increased number of Th17. Whereas the highest microbial load in the colon requires an influx of Treg cells into the mucosa, leading to the domination of FOXP3$^+$ subset [91].

Conversely, IgA-producing plasma cells bias towards IgA production increasing from ~75% of the plasma cells in the duodenum to ~90% in the colon [121]. Secretory IgA production is almost completely dependent on the presence of the microbiota and IgA have been shown to bind and mask LPS, avoiding overstimulation of mucosal immune system by the commensal microbiota.

Innate players of mucosal immunity are also different along the length of the intestine. The numbers of CD103$^+$ CD11b$^+$ dendritic cells in different segments of the intestine correlate with the presence of Th17 cells [29], indicating a potential role for these dendritic cells in intestinal Th17 homeostasis. Consistent with this possibility, selective reduction of this intestinal dendritic cell subset in mice results in reduced numbers of intestinal Th17 cells and in efficient Th17 differentiation in mesenteric lymph nodes [122]. In the colon, CD103$^+$CD11b$^-$ dendritic cells are the major CD103$^+$ dendritic cell subset but their functional specialization is unclear.

> The small intestine shows a bias towards processes that are associated with defense against extracellular infections, including the production of IL-17, IL-22 and antimicrobial peptides. Furthermore, it is directed mostly at establishing a tolerance to food antigens (at local and systemic levels), that can disseminate widely throughout the body.
>
> While the colon acts as the main reservoir for the commensal microbiota, and its immune system prevent inflammatory responses against them. Thus, the colon contains a particularly large numbers of mucosal IgA-producing plasma cells, IL-10-producing macrophages and FOXP3$^+$Tregs.

Macrophages are the most abundant innate immune cells in the healthy intestinal lamina propria. They phagocytose and degrade microorganisms and dead tissue cells, produce mediators that drive epithelial cell renewal. They also produce large amounts of IL-10, which not only prevents inflammation by blocking pro-inflammatory responses to stimuli such as TLR ligation [23], but also promote the survival and functions of local FOXP3$^+$Treg cells in the mucosa [79]. Absolute numbers and relative frequencies of macrophages are higher in the colon than in the small intestine [29,30,123], but what is their role in the colon physiology will be the focus of my PhD work. And entire chapter is dedicated to these cells below.

Chapter 3. Luminal gradients along the gut

The gut luminal content changes its chemical and physical properties along the length of the intestine, which plays a major role in the creation of local microenvironments and mucosal barriers. These gradients create the ecological niches permissive for certain microbiota. At the same time, the microbiota participates in creating such environments, reinforcing the tight physiological link between the host and the microbiome (Figure 4).

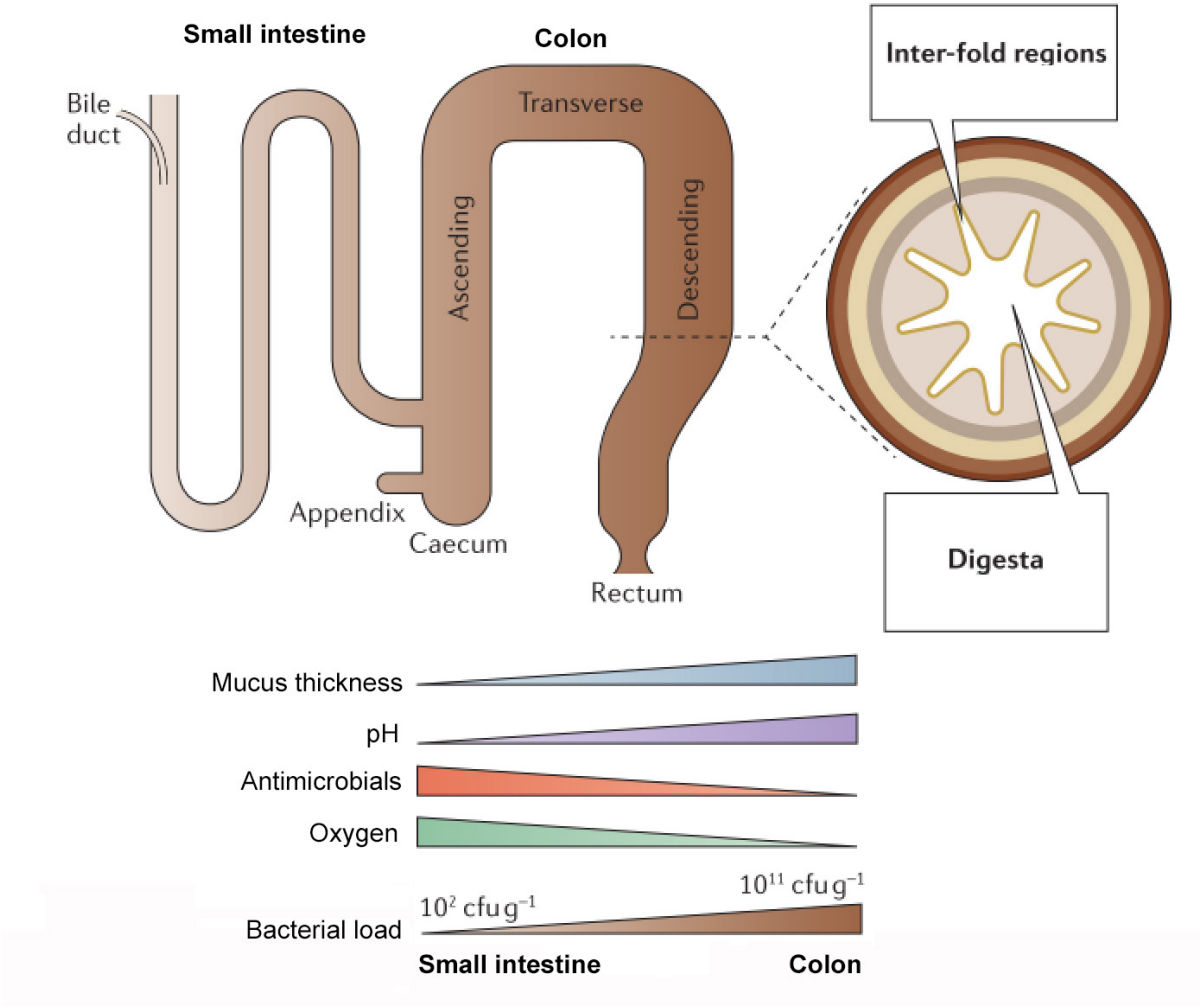


Figure 4. Luminal gradients along the gut.

Adapted from Donaldson et al, Nature Reviews Microbiology, 2015, 141 (1) 20-32

pH

While passing along the gut, the chyme changes its chemical composition during digestion, secretion and absorption. This process greatly affects ions concentrations, including protons.

Two pH gradients are described in the gut:

Luminal gradients: pH, mucus composition, and oxygen concentration, create local microenvironments within the intestinal lumen, that are permissive or not for given microbiota

(1) A luminal (longitudinal) pH gradient related to digestion. It forms due to the secretion of acidic or basic products by intestinal glands of the stomach, Brunner`s glands of duodenum, pancreas and liver. Even though the reported pH values of the chyme in different regions of the intestine vary from study to study, most likely due to the methodological differences, all of them point to the existence of the pH gradient along the intestinal tube [124,125]. The chyme is more acidic (pH 1.7-2) in the proximal region of the small intestine and reaches pH6 in the ileum. Due to the fiber fermentation followed by short-chain fatty acids production, sharp descent of the pH values is observed in the cecum [126], which then gradually rises towards the rectum [127]. Interestingly, luminal pH gradient is not dependent on the diet, as reported by early studies on dogs [128].

(2) A mucosal (transversal) pH gradient is formed due to the presence of a mucus layer, that captures hydrogen and bicarbonate ions, slowing down the diffusion in this zone [129]. This creates a shield of constant pH value near the apical surface of epithelial cells, protecting the epithelium from luminal pH changes. This phenomenon is observed in the small and large intestinal mucosa [130], and is called “pH-microclimate”[131]. Acidification of the luminal content is buffered by epithelial alkaline secretion, so a change of luminal pH from 7.6 to 2 causes only slight changes in mucosal pH values, which remains close to neutral [132]. Prostaglandins, in particular PGE2, are important mediators of the alkaline response to the luminal acids. When luminal pH is decreasing, PGE2 acts on epithelial cells and increases the rate of alkaline secretion. Faster alkaline secretion increases pH values close to the epithelium, which leads to the neutralization of the luminal acids and epithelial protection. As a consequence of this response mucosal (transversal) pH gradient sharpens.

Besides its protective role, pH-microclimate facilitates the absorption of weak electrolytes, such as folic acid, in the small intestine [133] and provides the basis for constant absorption of short-chain fatty acids in the colon [131].

Mucus

The epithelial lining of the gut is covered by a layer of mucus secreted by goblet cells. The proportion of goblet cells relative to enterocytes increases from 4% in the duodenum to 16% in the distal colon [134], which together with the repertoire of secreted mucins [135], modifies the mucus layer along the intestine.

Interestingly, the thickness of the mucus layer reaches 150 um in the colon of mice [136], which is almost the same thickness as the entire intestinal wall. This important component of the intestinal barrier has been poorly explored until recently, due to its collapse upon commonly used formaldehyde fixation.

Morphology of the mucus layer

Micropipette aspiration coupled with intravital microscopy allowed the examination of the thickness of the mucous in vivo and the rate of the mucus secretion over time [137]. It was found that: (1) the mucus layer is continuous and thicker than previously documented, most likely because of its shrinkage during the fixation in alcohol-based fixatives, such as Carnoy`s solution; (2) it consists of two layers-loosely adherent gel that is easily removed by suction, and firmly adherent gel that resists aspiration. The proportion of these two layers, rather than their composition, varies in different intestinal segments and is responsible for the establishment of the mucus gradient along the gut; (3) the mucus is constantly renewed with the renewal rates that are distinct for each gut segment but always within the range of hours.

The thickness of the mucus layer decreases with age in both sexes. Several genes involved in the biosynthesis of mucus are downregulated in old mice, especially in males [138]. These changes are followed by enhanced activation of the immune system illustrated by an increased percentage of cytotoxic T cells in the colonic mucosa. This highlights the importance of the proper mucus layers morphology and thickness in the host homeostasis.

Composition of the mucus layer

The main components of the mucus are mucins. Secreted mucins are large, heavily O-glycosylated glycoproteins assembled into net-like polymers, which gives to the mucus its viscous properties [139]. There are several mucins and they are produced in different regions of the gastro-intestinal tract, but the main gel-forming mucin in both small and large intestine is Muc2.

Muc2 is insoluble and stored in a condensed form in the granules of goblet cells. After release, Muc2 dramatically expands in volume, 100-1000 times [136]. In the transition-zone between the inner and outer mucus layers, Muc2 is cleaved, becoming soluble, which allows the formation of the outer mucus layer with further volume expansion and an increase in the net-size [140]. Such physical properties make the outer mucus layer a permissive niche for bacteria [141]. The presence of both mucus layers in the germ-free animals suggests that mucus maturation rather depends on cell intrinsic components (such as and proteases) [140].

Interestingly, within individual crypts of the large intestine, the adjacent goblet cells often produce different glycoforms of mucins forming striated mucus layers. Also, as observed in the human colon in homeostasis, all goblet cells within one crypt may synchronically switch to the production of the same mucin glycoform [117]. It is unknown what factors regulate this transition but speculated to be microbiota-related.

Proteomic analysis of the mucus layer revealed the presence of other components, such as Fcgbp, Clca3, Zg16, Agr2, immunoglobulins, plasma proteins and many more [142]. The origin of those proteins is unknown, as they also might come from cells that are continuously shed out into the lumen and trapped within the mucus and thus detected by proteomics. Some of them, such as Fcgbp, perform unconventional roles such as mucus cross-linker [136]. The proteins originating from cellular debris may also function as a carbon and nutrient source for the microbiota, participating in the creation of an ecological niche within the outer mucus layer [141].

The mucus of the small intestine

As mentioned above, Muc2 mucin is the main structural component, just as in the large intestine. Despite this, the properties of the mucus in these two locations are different.

There are conflicting reports on the morphological appearance of the mucus in the small intestine analyzed by histochemical methods. Some studies describe two mucus layers, with the outer mucus being easy to aspirate and remove [137]. In contrast, other studies describe a thin layer of non-removable mucus, which covers the villi. Similarly, some postulate that ileal mucus has only one layer attached to the epithelium [139], while others report that ileum has no mucus [117].

Nevertheless, the majority of physiological studies agree on several points:

(1) the mucus in the small intestine is thinner compared to the colon mucus [134,135,137]. Along the small intestine, the jejunum has the thinnest mucus [134,137], which probably reflects its major role in absorption, neutral pH of its luminal content, and lower microbial load.

(2) The mucus is secreted continuously with the lowest rate in the duodenum and the highest in the ileum [137], however, these rates might increase upon acid irritation [143]

(3) The small intestinal mucus network is more sparse than in the colon - penetrable to beads of similar size as bacteria [134]

(4) in the small intestine, the bacteria are found in direct contact with epithelial cells [144,145]

Thus, the mucus in the small intestine is more porous to allow nutrients and antigens, which can be relatively large, to come in contact with epithelium, and due to the lower microbial load.

The mucus of the large intestine

There are pronounced changes in the mucus layer across the colon, including its thickness, composition and penetrability to microbiota [135,139] .

- Proximal colon. The mucus layer's overall thickness is greater than the one in ileum [137], but still smaller than in the distal colon [117]. The proximal colonic mucosa forms stable traverse folds that project into the lumen and are immersed in liquid content. Accordingly, the mucus changes its properties depending on the morphological zone - between traversal folds or their tips. Between traverse folds, it is impenetrable to beads similar to the size of bacteria, whereas on folds` tips, it is thinner and permeable [134]. Indeed, bacteria were found to contact the epithelium at the folds' tips [146]. Thus, the permeability of the mucus barrier to bacteria shows an intermediate profile as compared to the distal colon.

- Distal colon. Mucus layer riches its highest thickness in the distal colon [117,134,137] and is composed of the different mucin repertoire [136]. The inner layer is not permeable to beads of the bacterial size [134] and bacteria were not found in contact with the epithelium. This gives an impressively large sterile zone of 50 um [136,139,147], which is comparable to the thickness of the entire mucosal wall. In part, sterility might be achieved by the highest rate of mucus secretion, 200 um/h, as shown for the distal colon [137,139]. Description of the outer mucus layer in the colon is technically challenging, because transiting solid feces remove it. Thus, the mucus layer appears different in the empty versus full distal colon. A recent study claims that the outer layer is only present around feces [146]. Authors explain this inconsistency with the previous findings by the sample preparation protocol, which lead to misinterpretation of the results: when two mucus layers were initially described by IHC staining, distal colons were fixed together with feces. This created an impression that mucus is two-layered, while in reality the outer one rather comes from the fecal pellet.

The function of the mucus layer

The mucus was initially thought to play solely a protective role by shielding the epithelium from the shear and mechanical stresses imposed by feces. Nowadays, it is recognized that the mucus plays additional important roles in the gut homeostasis, which show variations depending on the gut segment.

1. Protective role

In both, the small and large intestine the mucus protects the mucosa from luminal insults: while in the small intestine the mucus acts as a chemical barrier that prevents direct access of luminal enzymes and auto-digestion of host tissues [148], in the colon, the mucus acts as a physical barrier that prevents direct contact between the abundant microbiome and host epithelium [147]. This physical barrier protects the host immune system from overstimulation, colitis development [149] and increased susceptibility to pathogens, such as *C. rodentium* [150] and *Salmonella*, which swim in the outer mucus layer, probing for colon mucus heterogeneities [151].

2. Water absorption and feces consolidation

As discussed in Chapters 1 and 2, the distal colon has the unique capacity to absorb water against large hydraulic resistance, which requires developing of the osmotic pressure of 5-10 atmospheres to successfully consolidate feces [8]. This pressure can be reached only by numerous crypts acting simultaneously during fecal pellet transit through the distal colon. Thus, the mucus layer, being continuous, helps to build up the suction force by summing the suction created by each individual crypt. Also, feces consolidation requires time and tight sealing between pellet and the crypts. Under these circumstances, mucus layer acts as grease, which, firstly, seals the space between the crypt luminal opening and pellets, and secondly permits the feces to slide across the luminal surface, while suction is maintained. This hypothesis was confirmed by physiological studies, where Muc2-deficient mice develop diarrhea and fluid loss, along with the other issues [149].

3. Providing ecological niche

Recent studies show that the outer mucus layer is populated by specific members of the microbiota, that are distinct from their luminal counterparts [141]. The same member of microbiota, exhibit distinct transcriptomic profiles depending on if it populates the lumen or the mucus, suggesting that the mucus layer can create spefic ecological niches. This could be due to:

- *Physical mesh and anchoring point.* Mucins are used as ligands for bacterial adhesins [152]. Probiotic *Lactobacillus* adheres to mucus [153,154] through specific protrusions [155] and initiates colonization of the intestine, suggesting that the mucus can participate to the primary selection of microbial species [136]. The mucus also selects the microbes undergoing rapid renewal within a timescale of several hours. This means that microbes must be fit enough to be renewed or replenished at the same rate while competing with each other for resources [141].

- *Limited iron bioavailability.* Even though the molecular mechanisms of iron sequestering in the colon mucosa remain partly unknown, it is clear that the outer mucus layer has a restricted amount of ionic iron, consistent with the upregulation of iron uptake genes in bacteria found in the mucus [141]. Limited amount of ionic iron is a protective mechanism

against pathogenic microbes, because the vast majority of them need to assimilate iron in its ionic form.

- *Carbon source.* The mucus is rich in glycoproteins and polysaccharides, which serve as an alternative or even primary carbon source for mucus-resident bacterial species [156,157]. One of the intestinal generalist, *Bacteroides thetaiotaomicron,* can shift from dietary polysaccharides to mucus glycan metabolism in the absence of fibers, which helps maintain integrity in microbiome composition during dietary fluctuations and nutrient availability. However, in the long term, it negatively impacts the integrity of the mucus barrier and susceptibility to infections [157]. Interestingly, mucus glycosylation profile may also participate in the selection of symbionts; it influences species-specific microbiome composition [158] and mice lacking O-glycans exhibit microbiota differences in the cecal lumen [159].

4. Mucosal and systemic immune homeostasis

Besides the role of goblet cells and goblet-associated antigen pathways in antigen delivery and immune homeostasis, which constitutes the entire field of research [95,160,161], mucins directly interact with immune cells such as dendritic cells and macrophages in the small intestine. Luminal antigens (bacteria, or dietary antigens) bind Muc2 and suppress inflammatory, but not tolerogenic dendritic cells and macrophage-mediated responses, leading to secretion of tolerogenic cytokines, such as IL-10 and TGF-ß. Muc2-deficient animals show elevated inflammatory responses, completely abrogated by oral administration of Muc2 [145].

To summarize, the mucus barrier plays important role in mucosa protection, water absorption, immune homeostasis and commensalism. The gradient in mucus composition and its properties along the gut reflects distinct physiological roles of gut segments. It further introduces chemical and physical variability in local microenvironments, which participate in the creation of specific ecological niches occupied by the distinct microbiome.

Oxygen

Similar to pH and mucus gradients, the oxygen concentration also changes in the gut along the two axes:

(1) radial gradient, formed due to the oxygen diffusion from highly vascularized intestinal mucosa into the lumen[162]. The oxygen concentration is determined by the predominant type of oxygen metabolism of intestinal epithelial cells, chemical reactions that occur in the lumen of certain intestinal segments and the presence of aerobes and facultative anaerobes that actively consume oxygen.

(2) longitudinal gradient, formed due to change of the above-mentioned factors (epithelial cell metabolism, digestive reactions and microbiota composition) along the length of intestine.

In both small and large intestine, blood perfusions significantly fluctuate regularly forming highly unique oxygenation profile [163]. In the small intestine, blood flow is highly dependent on the absorption of ingested nutrients and increases 93-156% after the meal [164]. In the colon, the production of short-chain fatty acids (SCFAs) during fiber fermentation stimulates perfusion of capillaries with dose-dependent vasodilatation [165].

The highest luminal oxygen concentration is observed in the duodenum and the lowest - in the caecum and colon, where it is near zero[166]. Thus colonic epithelial cells are present in chronic hypoxia state, which is referred as physiologic hypoxia [163,167].

Mechanisms of oxygen gradient formation

Initially, it has been proposed that facultative anaerobes, which dominate in the microbiota of infant gut, consume oxygen, and thus by establishing hypoxia, create a suitable microenvironment for the obligatory anaerobes that populate the gut later in life [168,169]. However, further studies challenged this hypothesis. First, obligatory anaerobes are able to colonize the gut of germ-free animals successfully [170]. Second, direct oxygen concentration measurements *in vivo* revealed that the luminal oxygen gradient is in germ-free mice. Together, these findings suggested that microbiota-independent factors drive the formation of the luminal oxygen gradient is driven by microbiota-independent factors [166].

Two main microbiota-independent mechanisms are responsible for creating hypoxia in the gut: (1) chemical reactions, such as lipid oxidation [166] and (2) active epithelial oxygen consumption. Stimulation of colonocytes with short-chain fatty acids activates b-oxidation metabolism, which uses butyrate as the energy source [171]. B-oxidation additionally increases epithelial oxygen

consumption to the extent that the epithelium senses metabolic hypoxia and hypoxia-inducible factor is stabilized [172]. Thus, the energy metabolism of mature colonocytes is characterized by high oxygen consumption, which provides the host control over physiologic hypoxia of the gut lumen [173]. In inflammation disorders, which are often characterized by crypt hyperplasia, immature colonocytes are exposed to the lumen [174]. As anaerobic glycolysis is the main metabolic pathway in immature colonocytes, luminal oxygen is less consumed. This leads to elevated luminal oxygen concentrations, dysbiosis and change of the local immune landscape [175].

Importance of the oxygen gradient

- Epithelial barrier integrity. Physiological hypoxia preserves epithelial barrier function by maintaining restricted permeability [172], and tight junctions integrity [176].
- Ecological niche/commensalism. Oxygen concentration determines the taxonomic composition of the gut microbiota in each intestinal segment [166], as it provides the environment that suits the metabolic needs of the symbionts. In distal regions of the gut, epithelial cells limit the amount of oxygen that difuses into the gut lumen. This maintains the dominance of obligate anaerobes that digest the fibers into SCFAs. SCFAs, in turn, bind to PPAR-g, which is highly expressed in differentiated colonocytes. This shifts the energy metabolism of colonocytes toward oxygen consumption and thus reinforces luminal hypoxia [171] and survival of obligatory anaerobes.
  Failure of the host to limit the luminal oxygen concentration results in a shift in the microbial community, from obligate to facultative anaerobes [177], and consequently increases susceptibility to pathogens invasion [175,178].

To summarize, the oxygen gradient along gut axes is formed during the digestion process (lipid oxidation) and is maintained by the peculiar metabolic state of the epithelium. This promotes colonization of the distal region of the gut by obligate anaerobes, which ferment fiber and produce short-chain fatty acids necessary for the host.

Altogether, the chyme composition, mucus, pH and oxygen gradients along the gut create a variety of highly distinct ecological niches that form, maintain and reinforce the symbiosis with the particular microbiota. Hosting different members of the microbiota at the specific places creates

probably the most complex and sophisticated gradient – gradient of the local ecosystems, that live and interact with each other, providing advantages and challenges to the host and create our microbial self.

Chapter 4. Microbiota

Gradients of pH, nutrients, mucus and oxygen create gut ecological niches populated by different microorganisms, which in turn modify occupied microenvironments. This process creates complex ecosystems along the intestine, which evolve over time. Interestingly, microbial communities associated with some niches of the human body have various degrees of complexity. If vaginal microbiome is predominantly composed of a few different inhabitants [179], the intestine contains thousands of different microbes [171,180–182].

Intestinal microbial density increases from the duodenum and reaches its maximum in the colon [181]. The small intestinal microbiota has a higher capacity to degrade simpler carbohydrates. Thus, to limit direct competition between these microorganisms and the host for nutrients, the number and composition of microbiota must be tightly regulated. This is achieved by fast transit time, the secretion of antimicrobials, bile acids and the lower pH. These factors restrict numerical abundance and species diversity of small intestinal microbiota and favor the growth of species involved in lipid digestion and absorption [183]. Lipid oxidation in turn consumes oxygen and is a major driving force for generation of the hypoxic environment of the lower intestine [166]. Thus microbial communities of the small intestine shape the colon environment and thus impact on the microbial species that reside there [12].

Microbiota produces various metabolites that are beneficial for the host, and regulate many aspects of its physiology, ranging from being an energy source to the perfusion of the blood vessels, and reinforcing the T-cell differentiation.

While the great number of metabolites are beneficial, some of them perturb the intestinal barrier, and are employed by opportunists in their invasive strategies. For example, intestinal barrier is directly targeted by several fungal toxins, which can lead to the fungal invasion, dysbiosis and sepsis.

It is estimated that around 20–60 g of complex dietary carbohydrates [184] and proteins [185], that escape small intestinal digestion reach the colon each day. Thus colon microbial communities

use fermentation as the main route of extracting energy from fibers, which results in high short-chain fatty acids production in the proximal colon [63]. These nutrients are either used by colonocytes as a source of energy [174] or directly incorporated into the host metabolism as an additional carbon source. Distal colon microbial communities perform protein fermentation with the resulting production of phenols, indols and ammonia in case of a protein-rich diet.

Microbiota members interact not only with the host but also between each other, and all possible ecological interactions exist in the gut:

- truly symbiotic, such as mutual cross-feeding interactions between *Bifidobacterium longum* and *Eubacteria rectale* [186];
- parasitic, such as coccus TM7, found in human oral cavity, exhibit reduced genome, small size and lack of biosynthetic capacity for amino acids. It parasitizes on *Actinomyces Odontolyticus*, and fully relies on its metabolism [187].
- predatory, where *Bdellovibrio bacteriovorus* attacks and consumes other bacterial strains, including known pathogens, such as invasive strains of *E.coli, Salmonella typhimurium* and *Helicobacter pylori*, thus additionally protecting the host [188].

The distinct spatial distribution of microbiome components along the intestine allows the host to efficiently extract and absorb nutrients/electrolytes, adapt to dietary changes and fasting, and further shape both local and systemic immune responses.

Bacteria

Host-driven negative & positive selection of bacterial species in the small intestine

The small intestine has higher levels of oxygen and antimicrobials than the colon, therefore, the microbial community of the small intestine is dominated by fast-growing facultative anaerobes that tolerate the combined effects of bile acids and antimicrobials while competing with both the host and other bacteria for the simple carbohydrates that are available in this region of the gastrointestinal tract. Most facultative anaerobic bacteria belong to the families *Lactobacillaceae* (phylum *Firmicutes*) and *Enterobacteriaceae* (*Proteobacteria*) [171]. Small intestinal bacterial communities are less diverse than colon ones as they are subjected to both negative and positive selective environmental pressures applied by the host. `

Examples of negative selective pressures include:

- Oxygen that freely penetrates the stroma of the small intestine restricting the growth of obligate anaerobes in the lumen [166];
- Defensins, Paneth cell-derived antimicrobial peptides secreted in the upper small intestine selectively exclude segmented filamentous bacteria (phylum *Firmicutes*) from the small intestinal microbial community [189];
- Bile acids, secreted through the bile duct in duodenum, are bactericidal to certain species owing to their surfactant properties and are known to broadly shape the composition of the small intestinal microbiota. For example, feeding mice with an excess of bile acids generally stimulates the growth of *Firmicutes* and inhibits the growth of *Bacteroidetes* [190].

Examples of positive selection pressures include:

- the ability of bacteria to adhere to and metabolize host-derived mucins, which are the main driving force in shaping host-bacterial commensalism [191]. Shorter transit time in the small intestine compared with in the colon (despite the greater length of the small intestine, an order of magnitude is shorter) is thought to make bacterial adherence to tissue or mucus an important factor for persistent colonization of the small intestine.
- Higher concentration of simple sugars favors the growth of bacterial communities capable of importing and metabolizing them. Metatranscriptomic analysis revealed that, compared with bacteria isolated from faecal samples, small intestine bacteria show elevated expression of genes involved in central metabolism and in pathways responsible for the import of simple sugars [180].

Negative and positive host-driven selections result in the gradual increase of bacterial densities from 10^1–10^3 bacteria/ml in the duodenum to 10^4–10^7 bacteria/ml in the ileum. Only at the distal end of the small intestine, in the terminal ileum, bacterial densities reach saturating levels similar to those found in the large intestine [9]. Of note, any illness affecting these host control mechanisms may lead to small-intestinal bacterial overgrowth, which can in turn result in malnutrition and weight loss [192].

Colon physiology and bacterial products

The caecum and colon cultivate the densest and diverse communities of all body habitats. Mice, like most herbivorous mammals, have a large caecum between the small and large intestine, where plant fibers are slowly digested by the microbiota [9]. Interestingly, the composition of bacterial communities changes not only along longitudinal axis of the colon, but also depend on its physical location within the tissue a specific gut segment. In particular, it has been shown that bacterial communities present in between traverse folds (interfold region) of the proximal colon differ in their composition and morphological appearance from those present in its central lumen (digesta region) [113]. Another striking example is the distribution of aerobic and anaerobic bacteria within the crypt-lumen axis. While the colonic lumen is occupied by obligate anaerobes, it has been shown that 70% of caecal and proximal colonic crypts are rather populated by aerobic bacteria (*Acinetobacter genus*) at homeostasis. In contrast, small intestinal and distal colonic crypts remain bacteria-free [193].

Examination of the colonic mucus by FISH has shown that its inner layer is sterile, as compared to its densely populated outer layer [147]. In mice, a viscosity gradient of the gel-forming mucus increases from the proximal to the distal colon. Accordingly, there are more mucus-associated bacteria in the proximal than in distal colon [194]. Mucosal biofilm formation in the colon is conserved from mammals to amphibians [195], suggesting an ancient evolutionarily conserved function of the colon as a host-microbial interaction platform.

1. Short-chain-fatty acids (SCFAs) present in high concentrations in the proximal colon are essential for perfusion of mucosal blood vessels. The best human evidence for this was provided by Mortensen et al [165], who utilized resected colonic segments to determine the response of resistance vessels to varying concentrations of SCFAs. Treatment with low concentrations of SCFAs led to dose-dependent vasodilation.

2. Digestion. SCFAs are beneficial for the host as they are a result of microbial carbohydrates digestion and contribute up to 10% of the daily calorie intake [45]. Also, the microbiota supplies the host with several vitamins such as B1, B2, B3, B5, B6, B9, B12[46], and K [48].

3. Butyrate is a primary energy source for colonocytes. It has been shown that colonocytes from germ-free mice are constantly in an energy-deprived state, as NADH/NAD+ and ATP levels are diminished by 16 fold and 56%, respectively in germ-free colons. Such nutrient deprivation induces autophagy, which is a catabolic process where the cell degrades its own cellular components in an attempt to maintain energy homeostasis. When butyrate is added to germ-free colonocytes, it prevents them from undergoing autophagy and further rescues their deficit in mitochondrial respiration [173].

4. Butyrate stimulates sodium absorption and chloride secretion in colonocytes, thus participating in the regulation of electrolyte absorption in the colon [196,197].

5. Microbial vitamin B2 precursor governs the development of mucosa-targeted T-cells (MAIT-cells) and modulate systemic immune response. Vitamin B2 precursor, 5-OP-RU, is produced by bacteria and not by the host cells. It travels to thymus from colonic surfaces, where it controls the ontogeny of MAIT-cells. MAIT cells are absent in germ-free mice, but gradually increase upon bacterial colonization or 5-OP-RU supplementation. Upon microbial colonization MAIT cell frequencies increase first in the thymus, then in the spleen and lungs, suggesting a major role of this commensal`s metabolite in the development of both central and peripheral immune systems [198].

6. SCFAs were also shown to inhibit hyphal transformation of opportunistic fungi *C.albicans*, keeping it in a harmless yeast form [45], suggesting that SCFAs production might also constitute a defense mechanism against fungal invasion.

Fungi

Fungi have been long recognized as members of the “normal gut microbiota” [199], and recent studies revealed that the fungal ‘‘mycobiota’’ is also diverse. In comparison to bacteria, however, fungi correspond to a numerically smaller proportion of the gut microbiome. For this reason, analysis of the role of fungi in interaction with the host and with other members of the community has lagged behind the study of bacteria [200].

While it is true that fungi are vastly outnumbered by bacteria [180], one has to keep in mind that one of the main method to analyze intestinal microbiome was and still is metagenomics

sequencing, which does not allow to estimate biomass differences, and only addresses the numerical abundance of microbiota components. Size and volume differences between bacteria and fungi and the resulting differences in biomass are also excluded from this analysis.

It was estimated that the average bacterium relates to a yeast cell as a human to an elephant [201], thus the intestinal fungal biomass and the following metabolites production have most likely been underestimated. Recent studies identified 66 genera of fungi present in human stool samples of which *Saccharomyces, Candida,* and *Cladosporium* were the most abundant genera [202,203]. Still, how the mycobiome is shaped and how it influences the human host is largely unknown.

Importantly, many of the fungi most commonly detected in stool samples are also present in food or the oral cavity. Therefore, to recognize which gut fungi are likely to have a sustained influence on host physiology, there is a need to separate constant and transient mycobiota members [204]. As one of the approaches 18s rDNA sequencing of mucosa-adherent fungal communities became a promising tool, which allows to enrich the sample for fungi that live in the gut compared to those that just pass through. It showed that distribution of fungi is also gradual along the length of the intestine and is changing together with microbial communities, with higher fungal presence in the distal colon and absence in the small intestine [11,13].

Fungi directly contact the epithelium in the proximal but not distal colon. This suggests, that thick mucus layer of the distal colon prevents physical contact of fungal species with the host. Also, this mucus favors creation of a biofilm, where fungal and bacterial species establish strong ecological connections providing additional stability to the entire ecological consortium.

Fungal Pathogen Associated Molecular Patterns (PAMPs) that activate the inflammatory response are located in both the outer and inner layers of the intact fungal cell wall and include [205]: (1) mannans and glucans recognized by a range of C-type lectins and toll-like receptors (TLRs), which stimulate cytokine production and phagocytosis; (2) O-linked mannans (sensed through the TLR4 receptor); (3) β-mannan recognized by galectin-3; (4) α-linked N-mannans recognized by the mannose receptor (MR), dectin-2, mincle, and DC-SIGN; and (5) chitin taken up by the MR, which induces TLR9- and NOD2-dependent IL-10 production.

On the tissue level, fungi can be sensed through:

- Direct recognition by the epithelium

The epithelium as the first cell type that comes into the contact with the fungi employs several PAMPs-driven mechanisms to timely respond to fungal presence. In the oral cavity, recognition of chitin, mannan and b-glucan by epithelial cells leads to NF-kB and c-Jun activation of the first MAPK wave. Interestingly, while this wave simply informs the host about the presence of fungi, a second MAPK wave is specifically induced by the invasive *C.albicans* hyphae form, results in c-Fos activation and is pro-inflammatory [206]. Such mechanism allows the host to discriminate between the commensal yeast form of *C.albicans* and its invasive hyphae form already at the level of the epithelium.

- Direct recognition by macrophages

Tissue-resident macrophages represent the first line of defense against fungal invasion. When activated by fungi they produce cytokines and chemokines that can attract additional innate immune cells such as neutrophils [207]. Colonic macrophages use Dectin-1, Dectin-2, Mincle, TLR2, and TLR4 to recognize fungi cell-wall components and orchestrate antifungal immunity [12,13,208].

Similarly, to the epithelium, macrophages are able not only to detect the presence of fungi, but also its morphological forms, which in turn differentially affect the macrophage activation status and global physiological outcome. For example, while stimulation of macrophages with the yeast-form of *C.albicans* increases the expression of TLR4, Dectin-1 and stimulates IL-1β secretion, its hyphae-form induces the expression of TLR2, Dectin-2, and the secretion of IL-10. The phagocytic activity and NO production capacity of macrophages are also dependent on the length of the hyphae with longest hyphae inhibiting phagocytosis and NO production to a stronger extent than short ones [209].

- Recognition of fungal toxins

Fungi produce an assortment of immune-modulating compounds and their secondary metabolites, such as aflatoxins, fumonisins, gliotoxin, trichothecenes and others exhibit broad immunosuppressive effects [210]. Fungal metabolites can be sensed by both epithelium and by immune cells and the most studied example is Candidalysin, a toxin and virulence factor of *C.*

albicans, secreted during hyphal invasion [211]. Epithelial recognition of Candidalysin is PAMPs independent, as it directly activates EGFR, causes its phosphorylation. This initiates the early epithelial response [212] and release of alarmins [213]. Exposure of macrophages to Candidalysin induces dose-dependent inflammasome activation and IL-1b release [214], even though signaling pathways are currently unknown.

Host recognition

Fungal Pathogen Associated Molecular Patterns (PAMPs) that activate the inflammatory response are located in both the outer and inner layers of the intact fungal cell wall and include [205]: (1) mannans and glucans that are recognized by a range of C-type lectins and toll-like receptors (TLRs) and stimulate cytokines production and phagocytosis; (2) O-linked mannans (sensed through the TLR4 receptor); (3) β-mannan that is recognized by galectin-3; (4) α-linked N-mannans are recognized by the mannose receptor (MR), dectin-2, mincle, and DC-SIGN; and (5) chitin is taken up by the MR and induces TLR9- and NOD2-dependent IL-10 production.

On the tissue level, fungi can be sensed through:

- direct recognition by the epithelium

Epithelium as the first cell type that comes into the contact with the fungi employ several PAMPs-driven mechanisms to timely respond to fungal presence. In oral cavity and vagina recognition of chitin, mannan and b-glucan by epithelial cells leads to NF-kB and c-Jun activation of the first MAPK phase. Interestingly, while the first MAPK wave simply informs the host about fungal presence, second MAPK phase results in c-Fos activation, and is specifically induced by invasive *C.albicans* hyphae form, correlates with pro-inflammaroty responses and a cell damage in a dose-dependent manner [206]. Such mechanism allows the host to discriminate between commensal yeast form of *C.albicans* and invasive hyphae form already on the level of the epithelium.

- direct recognition by macrophages

Tissue-resident macrophages represent the first line of defense against fungal invasion and in case of the activation lead to the localized production of chemokines that attract additional innate

immune cells [207]. Colonic macrophages use Dectin-1, Dectin-2, Mincle, TLR2, and TLR4 to recognize fungi cell-wall components and orchestrate antifungal immunity [12,13,208].

The same as the epithelium, macrophages are able not only to detect fungal presence, but also its morphological form, which in its turn affect differently the activation status of the macrophages and global physiological outcome. It has been shown that while stimulation of macrophages with yeast-form of *C.albicans* increases expression of TLR4, dectin-1 with following release of IL-1β, hyphal-form stimulates expression of TLR2, dectin-2, and release of IL-10. Interestingly, phagocytosis activity and NO production by macrophages were also dependent on the length of the hyphae: the longest hyphae inhibited phagocytosis and NO production more, than the short ones [209].

- recognition of fungal toxins

Fungi produce an assortment of immune-modulating compounds and their secondary metabolites, such as aflatoxins, fumonisins, gliotoxin, trichothecenes and others exhibit broad immunosuppressive effects [210]. Fungal metabolites can be sensed by both epithelium and by immune cells and the most studied example is Candidalysin, a toxin and virulence factor of *C. albicans,* secreted during hyphal invasion [211]. Interestingly, epithelial recognition of Candidalysin is PAMPs independent, as it directly activates EGFR, causes its phosphorylation. This initiates the early epithelial response [212] and release of alarmins [213]. Exposure of macrophages to Candidalysin induces dose-dependent inflammasome activation and IL-1b release [214], even though signaling pathways are currently unknown.

Colon physiology and fungi

As bacteria, fungi possess multiple traits that are beneficial for host physiology:

1. Contribution to digestion and SCFAs production. Since anaerobe fungi contribute to the digestion of fibrous materials in ruminants and herbivores [215], they may play a similar role in non-ruminant animals [11].

2. Dampen local and systemic inflammatory responses. Treatment of mice with antifungal drugs increase disease severity in several models of experimental colitis and exacerbate development of

allergic airway disease [13,59]. Additionally, in humans a polymorphism in the gene encoding Dectin-1 has been linked to a severe form of ulcerative colitis, which is released by treatment with antifungal drugs. However, whether this results from direct alteration of the fungal communities, or of the production of fungal toxins, or is rather due to secondary effects on bacteria populations - which can expand or shrink in response to antifungal drugs- is unclear. Of note, the immunosuppressive properties of fungal toxins, such as cyclosporine, allows their use in clinic to treat host versus graft disease [216].

3. Maintain bacterial (*Lactobacillus)* populations. Antifungal treatments result in substantial reduction of lactobacillus species [59], which are thought to be protective in the context of both intestinal and allergic airway inflammation [217–219]. However, it is not known whether commensal fungi play a protective or detrimental role for the host under steady-state conditions.

In conclusion, fungi have significant effects on the gut ecosystem, and immune responses despite their numerical inferiority. Treatments that reduce the fungi load often result in perturbation of bacteria communities and stimulate immune responses [59].

Host control over the development of intestinal microbiota

Mammals employ positive selection mechanisms to shape infant microbial communities during breast-feeding. Milk oligosaccharides are complex carbohydrates that cannot be broken down by enzymes in the upper gastrointestinal tract of the infant and thus reach the colon [45]. There they foster the development of a microbiota dominated by species belonging to the *Bifidobacterium* genus (phylum *Actinobacteria*)accounting for up to 70% of the bacteria present in the infant feces [220]. These bacteria carry a gene cluster for a fermentative breakdown of milk carbohydrates. They are facultative anaerobes. They consume the residual oxygen left from the limited lipid oxidation in the developing gut, creating hypoxic conditions over time. Once this nutritional control mediated through milk oligosaccharides is relieved at weaning, the dominance of the genus *Bifidobacterium* gives way to a diverse microbial community, predominantly composed of obligate anaerobic bacteria belonging to the phyla *Firmicutes* and *Bacteroidetes* [221].

On the level of species, the composition of the human gut microbiota strongly shifts with changes in the diet [222], thus supporting the idea that the diet is one of the main drivers in shaping the gut microbiota in adults. Fiber-rich and low-fiber diets cause profound changes in the microbiome, even during daily shifts in nutrient supplementation [157].Low-fiber diet induces a thrive of mucus-degrading bacteria and enhance the susceptibility to colonic infections. Importantly, fibers/fat diet variations (high-fat vs high-fiber) can also foster the development of microbial communities that are stable and affect the host's body composition. For example, transplantation of an "obese microbiome" into germ-free animals causes an increase in body fat as compared to control animals inoculated with a "lean microbiome" [223], indicating that the increased capacity to harvest energy is transferred with the stable microbial ecosystem.

The host and the microbiome thus evolve together and establish an ecosystem with complex symbiotic relationships. The perturbation of this ecosystem affects the host's physiology and leads to dysbiosis, which in turn renders the ecosystem less resilient to pathogens [174].

For example, the metagenomic analysis revealed that colon cancer patients often experience intestinal dysbiosis [224]. Moreover, metagenomics sequencing has detected significant shifts in the abundance of commensal bacteria in colorectal tumors, compared to the adjacent normal tissues, more precisely 2 dominant phylas, *Bacteroidetes* and *Firmicutes* were replaced by *Fusobacterium*. [225,226]. This is probably explained by the loss of proper host selection mechanisms that are often driven by the epithelium. For example production of specific mucins and oxygen gradient, that cannot be achieved by transformed epithelium.

Interestingly, colorectal tumors can bring along gut bacteria, such as *Fusobacterium nucleatum,* during their metastasis to the liver [227]. *Fusobacterium nucleatum* stimulated proliferation of cancer cells and protected the tumor from cytostatic drugs, since reducing the bacterial load by treating the mice with antibiotics increase chemotherapy efficiency and T cell infiltration.

Not only bacteria have been associated with tumor growth. Fungal loads of pancreatic tumors are 3000 times increased compared to the normal pancreas, due to the overgrowth of *Malassezia species*, commensal fungi of the oral cavity in humans and mice. During dysbiosis, they migrate into the pancreatic tissue, which is directly linked to the gut via pancreatic duct and promotes tumorigenesis [228].

Change in microbial metabolites production profile associated with tumorigenesis greatly affect and shape anti-tumor immune response. Metabolites derived from bile acids by intestinal bacteria modulate the recruitment of NKT cells to the cancer in the liver [229], while short-chain fatty acids promote the memory potential of antigen-activated $CD8^+$ T cells [230].

Chapter 5. Intestinal Macrophages

At homeostasis, in intestinal lamina propria macrophages are the most abundant leukocytes type and represent the largest pool of macrophages in the body [72].

Absolute numbers and relative frequencies of macrophages are higher in the colon than in the small intestine. [29,30,123]. Interestingly, mucosal macrophage numbers correlate closely with the relative bacterial load and thus are highest in the caecum and colon, where the number of microbiota is the highest.

Regarding tissue distribution as it was shown for gastric, duodenal, ileal, colonic and fetal intestinal mucosa, the majority of macrophages are localized right under the epithelium [30,231]. Sub-epithelial intestinal macrophages are more intensely stained for MHCII and CD74 [30] than their counterparts that are located deeper in the stroma and also to the macrophages in other tissues, such as splenic red pulp, lung, sinus macrophages in lymph nodes and Kupffer cells in the liver.

Intestinal macrophages form additional line of defense right below the epithelial barrier, and are ideally positioned to capture the invaders or their metabolites.

These macrophages are anegric as they do not respond to the commensal microbiota. They clean apoptotic bodies silently, without inducing the inflammation from host- or host communities-derived signals. At the same time, they remain highly responsive to pathogenic signals.

Mature steady-state gut macrophages have unique physiological properties. They can encounter a huge load of commensal microbiota, food antigens, and apoptotic bodies without undergoing subsequent activation [232,233]. The most studied examples are response of intestinal macrophages' towards microbial antigens and apoptotic bodies.

Mechanisms of such tolerance rely on regulatory circuits that balance cytokines and pattern recognition receptor signaling cascades, and are imprinted by the intestinal stroma during macrophage differentiation [234]. Macrophages also protect the tissue from immune overreaction

in response to apoptotic bodies by secreting DNAse 1L3. DNAse1L3 degrades dsDNA, present in apoptotic bodies, and prevents its recognition by the immune system, as shown for lung alveolar space, pleural and peritoneal cavities [20]. The same macrophage feature was also recently demonstrated in the gut. Engulfing of apoptotic bodies derived from intestinal epithelial cells in Villin-hDTR model induced expression of negative regulators of the immune response in macrophages, and shifted their metabolism towards lipids and amino acid catabolism as shown for the small intestine [19]. Interestingly, when macrophages are removed from the tissue of residence they can no longer avoid immune recognition of dsDNA from apoptotic bodies. This increase of macrophage responsiveness after extraction from the tissue is called "deprogramming", suggesting that constant uptake of apoptotic bodies, influenced by the tissue-specific factors, imprint silent uptake of apoptotic bodies program that is fully reversible [235]. In sharp contrast macrophages' anergy towards microbiota-derived antigens has been shown to be stable over time, since the removal of macrophages from the intestine and their culture up to 45 days did not increase their response towards an array of stimuli, including *H. pylori* urease, heat-killed (HK) *Staphylococcus aureus*, IFN-γ, and PMA, measured by the release of IL-1, IL-6, or TNF-α, and IL-8, whereas similarly treated monocytes produced large amounts [236].

How such programming is shaped during macrophage differentiation in intestinal tissue remains an open question.

Origin, development and differentiation of intestinal macrophages

Development

In developing intestine macrophages express pro-inflammatory cytokines, as shown for the human fetus and pre-mature neonates [237]. But during intestinal development TGF-b2 suppresses macrophage activation by guiding their differentiation towards the acquisition of anergic phenotype, and macrophages in full-term neonates are already characterized by anti-inflammatory nature. Accordingly, impaired tissue expression of TGF-b2 or decreased TGF-b2 bioactivity is associated with the development of necrotizing enterocolitis (NEC) – an intestinal inflammatory condition, which typically occurs in 7% of pre-term newborns, and leads to the complete necrosis of the portion of the bowel [238,239]. In line with these results, internally administered

recombinant TGF-b2 suppresses macrophage inflammatory responses and protects against NEC in experimental models [237].

Origin in adults

In terms of macrophage`s origin, adult tissues can be classified as: (1) closed, without homeostatic monocyte recruitment (brain, epidermis, lung, and liver). Macrophages in such tissues are directly derived from embryonic precursors and are self-maintained throughout the live; (2) open, with fast steady-state monocyte recruitment, such as gut (where 80% of macrophages are of monocytic origin) and dermis (where 70% of macrophages are of monocytic origin) [240]. Of note, trascriptomic analysis has recently showed that the closest macrophage population to the intestinal macrophages are the once, which resides in dermis; (3) open, with slow homeostatic recruitment, such as heart and pancreas [240].

This was shown by using Ms4a3: Cre/Rosa^{TdT} model, where monocytes and their progeny are irreversibly labeled with tdTomato, as no postnatal changes in tdTomato labeling in brain microglia, epidermal LCs, or liver KCs during steady-state development was observed. In contrast, tdTomato labeling in macrophages slowly increased with age in the lung, spleen, peritoneal cavity, and kidney. Eight weeks after birth, a rapid increase in tdTomato labeling of macrophages was observed in the small intestine and colon, with a faster rate in the colon than in the small intestine. [240], suggesting a dominant pathway in mucosal macrophage maintenance to be a constant recruitment of monocytes into the intestinal wall and their further differentiation.

Circulating monocytes in the blood have a limited half-live, by BrdU assay it was determined to be 20h [241]. On demand, Ly6C+ monocytes are rapidly recruited to sites of need: for homeostatic replenishment of resident macrophages/dendritic cell pools or to the cites of injury and inflammatory challenge [234]. In both situations CCR2-CCL2 axis is the main driver of tissue monocytes recruitment, as in Ccr2$^{-/-}$ mice number of macrophages in the gut is significantly reduced, while adoptive transfer of monocytes rescues this phenotype [242–244].

In addition to the chemokine axis CCR2-CCL2, monocyte recruitment can be induced by the exposure to commensal bacteria and to antigens ingested with the diet [14]. A number of studies underlined the key role of microbiota in shaping macrophage populations in the mucosa: it has

been demonstrated that microbial colonization, particularly during weaning, induces changes in colonic macrophage compartment, while administration of broad spectrum antibiotics negatively affects macrophage turnover. Accordingly, a reduced macrophage number can be found in the gut of germ-free mice [243].

Monocytes differentiation into intestinal macrophages takes 5-6 days, and is characterized by a process known as "monocyte waterfall" [241,243]. Briefly, Ly6C^{hi} MHCII^{-} (P1) monocytes enter the intestinal tissue and, progressively, acquire the expression of MHCII and becoming Ly6C^{hi} MHCII^{high} (P2). As the third step, they downregulate Ly6C (P3), together with other proteins responsible for monocyte extravasation (including CCR2, CD62L, LFA-1 and VLA-1), and, finally, upregulate the expression of CX3CR1, giving rise to mature macrophages (P4) [245].

Identity of macrophages is further shaped by the local microenvironment, which imprints enhancer landscapes specific for each particular tissue [246], particularly through TGF-b in the colon [247] and Notch-signaling in the small intestine [248]. The importance of Notch1 and Notch2 in macrophage differentiation in the small intestine requires further investigations, since the studied population was defined as CD11c^{+}CX3CR1^{+} cells, a population that can also include dendritic cells.

Although embryonic macrophages seeded in the gut are rapidly replaced in a microbiota-dependent manner by Ly6C^{hi} monocytes in the gut mucosa, it has been recently shown, that macrophages in different parts of intestinal wall, namely in sub-mucosa and muscle layers, of the small intestine are an exception. They represent a self-maintained pool which has no input from circulating monocytes [249]. Thus, intestinal self-maintained macrophages can be further separated into the following categories based on their submucosal localization: within enteric-nervous system (neuronal-associated self-maintaining gMacs); within vasculature (blood vessel-associated self-maintaining gMacs), within Peyer`s patches (gut-associated lymphoid tissue-associated self-maintaining gMacs), and near Paneth cells (Paneth cell-associated self-maintaining gMacs).

Maintenance of adult intestinal macrophages

Several regulatory circuits are involved into the differentiation, survival and anergy of intestinal macrophages and include:

1. CSF1 is involved in the differentiation and survival of intestinal macrophages. Genetic deletion of Csf1 gene, as well as the administration of anti-CSFR1 antibody, result in a reduced number of intestinal macrophages in most organs, including the gut [17,18]. To the opposite, treatment of mice recombinant CSF1-Fc conjugate, induces extensive macrophage infiltration into tissues [250].

2. The IL-10/IL-10-receptor (IL-10R) axis is important for establishment and maintenance of macrophages' anergy. Disruption of this axis results in higher macrophage expression of pro-inflammatory mediators, as well as macrophage hyper-responsiveness to TLR engagement, leading to the occurrence of intestinal inflammation [25]. Accordingly, polymorphism in IL10RA and IL10RB genes is associated with the early onset of inflammatory bowel diseases (IBDs) in humans [243].

3. The CX3CL1-CX3CR1 axis is crucial for colonic macrophage differentiation, as indicated by their high expression of CX3CR1 and their localization close to the CX3CL1-positive intestinal epithelial cells [251]. Absence of CX3CR1 expression by colonic macrophages results in failure in stimulating Treg cell expansion: accordingly, lack of CX3CL1-CX3CR1 signaling leads to a more sever dextran sulfate sodium (DSS)-induced colitis [252]. In line with this observation, although in humans CX3CR1 expression by intestinal macrophages is reduced compared to mice, a missense mutation in the CX3CR1 gene has been identified in patients with Crohn's disease, in association with an impaired antifungal response [12].

4. The TGFβ/TGFβ-receptor axis is fundamental for the terminal differentiation of mucosal intestinal macrophages, modulating the expression of genes associated with their homeostatic profile (CX3CR1, IL-10, and αvβ5 integrin) and turnover (CCL8) [253].

5. Microbiota-derived SCFAs and aryl hydrocarbon receptor (AhR) ligands, originating from cruciferous vegetable indole derivatives stimulate the acquisition of anergic phenotype in macropahges [243]. Specifically, treatment of macrophages with butyrate leads to the downregulation of LPS-induced pro-inflammatory mediators, including NO, IL-6, and IL-12 [254], and induces metabolic and transcriptional changes [28]. Interestingly, it has been demonstrated that microbiota also indirectly affects gut macrophages via the interaction with RORγt+ Innate Lymphoid Cells (ILC) 3: microbiota stimulates macrophages to produce IL-1β which, in turn, induces

the release of CSF2 by ILC3, leading to the secretion of IL-10 by macrophages and, finally, the regulation of gut homeostasis via Treg cell expansion [255].

In terms of the **lifespan**, intestinal monocyte-derived macrophages fall into 2 categories: (1) short-lived (2-3 weeks), and (2) long-lived cells (up to 8 months) with self-renewing capacity. The second population might also include remnants of embryonic populations [234,256,257]. The lifespan of embryonically-derived self-renewing macrophage populations is not yet established.

Differences of monocytes differentiation the small and large intestine

Adoptive monocytes transfers into macrophage-depleted recipients allowed monocytes` synchronization in terms of development, and further transcriptomic comparison of monocytes/macrophages differentiating in the small intestine (ileum) and colon [234].

Firstly, engrafted colonic and ileal macrophages segregated in gene expression according to tissue. Secondly, the majority of changes in gene expression, both in fold change and numbers, occurred in the transition from monocytes to either colonic or ileal macrophages at day 4 post transfer, which is immediately after extravasation, suggesting the major impact of the local cues into tissue-resident macrophages differentiation. Thirdly, several samples of engrafted ileal macrophages from this study clustered with the colonic samples rather than the ileal ones, suggesting that the colonic signature is default [234].

458 genes were up-regulated during monocyte differentiation in a segment-specific manner: 351 in colonic macrophages and 107 in ileal macrophages. Monocyte differentiation into ileal macrophages was accompanied by induction of Gata and Hbox TF family members, such as Gata5 and Hbox3, as well as genes encoding the chemokine Ccl5 and the chemokine receptor CCR9. Monocytes that entered colon preferentially up-regulated Foxd2, the nuclear receptor Nr3c2, and the dominant negative helix-loop-helix protein Id2. Of the genes, which were specifically down-regulated in only one intestinal segment, 78 genes followed this trend in colonic and 99 in ileal macrophages. The latter down-regulated genes included 7 TFs, such as Foxp1 and Trim16, while Arid5a and Elk3 were specifically down-regulated in the colon [234].

Many genes related to immune reaction and response to challenge displayed higher expression in ileal macrophages than their colonic counterparts. For example Arid5a, whose gene product

regulates IL6; Elk3, which encodes a member of the ETS TF family and was reported to modulate the phagocytosis of bacteria by macrophages, and Ano6, that is down-regulated in colonic macrophages, and reportedly supports microbiocidal activity of macrophages involving P2X7 receptor signaling (Ousingsawat et al., 2015) [234]. These findings suggest that overall anergic phenotype of intestinal macrophages is even more pronounced in the colon.

In agreement with this results, it has been recently reported that mice lacking IL10Ra develop severe gut inflammation in the colon, but not the ileum [25,258], as do children that harbor an IL10RA deficiency [259].

Physiological roles of macrophages in the small intestine

Macrophages perform multiple physiologic functions in the small intestine, ranging from classical onces, like scavenging and dead-cells removal, to the site-specific, like establishment of the food tolerance, maintenance of epithelial stem cells and neurons.

1. Maintenance of $Lgr5^+$ stem cells pool by regulation of Paneth cells development. $Csf1r^{-/-}$ mice lack Paneth cells, and show a reduction in Lgr5 expression and cell proliferation within small intestinal crypt [260,261]. Immunostaining with Csf1r antiserum suggested that Paneth cells express Csf1r-/-, implying that CSF1 directly regulates their development.

Further studies did not confirm Csf1r presence on Paneth cells. The absence of detectable fluorescence in Paneth cells of "MacGreen" Csf1r-EGFP mice; negligible expression of Csf1r mRNA in Paneth cells by RT PCR; the absence of Csf1r mRNA in sequencing of Paneth cells; lack of the signal in Csf1r mRNA *in situ* hybridization and finally no Paneth-cell or other epithelial phenotype in conditional epithelial-restricted Csf1r-knockout using Villin-Cre mice have questioned the direct link between CSF1 and Paneth cells and proved no direct effect of CSF1 signaling in the Paneth and $Lgr5^+$ cells differentiation [250]. Therefore, the effect of CSF1R blockade on the maintenance of intestinal epithelial homeostasis was proven to be indirect. It was shown that CSF1R mRNA expression was restricted to macrophages which are intimately associated with the crypt epithelium [250]. The depletion of these macrophages following prolonged CSF1R blockade disturbed intestinal crypt homeostasis, affecting the differentiation of Paneth cells, $Lgr5^+$ intestinal

stem cell with the subsequent shift in differentiation of epithelial cell lineages, changing the balance between M- and goblet cells towards the latest.

2. Maintenance of the vasculature. Recently, a role for tissue-resident self-renewed CX3CR1^{+} macrophages has been also unraveled in the maintenance of the intestinal vasculature: targeted depletion of this macrophage population results in morphological abnormalities, disruption, reduced abundance of mucosal and submucosal blood vessels [249].

3. Silent disposal of microbial and enterocytes' material. As throughout the entire gut, small intestinal macrophages are avidly phagocytic and bactericidal, but ingestion of microbiota components is not associated with the release of pro-inflammatory mediators [262]. The ability to ingest and dispose of material in a non-inflammatory way manner also extends to removal of senescent enterocytes and leucocytes, thus ensuring homeostasis in a tissue with rapid turnover of all its components [232].

4. Establishment of food tolerance. CX3CR1^{+} macrophages were found to take up soluble fed antigens and quickly transfer them to CD103^{+} dendritic cells in the small intestine. Antigen transfer occurs via a mechanism that is Connexin 43-dependent and required membrane transfer, indicating a physiological role of gap junctions and division of labor between intestinal phagocytes in antigen presentation [27]. When this transfer was inhibited by genetic deletion of Cx43 in antigen-presenting cells, T regulatory cell differentiation and oral tolerance failed to be established. Additionally, small intestinal macrophages additionally maintained local Treg cell pools by producing retinoic acid in response to CSF2 stimulation [255].

5. Control of intestinal motility through support of enteric neurons. Mice with depleted self-maintained macrophages (gMacs) pool showed a significantly reduced small intestinal transit time and a prolonged total transit compared to controls. This phenotype was a result of the loss of macropahges' support of enteric neurons, that regulate intestinal motility. In the absence of gMacs great amount of enteric neurons underwent apoptosis in submucosa and in myenteric plexus. Consistent with the observed decreased intestinal function, these mice exhibited a reduction in body weight compared to control animals [249].

Physiological roles of macrophages in the colon

Macrophages possess multiple physiological functions, specific to the colon, that include: mounting of efficient anti-fungal response, regulation of epithelial healing during ulcerative colitis and are characterized by even more anergic phenotype that their small intestinal counterparts, probably reflecting higher microbial loads in the local microenvironment.

1. Anti-fungal immune response. CX3CR1^{+} MNPs recognize (through dectin-1 and dectin-2) and respond by the induction of Th17 immune response to the colonic fungal infection. Th17 cells are crucial for the control of fungi at other gastro-intestinal sites such as the oral cavity [263]. Upon colonization with *Candida albicans* a strong Th17 response was also observed in the colon. Depletion of CX3CR1^{+} MNPs resulted in the loss of efficiency of such response in the colon, mesenteric lymph nodes, but not in the small intestine. Interestingly, depletion of CD11b^{+}CD103^{+} and CD11b^{-} CD103^{+}dendritic cells had no inhibitory effect. This processes wash shown to be orchestrated by spleen tyrosine kinase (Syk) signaling and important to control the fungal loads during experimental colitis. Conversely, in humans, CX3CR1 polymorphism is strongly associated with a decrease of anti-fungal antibody responses in Crohn`s disease patients [264].

2. Involvement into gut-lung axis. CX3CR1^{+} MNPs that are involved in the uptake of intestinal fungi were essential for mediating the effect of gut fungal dysbiosis on peripheral immunity on other body sites, such as lungs. Depletion of CX3CR1^{+} gut-resident MNPs (or selective inhibition of Syk) signaling within these intestinal phagocytes ameliorated the symptoms of HDM-induced lung allergy. These results suggest that perturbation of healthy intestinal fungal communities can lead to the expansion of specific fungi that can affect systemic immunity through an interaction with CX3CR1^{+} MNPs in the gut [208].

3. Silent disposal of microbial and enterocytes' material. As discussed above, local microenvironment of the colon and microbiome composition [31], drive the monocyte differentiation towards colon-specific macrophages, with the unique transcriptional profile [31,245], where both steady-state and inflammatory macrophages arise from the same monocytic precursors. While homeostatic macrophages are resistant to TLR stimulation, TLR-responsive macrophages locally differentiate and accumulate in the tissue during experimental colitis [242].

Interestingly, both pro- and anti-inflammatory colon macrophages express a wide array of TLRs. Thus, it seems that colonic macrophage TLR blockade happens in the downstream signaling. This may reflect a number of different mechanisms, including the absence of key adaptor signaling molecules such as MyD88, IRAK and TRAF6, or the presence of inhibitory molecules such as IRAK-M [18]. Overall, this results in the failure to translocate NF-kB to the nucleus and/or inability of NF-kB to bind and activate gene transcription once there [265]. Additionally, colonic macrophages down-regulate co-stimulatory molecules responsible for respiratory burst and NO production [266–269].

Multi-level blockade of inflammatory responses in homeostatic colonic macrophages gives them ability to engulf microbial products and apoptotic bodies in a silent manner, avoiding the induction of the immune response towards commensals or self-antigens.

Interestingly, while macrophages in the colon manage to stay anergic while encountering huge microbial load and a cell-death derived antigens, they are highly sensitive towards dietary fat. High-fat diet (HFD) induced profound inflammatory response in homeostatic macrophages, which results in the increase of epithelial permeability (by decrease of Claudin-1 expression in epithelial cells), metabolic endotoxemia and macrophage infiltration into the adipose tissue [270].

While at homeostasis colon macrophages do not respond to LPS-stimulation by TNFa secretion, macrophages from mice fed with HFD expressed high TNFa levels even at the absence of LPS. The concentration of other pro-inflammatory cytokines, such as IL1b, Ccl1, and Ccl2, was also elevated. Accordingly, these mice had a significantly shorter colon, which is one of the hallmarks of colitis, compared to mice fed a normal chow diet. Interestingly, colon macrophages in HFD-fed mice also expressed H_2O_2 indicating oxidative stress after a month on HFD, while H_2O_2 production in epididymal fat increased only after 12 weeks. These data suggest that pro-inflammatory changes in colonic macrophages induced by HFD precedent a response of the adipose tissue [271]. Consistent with these findings, metabolic endotoxemia (measured by the level of LPS in the portal vein) and impair of intestinal barrier function (measured by the Claudin-1 expression) was rescued in macrophage-specific Ccr2 knockout and epithelial cell-specific tamoxifen-inducible Ccl2 knockout, proving the direct role of macrophages' recruitment through CCR2-CCL2 axis in this process.

4. Maintenance of Treg pool. Reduction of macrophage numbers with the following decrease of IL-10 production disrupts Treg homeostasis [255]. Disturbance of this axis resulted in low Treg numbers, especially in the colon with a subsequent development of IBD.

5. Regulation of epithelial proliferation in response to injury. When recruited to a site of injury and activated by the microbiota, colon inflammatory macrophages support and promote proliferation of epithelial precursors, accumulating closer to the crypt base [21]. This resulted in crypts elongation, and passive moving of the stem-cell zone deeper into the stroma in regions near ulcers. Accumulation of epithelial precursors has caused a shift in epithelial homeostasis, where goblet-cell differentiating pathway was dominating. Depletion of microbiota or macrophages did not affect the crypts` length compared to non-treated controls, with the shortest crypts observed in a macrophage-depleted, microbiota-depleted condition. Thus colon macrophages shape the crypt progenitor cell niche in a way that allow colonic epithelium to minimize stem-cell injury and mount an appropriate regenerative response.

To summarize, intestinal macrophages have evolved to live on the interface between the host immune system, injected products, and microbiome. They recognize pathogens, commensals and food antigens to guide and direct host immune responses towards maintaining an ecological equilibrium in the microbiota, symbiotic relationships with its members, and a tissue

Chapter 6. Summary

The intestinal tract provides a unique environment as it is continuously exposed to food antigens as well as to the commensal microbiota. To allow an efficient absorption of nutrients and electrolytes intestinal barrier is relatively thin, which creates additional challenges for the host, as toxic luminal substances may also reach the blood circulation [1]. Accordingly, disruption of the intestinal barrier leads to multiple pathological situations ranging from nutrient deprivation [2] and inflammatory bowel diseases [3,4] to sepsis [5] and multi-organ failure [1,6,7].

Among the different regions of the intestine, the epithelial barrier of the distal colon faces particular challenges. On the one hand, the distal colon epithelium is exposed to the extreme osmotic pressure of 10 atm needed to absorb water and solidify feces [8]. On the other hand, microbiota, including bacteria, fungi, archaea, and viruses, reaches its maximum in this region of the gut [9–12]. In

particular, fungi are more abundant in the distal colon [13] and can produce metabolites that trigger apoptosis of intestinal epithelial cells [14]. Accordingly, intestinal barrier is the main target for many fungal toxins, such as gliotoxin [14], aflatoxin [15], thrichothecenes [16] and candidalysin [17].

Thus, the colonic mucosa must therefore tightly regulate fluid absorption to avoid potential entry of toxic fungal metabolites into epithelial cells and further into the blood circulation. The mechanisms underlying such regulation remain unknown.

In homeostatic conditions, one of the most abundant type of intestinal immune cells are macrophages, which mainly differentiate from monocytes in response to local cues. Intestinal macrophages reside either within the lamina propria or the muscle layer, where they participate in a variety of biological processes, including the degradation of microorganisms [18], silent clearance of apoptotic bodies [19,20], tissue repair [21], and gastro-intestinal motility [22]. Intestinal macrophages also limit inflammation [23–25], facilitate the survival of local $FOXP3^+$ T regulatory cells and tolerance to food [26,27]. The function of macrophages is tightly regulated by the microbiota [28] and, accordingly, they are more abundant in the colon than in the small intestine [29,30].

Interestingly, in the colon, macrophages can be found in close association with epithelial cells [30,31]. Disruption of macrophages' sub-epithelial localization participates in the loss of intestinal barrier integrity observed in inflammatory bowel diseases such as ulcerative colitis and Crohn's disease [32]. Macrophages are, therefore, ideally positioned to orchestrate epithelial cell-microbiota interactions for maintenance of colon homeostasis.

The main question of my thesis was to **identify the role of colonic macrophages in integrity and function of intestinal epithelial barrier in homeostasis**.

Below, I highlight the milestone findings that let us address this question.

1. Macrophages control epithelial cell survival and barrier integrity in the distal colon

To address the role of macrophages in colonic barrier, I analyzed the integrity of the intestinal epithelial barrier in macrophage-depleted animals. Independently, in two different mouse models of macrophage depletion, I observed massive apoptosis of colonic epithelium upon macrophage depletion.

Strikingly and surprisingly, epithelial death occurred only in the distal, but not proximal colon, while the efficiency of macrophage depletion was the same in these two segments. Epithelial death was followed by an increase of the dye absorption infused into the colonic lumen, indicating a failure of the intestinal barrier.

2. Distal colon macrophages insert “balloon-like” protrusions (BLPs) in between epithelial cells and have a distinct transcriptomic profile

I observed that sub-epithelial macrophages of the distal colon are morphologically different from their proximal counterparts. They form peculiar protrusions, shaped as balloons (“balloon-like” protrusions, or BLPs), that penetrate the basement membrane and physically interact with the epithelium. Then we performed Single Cell RNA sequencing of the macrophages isolated from proximal and distal colon, and found that BLP^{+} macrophages display a distinct transcriptomic profile, enriched for the microbiota-sensing genes.

3. Fungal metabolites absorbed together with the fluids stimulate BLPs formation in the distal colon

Sequencing results led us to hypothesize that macrophages form BLPs to sense the microbiome members. To test this, I treated animals with antibiotics or antimycotics, and observed that BLPs formed in response to the local fungi, but not bacteria. The opposite was true as well: macrophages in the germ-free mice formed an increased number of BLPs after fungal recolonization, while bacterial reconstitution had no effect. But how do macrophages sense the fungi present in the colonic lumen through the thick and sterile mucus layer using protrusions that do not penetrate the epithelium? Indeed, we found that distal colon macrophages do not upregulate any of the “classical” fungi-sensing receptors, such as dectin-1 and dectin-2. In line with this, the knock-out of dectin-1 did not affect the number of BLPs. Because the main physiological role of the distal colon is to absorb water from an environment that is highly populated by microbes and particularly fungi, it is possible that BLPs sample absorbed fluids and respond to the presence of fungi-derived metabolites.

I have collected several pieces of evidence to support this hypothesis: (1) BLPs increase in numbers after stimulation of water absorption, and this response is lower, if mice were pre-treated with

antimycotics; (2) BLPs directly sample the absorbed fluids, as shown by low molecular water-tracer; (3) BLPs are greatly increased in numbers in response to fungal toxins, such as gliotoxin, candidalysin and T-2 toxin. Based on this evidence we have concluded that distal colonic macrophages form BLPs in response to fungal toxins, present in absorbed fluids.

4. Macrophages protect epithelial cells from being poisoned by fungal toxins

Toxin-infusion experiments showed that in homeostasis epithelial cells of the distal colon can stop the absorption of fungi-toxin reach fluids. Interestingly, this phenomenon was not observed in macrophage-depleted mice, where uncontrolled absorption of fungal products led to the death of the intestinal epithelium. These results suggested a major role of macrophages in controlling the epithelial absorption, but the role of BLPs remained to be investigated.

Interestingly, we have observed that CD74 is critical for the BLPs-mediated fluid sampling, as in $CD74^{KO}$ animals BLPs did not uptake the fluid as efficiently as in $CD74^{WT}$ littermates, giving us a mouse model where BLPs were “deficient” in their ability to sample. Strikingly, colonic epithelium in $CD74^{KO}$ animals could not distinguish between pure or toxin-containing infused fluids, and underwent apoptosis soon after the infusion. These findings strongly suggested that BLPs orchestrate fluid sampling by distal colonic macrophages, which is critical to protect epithelial cells from absorbing fluids enriched in fungi toxins/metabolites.

To summarize, here, I describe a mechanism by which the innate immune system allows rapid quality-check of absorbed fluids to avoid intoxication of colonocytes. This mechanism relies on a population of distal colon macrophages that are equipped with "balloon-like" protrusions (BLPs) inserted in the epithelium, which sample absorbed fluids. In the absence of macrophages or BLPs, epithelial cells keep absorbing fluids containing fungal products, leading to their death and subsequent loss of epithelial barrier integrity.

These results reveal an unexpected and essential role of macrophages in the maintenance of colon-microbiota interactions in homeostasis.

Results

Macrophages control epithelial cell survival and barrier integrity in the distal colon

The gut immune system is highly compartmentalized, with different cell types distributed in gradients along the intestine [72]. This particularly concerns macrophages (Mϕ), which are present in greater amounts in the colon as compared to the small intestine. Colonic Mϕ display an anergic phenotype [242,262] and their loss correlates with the development of ulcerative colitis and Crohn's disease [272], suggesting a contribution to the maintenance of epithelium integrity. However, the mechanism(s) by which Mϕ achieve such a homeostatic function *in vivo* remains unknown. To address this question, we depleted Mϕ using the $CD64^{DTR}$ mouse model [273] and evaluated the state of the epithelium (Fig. 5A). We analyzed both proximal and distal colons as they are known to exhibit many differences both in terms of physiology [274–276] and microbiota composition [10,12]. The efficient depletion of colonic Mϕ was verified by flow-cytometry and immunostaining in both colon segments (Fig. 6A). Unexpectedly, we found that Mϕ depletion led to massive apoptosis of epithelial cells in the distal but not the proximal colon (Fig. 5B, C). Death of epithelial cells in the distal colon was also observed when Mϕ were depleted by injecting anti-CSF1 receptor antibodies in C57BL/6J mice (Fig. 6B, C). Of note, if the presence of apoptotic cells merely resulted from the lack of scavenging by Mϕ, equal numbers of dead cells should be detected in distal and proximal colons (Fig. 5C). Our results, therefore, suggests that Mϕ facilitate the survival of epithelial cells in the distal colon specifically.

To evaluate the impact of epithelial cell death on epithelium permeability, we infused $CD64^{WT}$ and $CD64^{DTR}$ mice intra-rectally with a hypotonic solution containing the small fluorescent molecule hydrazide and measured its appearance in the blood. We found that hydrazide was more abundant in the blood of Mϕ-depleted mice compared to control animals (Fig. 5D), indicative of a loss in barrier integrity in these animals. Altogether, these results show that Mϕ are needed for epithelial cell survival and intestinal barrier integrity in the distal colon.

Figure 5. Macrophages are required for epithelial cell survival in the distal colon and form "balloon-like" protrusions inserted in between epithelial cells.

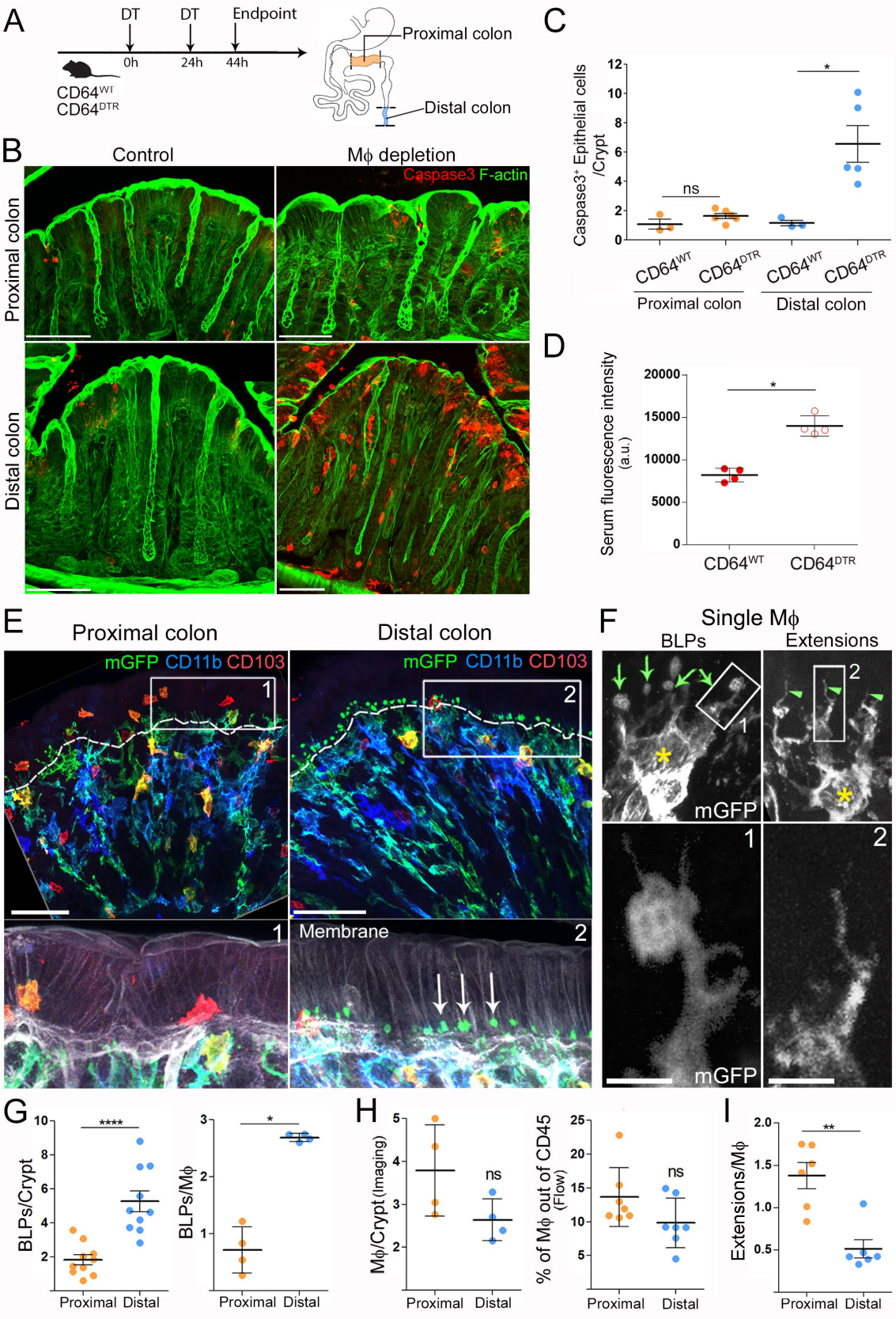


Figure 5. Macrophages are required for epithelial cell survival in the distal colon and form "balloon-like" protrusions inserted in between epithelial cells. (A) Scheme of Mϕ depletion using the $CD64^{DTR}$ mouse model. $CD64^{WT}$ or $CD64^{DTR}$ littermates received two injections of diphtheria toxin (DT) 24h apart. 44h after the first injection proximal and distal colon were processed for IHC. **(B)** Maximum z-projection (30 µm) of proximal and distal colon transversal sections 44h after the first DT injection. The global architecture of the tissue was visualized with F-actin staining (green) and apoptotic cells were revealed with cleaved caspase 3 staining (red), scale bar – 50 µm. **(C)** Number of apoptotic epithelial cells per crypt in the distal or proximal colon of $CD64^{WT}$ or $CD64^{DTR}$ mice. Pooled data from 3 independent experiments, dots represent average number per individual mouse. Results are presented as mean ± SEM, multiple comparison Kruskal-Wallis test, *P<0.05. **(D)** Serum fluorescence intensities of $CD64^{WT}$ or $CD64^{DTR}$ littermates 5-10 min after intra-rectal administration of hypotonic solution of Hydrazide-AlexaFluor633. All mice were injected with DT. Pooled data from 2 independent experiments, dots represent average number per individual mouse. Results are presented as mean ± SEM, Mann-Whitney test, *P <0.05. **(E)** Morphological differences of Mϕ in the proximal and distal colon. Whole-mount staining of the distal and proximal colon of CD11c: $Cre/R26^{mTmG}$ mice. Green – membrane GFP, blue – CD11b staining, red – CD103 staining, gray – membrane tdTomato. BLPs are indicated with arrows, the border between epithelium and the stroma is indicated with the dashed line. Z-projections of 20-40 µm, scale bars – 50 µm. **(F)** Single Mϕ forming BLPs (left) or thin extensions (right). Cell bodies are indicated with the yellow star, BLPs with green arrows, extensions with green arrowheads. Maximum z-projection of 10-15 µm, scale bar - 2 µm. **(G)** Number of BLPs, normalized per crypt (left) or per Mϕ (right) in the distal and proximal colon. Dots represent average number per individual mouse, left – pooled data from 7 independent experiments, right – pooled data from another set of 2 independent experiments. **(H)** Amount of Mϕ in the proximal and distal colon, analyzed by imaging (presented as amount of $F4/80^{+}MHCII^{+}CD103^{-}$ cells per crypt, each dot represents average number per individual mouse, data pooled from 3 independent experiments) and by flow cytometry (presented as percentage of $CD45^{+}$ cells, dots represent individual mouse, data pooled from 4 independent experiments). **(I)** Number of extensions, normalized per Mϕ in the distal and proximal colon. Dots represent average number per individual mouse, pooled data from 4 independent experiments. **(G-I)** Results are presented as mean ± SEM, Mann-Whitney test, *P <0.05, **P <0.01, **** P<0.0001.

Figure 6.

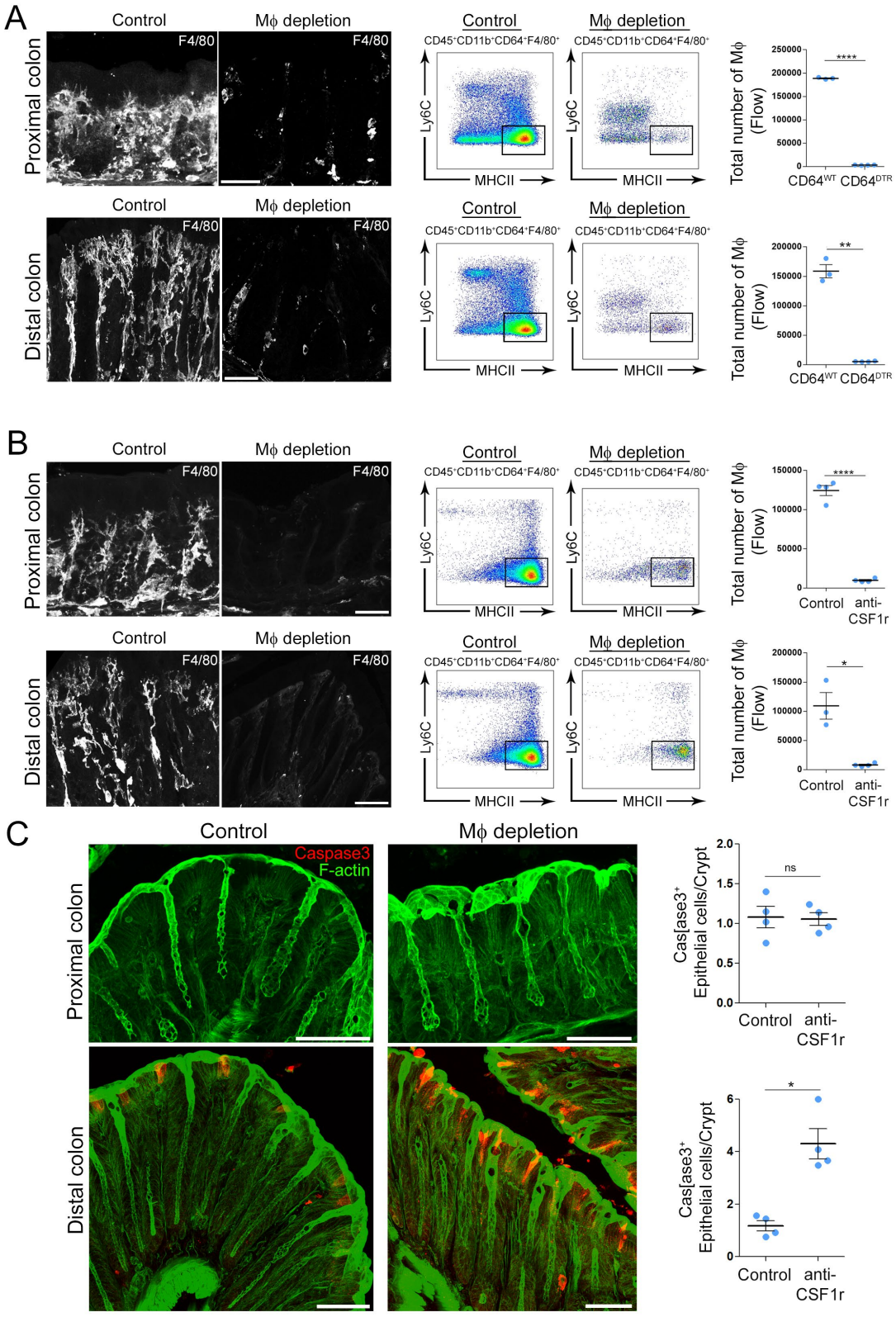

A
Control
Mϕ depletion
F4/80
Proximal colon
Distal colon
CD45+CD11b+CD64+F4/80+
Ly6C
MHCII
Total number of Mϕ (Flow)
****
**
CD64WT CD64DTR
B
Control anti-CSF1r
*
C
Caspase3
F-actin
Cas[ase3+ Epithelial cells/Crypt
ns

Figure 6. (A) Mϕ depletion efficiency using CD64DTR model analyzed by imaging and flow cytometry in the proximal and the distal colon. **(B)** Mϕ depletion efficiency using anti-CSF1R antibody – mediated model analyzed by imaging and flow cytometry in the proximal and the distal colon. **(C)** Number of apoptotic epithelial cells per crypt in the distal or proximal colon of control or anti-CSF1R antibody-injected mice. Maximum z-projections of ~30 µm, scale bar - 50 µm. Data pooled from 2 independent experiments, dots represent average number per individual mouse. Results are presented as mean ± SEM, Mann- Whitney test, *P<0.05, **P<0.01, ****P<0.0001.

Distal colon macrophages insert "balloon-like" protrusions in between epithelial cells

These results prompted us to investigate tissue distribution of Mϕ and/or their physical interaction with epithelial cells in the proximal and distal colon. To address this question, we performed whole-mount immunostaining of proximal and distal colon sections isolated from CD11c-Cre/R26^{mTmG} mice [277,278]. In this mouse model, all cells that express CD11c throughout their differentiation, which include intestinal Mϕ (and dendritic cells), switch from membrane-tomato to membrane-GFP expression, allowing better visualization of these phagocytes in the tissue.

Using these animals, we observed a phagocyte population in the distal colon that physically interacted with epithelial cells through membrane protrusions shaped as balloons (Fig. 5E, F), which we will refer to as "balloon-like" protrusions (BLPs) hereafter. The cell bodies of these cells were localized around the opening of the crypts. On average, each cell displayed three BLPs that crossed the basement membrane and contacted the base of epithelial cells. Of note, BLPs do not correspond to the "trans-epithelial dendrites" previously described in the small intestine [279,280] as they do not reach the lumen of the colon. Immunostaining showed that BLP$^+$ cells resembled bona-fide intestinal Mϕ (CD11b$^+$ MHCII$^+$ F4/80$^+$ CX3CR1$^+$ CD64$^+$ CD103$^-$ CX3CR1-GFP$^+$; Fig. 7) and accordingly, they were lost in toxin-injected CD64^{DTR} mice (Fig. 6A) [281]. Strikingly, reduced numbers of BLPs were observed in the proximal colon (Fig. 5E, G), even though proximal crypts contained a similar number of Mϕ as their distal counterpart (determined by flow cytometry and by imaging, Fig. 5H). Of note, observation of proximal colon Mϕ at higher resolution showed that they also displayed protrusions, which, however, were rather thin and did not end in a balloon-like structure (Fig. 5F, I). We conclude that the distal colon is enriched with Mϕ equipped with peculiar balloon-like membrane protrusions inserted at the base of epithelial cells.

Figure 7.

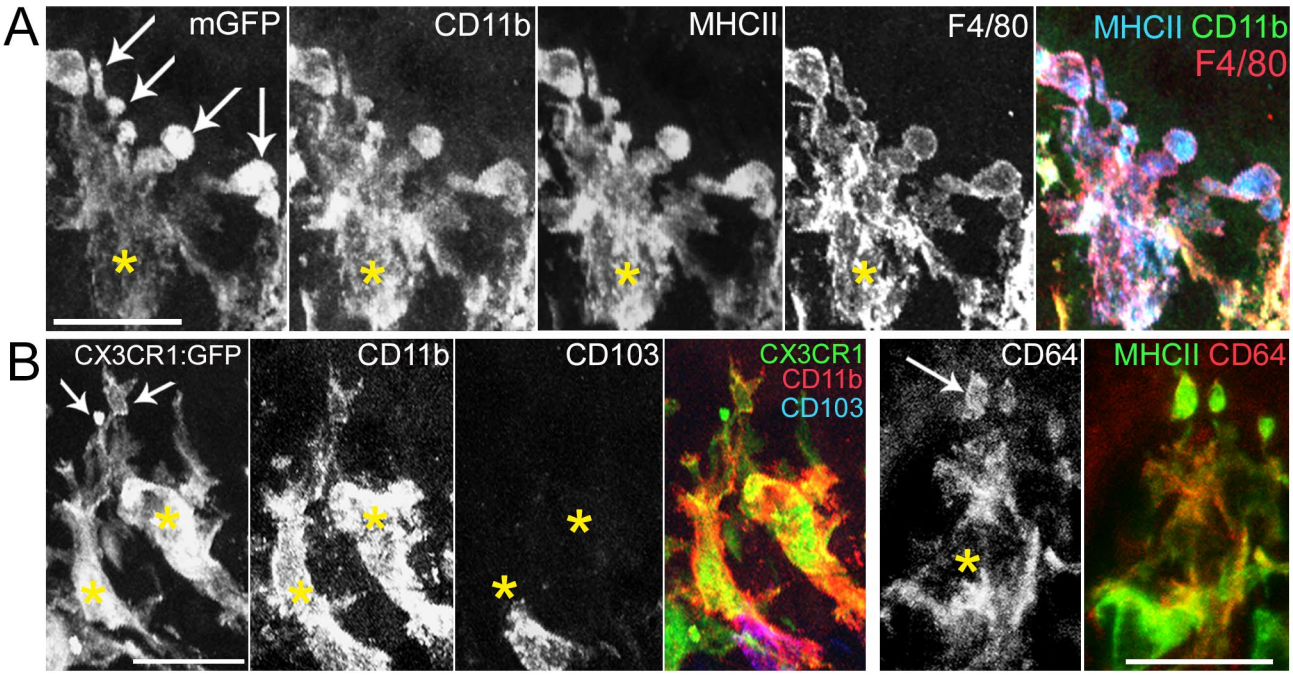


Figure 7. (A) BLP-forming macrophages express common intestinal macrophage markers. Cell bodies of Mϕ are indicated with yellow stars, arrows indicate BLPs. CD11b, MHCII, F4/80 staining of distal colon Mϕ from CD11c: Cre/R26^{mTmG} mouse, z-projection of 12 μm. Bottom panel (left): CD11b, CD103 staining of CX3CR1-GFP mouse, z-projection of 14 μm. **(B)** CD64 and MHCII staining of colon Mϕ from CD11c: Cre/R26^{mTmG} mouse, z-projection of 11 μm, scale bars – 20 μm.

BLPs are filled with epithelial cell membranes and endo-lysosomal compartments

We next analyzed the inner structure of BLPs using high-resolution confocal microscopy. We found that BLPs were approximately 1-5 μm in diameter, some of them forming thin extensions (about 0.3 μm in diameter and 5-10 μm in length) that extended between epithelial cells (Fig. 8A, left). BLPs were filled with membranes and vesicles devoid of actin (Fig. 8A, right). Most BLP internal vesicles in CD11c-Cre/R26^{mTmG} mice were Tomato^{+}, indicating that they originated from cells that do not express CD11c (Fig. 8B upper panel). Given the intra-epithelial localization of BLPs we hypothesized that these membranes might come from epithelial cells. To test this hypothesis, we generated Villin: Cre-ER^{T2}/R26^{mTmG} mice [277,282] in which intestinal epithelial cells express membrane GFP. Analysis of distal colon sections from these animals showed that BLPs were filled with GFP-positive membranes (Fig. 8B, lower panel), showing that they contain membranes and vesicles of epithelial origin.

Figure 8. BLPs contain epithelial cell membranes and are enriched in endo-lysosomal compartments.

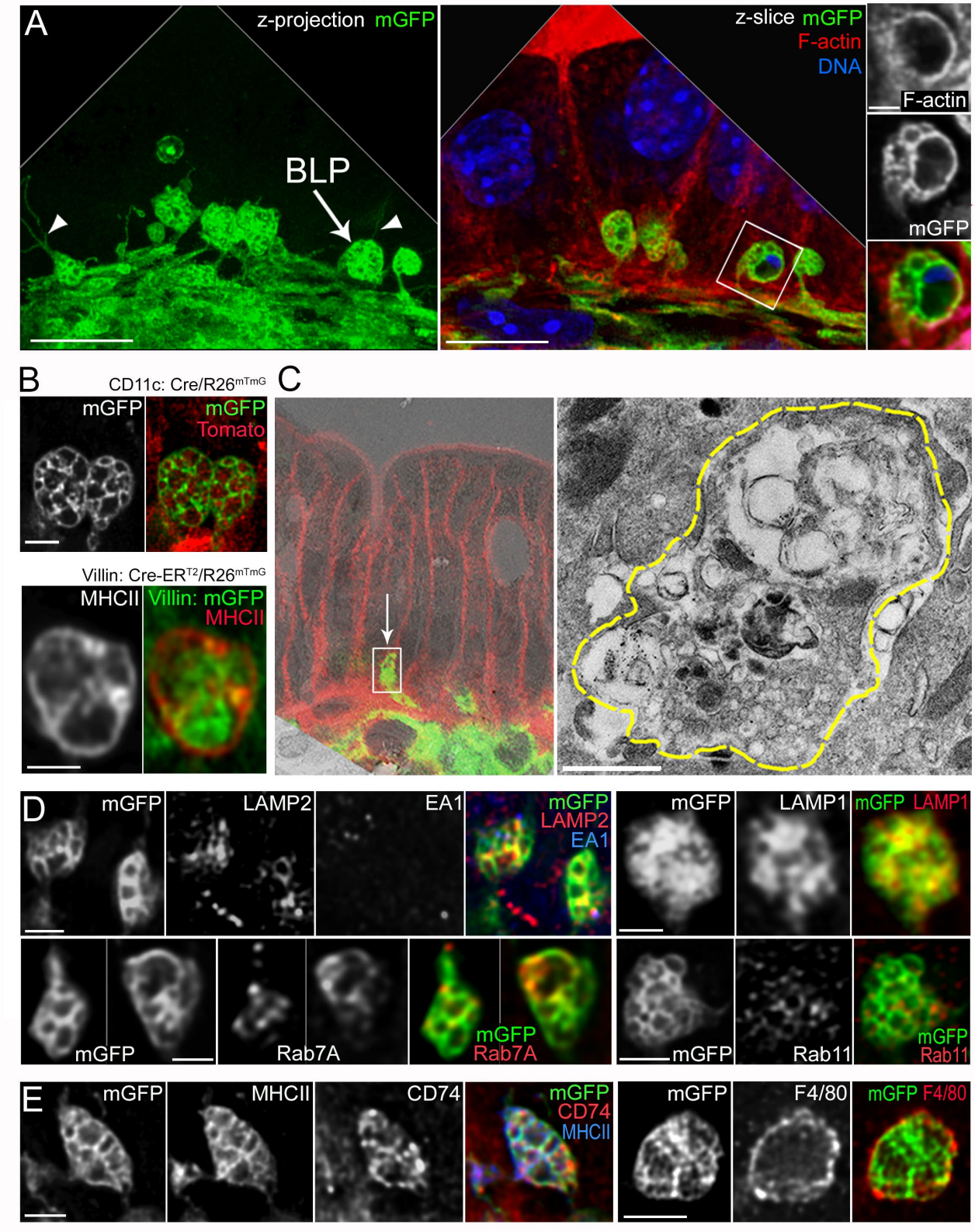


Figure 8. (A) BLPs (arrow) with thin membranous extensions (arrowheads). Maximum z-projection of a 7 µm (left) and a single slice (right) of distal colonic Mϕ from CD11c: Cre/R26^{mTmG} mouse, green

– mGFP; red – F-actin staining; blue – DNA staining, deconvolved. Scale bars – 10 µm, 1 µm on the magnified inset. **(B)** Inner compartments of BLPs are filled with membranous material, derived from CD11c-negative cells (top panel, distal colon of CD11c: Cre/R26^{mTmG} mouse), in part from the epithelium (bottom panel, distal colon of Villin: Cre-ER^{T2}/R26^{mTmG} mouse, intestinal epithelial cells express membranous GFP (green)), BLPs were visualized with MHCII staining (red). Maximum z-projections of 1 µm, deconvolved. Scale bar – 1 µm. **(C)** Correlative electron microscopy (left) of BLP from distal colon of CD11c: Cre/R26^{mTmG} mouse, arrow indicates a BLPs found on the confocal image (green – membrane GFP, red – membrane tdTomato, boxed) and overlaid with the low magnification TEM image, borders or the same BLPs are high-lighted with yellow dashed line on the higher-magnification TEM image (right). Scale bar – 1 µm. **(D)** LAMP2, LAMP1, Rab7A, Rab11 staining of BLPs, maximum z–projections of 1-2 µm, deconvolved. Scale bars – 2 µm. **(E)** MHCII, CD74 and F4/80 staining of BLPs. Maximum z-projection of 1-2 µm, deconvolved. Scale bars – 2 µm.

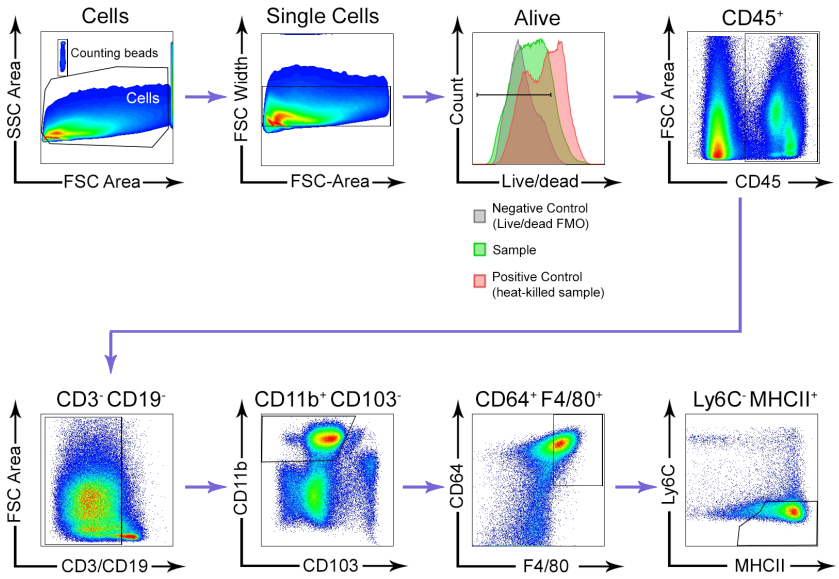
Correlative light-transmission electron microscopy analysis showed that BLP inner vesicles varied from 10 to 200 nm in diameter and were partly filled with electron-dense material, suggesting that they might contain lysosomes (Fig. 8C). Accordingly, most BLPs were positive for the LAMP1, LAMP2 and Rab7A late-endosomal/lysosomal markers (LAMP1-positive, 73,3% ± 3.5%; LAMP2-positive, 62% ± 2.5%; Rab7A-positive, 63,6% ± 3%) (Fig. 8D). In contrast, the marker of early endosomes, EEA1, was barely detected in BLPs (EEA1-positive, 8.8% ± 3.6%, Fig. 8D). Consistent with their late-endosomal/lysosomal origin, all BLPs were also enriched in MHC class II and associated Invariant chain, CD74 or Ii (100%, Fig. 8E). Of note, as we did not observe these two molecules in the epithelium, this result suggests that the endo-lysosomal markers found within BLPs were most likely expressed in the Mϕ themselves rather than internalized from neighboring cells. These data show that BLPs are filled with endo-lysosomal compartments that contain membranes internalized from epithelial cells.

BLP$^+$ Macrophages are CD11c^{high}

We next asked whether BLP$^+$ Mϕ constitute a unique cell population, distinct from its BLP$^-$ counterpart. To address this question, we FACS-sorted terminally differentiated Mϕ from both proximal (majority of Mϕ are BLP$^-$) and distal colons (majority of Mϕ are BLP$^+$) of a C57BL/6J mouse and compared their gene expression profiles using single-cell RNA-Sequencing [283] (Fig 9 for gating strategy, Fig. 10A).

Figure 9.

Gating strategy used to isolate macrophages from the distal and the proximal murine colon. The gating strategy begins on the top row, left.



To reliably identify transcriptionally different Mϕ sub-populations, we adopted a semi-supervised approach to group the cells based on their gene expression profile. First, we explored different solutions obtained by varying the input with a graph-based clustering algorithm [284] to identify the cluster whose relative abundance was greater in the distal than in the proximal colon, as observed for BLP$^+$ Mϕ. Then, based on the percentages of BLP$^+$ Mϕ quantified from colon sections (Fig. 10B), we selected feasible solutions as the ones where the fraction of putative BLP$^+$ Mϕ was between 50% and 70% in the distal colon and below 40% in the proximal colon. Second, we scored the solutions using the silhouette width, a measure of the similarity of each cell to the cells of the same cluster compared to the cells belonging to the neighboring cluster. The optimal solution was then defined as a feasible one whose average silhouette width of all cells (*silh(C)*) and of putative BLP$^+$ Mϕ (*silh(BLP$^+$ Mϕ)*), was maximal.

The optimal solution identified with this approach contained five clusters (Fig. 11 A, B). Only two of them, clusters 0 and 1, expressed high levels of all Mϕ markers (CD45, CD11b, F4/80, CD64, MHCII), hence the other three, comprising 140 cells overall, likely contained contaminants (e.g. epithelial cells and fibroblasts, Fig. 11, C) and were therefore removed. In total, we collected 2106 macrophages: 1354 cells in cluster 0 and 1752 cells in cluster 1 (Fig. 10B). While the distal colon sample included 58% of cells from cluster 1, the proximal colon only included 18%. This result suggested that cluster 1 is enriched for BLP$^+$ Mϕ, whereas cluster 0 is enriched for BLP$^-$ Mϕ. To test this hypothesis, we stained tissue sections with anti-CD11c (*Itgax*) antibodies, as the CD11c gene was found to be more expressed in cluster 1 as compared to cluster 0 (Fig. 10E). Strikingly, we observed

that these antibodies specifically labeled sub-epithelial BLPs^{+} Mϕ in the distal colon (Fig. 10C). Importantly, the percentage of BLP^{+} Mϕ found by tissue staining (Fig. 10B) was similar to the percentage of CD11c^{high} Mϕ defined by flow cytometry and imaging in the distal colon (Fig. 10D), suggesting that tissue disaggregation leads to the limited death of BLP^{+} Mϕ. Altogether these results strongly suggest that cluster 1 is enriched for BLP^{+} Mϕ.

Figure 10. BLPs^{+} Mϕ have distinct transcriptomic profile and express CD11c as a specific marker

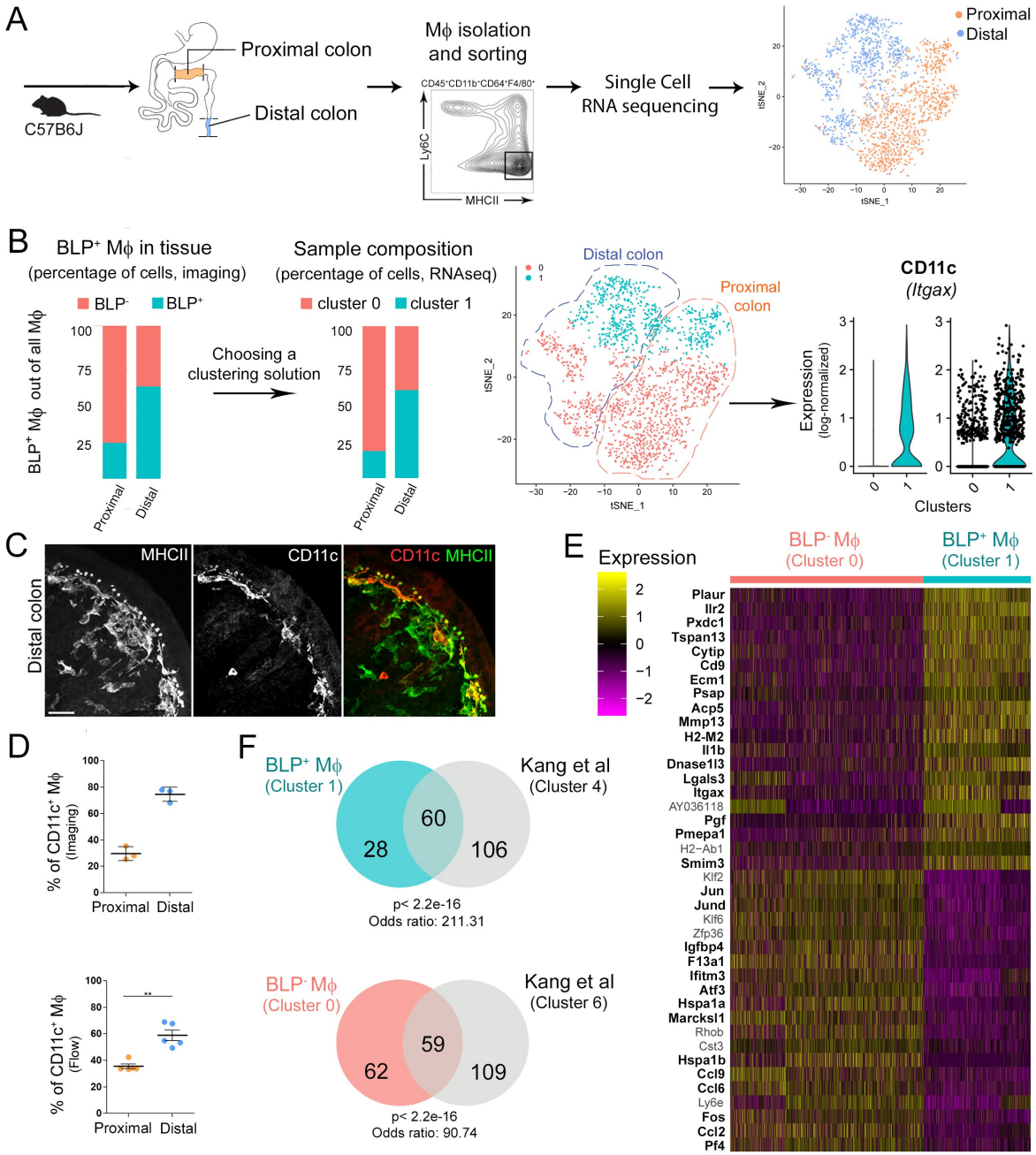


Figure 10. BLPs$^+$ Mϕ have distinct transcriptomic profile and express CD11c as a specific marker. **(A)** Single-Cell RNA-sequencing experiment workflow. Mϕ were isolated from proximal/distal colon by FACS (gated on alive, CD45$^+$, CD3$^-$, CD19$^-$, CD103$^-$, CD11b$^+$, F4/80$^+$, CD64$^+$, Ly6C$^-$, MHCII$^+$) and sequenced. 2106 Mϕ were identified, n = 1176 for proximal and n = 930 for distal colon, respectively, and shown on a tSNE representation, orange – cells isolated from proximal, blue – cells from distal colon (top 22 PCs computed on the top 1000 variable genes, vst method). **(B)** Selection of clustering parameters was based on the silhouette score and expected fraction of BLP$^+$ Mϕ in proximal and distal colon, obtained from IHC (results are presented on the stacked bar chart as a mean fraction of BLP$^+$ Mϕ out of all Mϕ, data pooled from 2 independent experiments). The selected clustering solution (graph-based clustering, 30 neighbors, resolution = 0.3) revealed the presence of two Mϕ sub-populations, displayed on the same tSNE as in (A) and colored accordingly: cluster 0, containing 964 cells in proximal and 390 cells in distal colon, and cluster 1, containing 212 cells in proximal and 540 cells in distal colon. Cluster 1 expresses CD11c as a specific marker. **(C)** Co-staining of MHCII and CD11c of the distal colon from C57B6J mouse. Maximum z-projection of 30 µm, scale bar – 20 µm. **(D)** Percentage of CD11c$^+$ Mϕ out of all Mϕ in proximal and distal colon determined by imaging (top, % of CD11c$^+$ Mϕ out of F4/80$^+$ CD103$^-$ MHCII$^+$ cells) or flow-cytometry (bottom, (% of CD11c$^+$ Mϕ out of CD45$^+$CD3$^-$CD19$^-$CD11b$^+$CD103$^-$CD64$^+$F4/80$^+$Ly6C$^-$MHCII$^+$ cells), dots represent average number per individual mice, data pooled from 3 independent experiments, results presented as mean ± SEM, Mann-Whitney test, **P <0.01. **(E)** Heatmap of the top 20 significantly up- and down-regulated genes between BLP$^+$ Mϕ (cluster 1) and BLP$^-$ Mϕ (cluster 0), respectively, sorted by non-decreasing p-value; entries represent the scaled (Z-score) normalized expression, values < -2.5 or > 2.5 are clipped; genes found respectively up- and down- regulated in Kang *et al* are highlighted in bold (see (F)). **(F, top**) Comparison of significantly up-regulated genes in BLP$^+$ Mϕ (cluster 1, 88 genes, in blue) and in cluster 4 from Kang *et al* (166 genes, in grey). Fisher's exact test using 10768 detected genes in the 2106 Mϕ as background. **(F, bottom)** Comparison of significantly up-regulated genes in BLP$^-$ Mϕ (cluster 0, 121 genes, in pink) and cluster 6 from Kang *et al* (168 genes, in grey).

BLP$^+$ macrophages exhibit a distinct gene expression profile

To identify the genes specific for BLP$^+$ Mϕ, we then extracted the genes that are differentially expressed in clusters 0 and 1. We found that 88 and 122 genes were respectively up- and down-regulated in BLP$^+$ Mϕ as compared to BLP$^-$ Mϕ (Fig. 10E). Among them, several genes could be directly or indirectly linked with microbiota recognition and inflammatory disorders in the colon, such as *lgal3* [285–287]*, plaur* [288,289]*, Il1b* (Seo et al., 2015)*, Ilr2* [291] *and cd9* [292].

We next compared our results to a recently published study [31] where single-cell RNAseq was used to identify the presence of distinct Mϕ sub-populations in the murine colon. This comparison showed that one of these sub-populations, “cluster 4”, which corresponded to terminally differentiated Mϕ (Fig. 11D), shared 60 genes with the signature of our BLP$^+$ Mϕ, including CD11c (Fig. 10F). In contrast, the cluster described in that study as “cluster 6” strongly resembled our BLP$^-$ Mϕ, with 59 overlapping genes. Consistent with our results, these two sub-populations were found to be spatially segregated within the colonic stroma, cluster 4 being localized closer to the epithelium, whereas cluster 6 was closer to the muscle layer. Interestingly, both clusters 4 and 6 were decreased in germ-free mice [31]. These results suggest that BLP$^+$ colonic Mϕ correspond to a specific Mϕ sub-population that is enriched in the distal colon, forms tight interactions with epithelial cells, and might be influenced by the microbiota.

Figure 11.

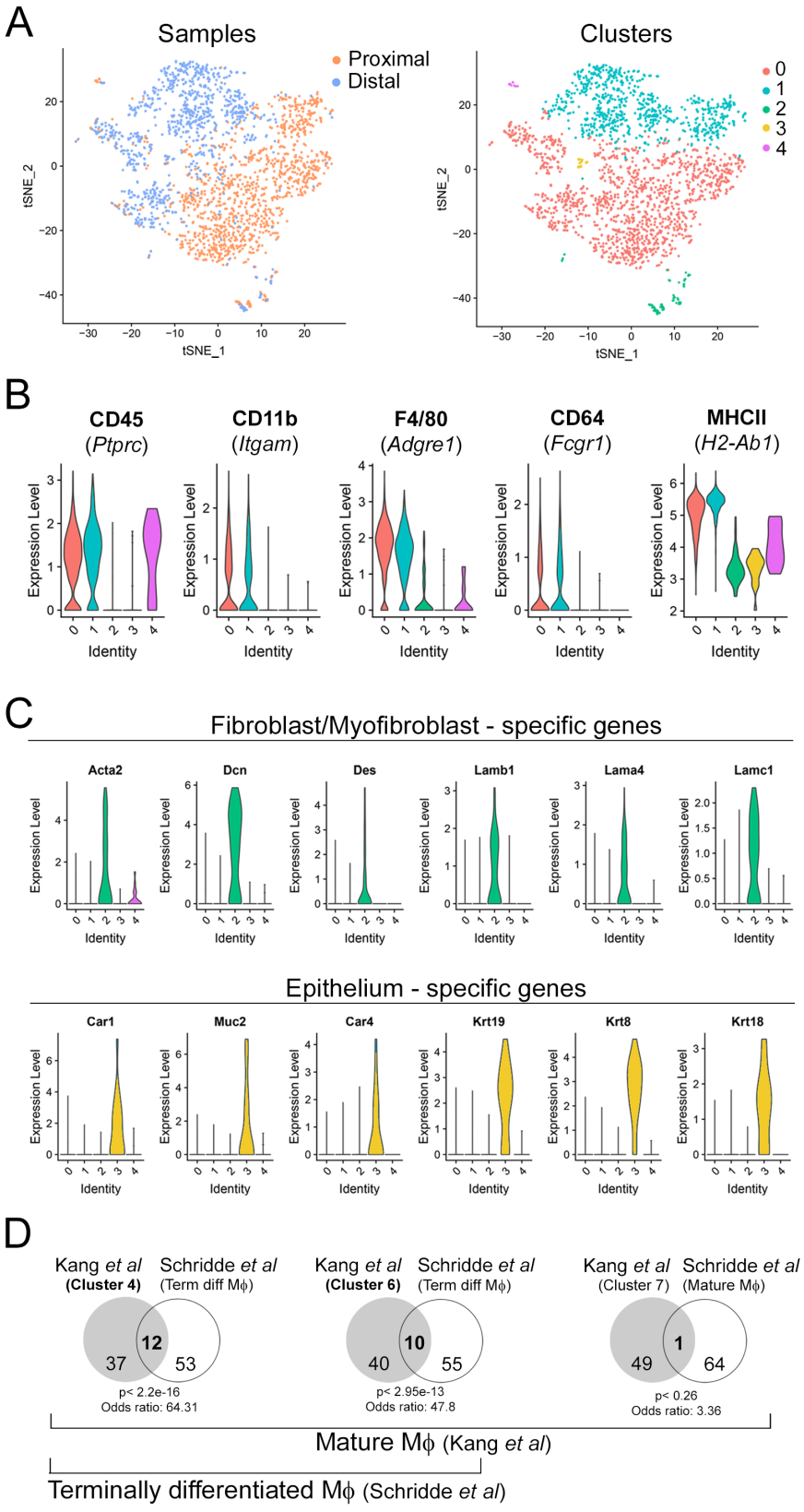

A
Samples
Proximal
Distal
Clusters
0
1
2
3
4
tSNE_1
tSNE_2
B
CD45 (Ptprc)
CD11b (Itgam)
F4/80 (Adgre1)
CD64 (Fcgr1)
MHCII (H2-Ab1)
Expression Level
Identity
C
Fibroblast/Myofibroblast - specific genes
Acta2
Dcn
Des
Lamb1
Lama4
Lamc1
Epithelium - specific genes
Car1
Muc2
Car4
Krt19
Krt8
Krt18
D
Kang et al (Cluster 4)
Schridde et al (Term diff Mϕ)
37
12
53
p< 2.2e-16
Odds ratio: 64.31
Kang et al (Cluster 6)
Schridde et al (Term diff Mϕ)
40
10
55
p< 2.95e-13
Odds ratio: 47.8
Kang et al (Cluster 7)
Schridde et al (Mature Mϕ)
49
1
64
p< 0.26
Odds ratio: 3.36
Mature Mϕ (Kang et al)
Terminally differentiated Mϕ (Schridde et al)

Figure 11. (A, left) tSNE computed on the top 22 PCs obtained on the 1000 most variable genes (vst method). Cells are colored by the sample. **(A, right)** tSNE computed on the top 22 PCs obtained on the 1000 most variable genes (vst method). Cells are colored by the cluster (number of neighbors = 30, resolution = 0.3). **(B)** Distribution of the log-normalized expression levels of genes used for sorting terminally-differentiated macrophages across clusters (gated on alive, $CD45^+$, $CD3^-$, $CD19^-$, $CD103^-$, $CD11b^+$, $F4/80^+$, $CD64^+$, $Ly6C^-$, $MHCII^+$). **(C, top panel)** Distribution of the log-normalized expression levels of fibroblast/myofibroblasts markers across clusters. **(C, bottom panel).** Distribution of the log-normalized expression level of epithelial cell markers across clusters. **(D)** Clusters 4 and 6 from Kang *et al*, consist of terminally differentiated (mature) Mϕ. Venn diagram of the set of cluster 4, 6 and 7 markers (top 50 up-regulated genes, gene AF251705 is excluded because it is not associated to any official gene name, Kang *et al*) and the terminally differentiated macrophage signature, defined as the genes showing log2(FC) ≥ 3 from P1 (monocytes) to P4 (mature macrophages) by Schridde *et al* (65 genes).

Intestinal fungi augment the formation of macrophage BLPs

These results prompted us to evaluate the impact of the microbiota on BLP$^+$ Mϕ. The colon harbors the largest amount of microorganisms in the body, where commensal bacterial and fungal populations share the intestinal niche [9,12]. To assess the potential effect of bacteria and fungi on the formation of BLPs, we targeted each population with a broad-spectrum antibiotic cocktail or anti-fungal agents respectively. No effect of antibiotics was observed (Fig. 12A). In sharp contrast, two antifungal agents, fluconazole and amphotericin B, significantly decreased the number of BLPs (Fig. 12A, B) without altering the total number of Mϕ, as shown by flow cytometry (Fig. 13A). We have previously highlighted that these drugs efficiently reduce the amount of intestinal fungi in mice [59] but using distinct mechanisms of action [293–295]. Tissue staining showed that the number of subepithelial Mϕ was also unchanged in mice treated with anti-fungal drugs (Fig. 13A), and that these cells displayed long thin protrusions instead of BLPs (Fig. 13B), as observed in the proximal colon. Of note, the combination of fluconazole or amphotericin B with antibiotics showed no additive effect (Fig. 12C), suggesting that these two anti-fungal agents do not act on BLPs indirectly, i.e. by leading to the expansion of colonic bacteria. These results, therefore, suggest that distal colon-resident fungi might promote the formation of BLPs in subepithelial Mϕ.

To directly asses the role of fungi in the induction of BLPs, we colonized germ-free mice with altered Schaedler flora (ASF), a well-defined community of eight bacterial species [208] or with the gut fungal pathobiont *Candida albicans*. Notably, fungal colonization induced strong BLP formation by Mϕ in the distal colon of germ-free mice that were otherwise devoid of these structures, while bacterial colonization did not influence the formation of BLPs (Fig. 12D). No change in the number of subepithelial macrophages was observed (Fig. 13A). While colonization of germ-free mice with pathobiont, *Candida albicans,* led to epithelial cell death, bacteria had no effect (Fig. 12E). Altogether, these results support a role for the mycobiota in the formation of BLPs in the distal colon, where these microorganisms are particularly abundant. Nevertheless, although we did not obtain any evidence for bacteria implication in BLP formation, we cannot exclude that specific bacteria species that are not present in ASF and resist the antibiotics used could also influence these protrusions.

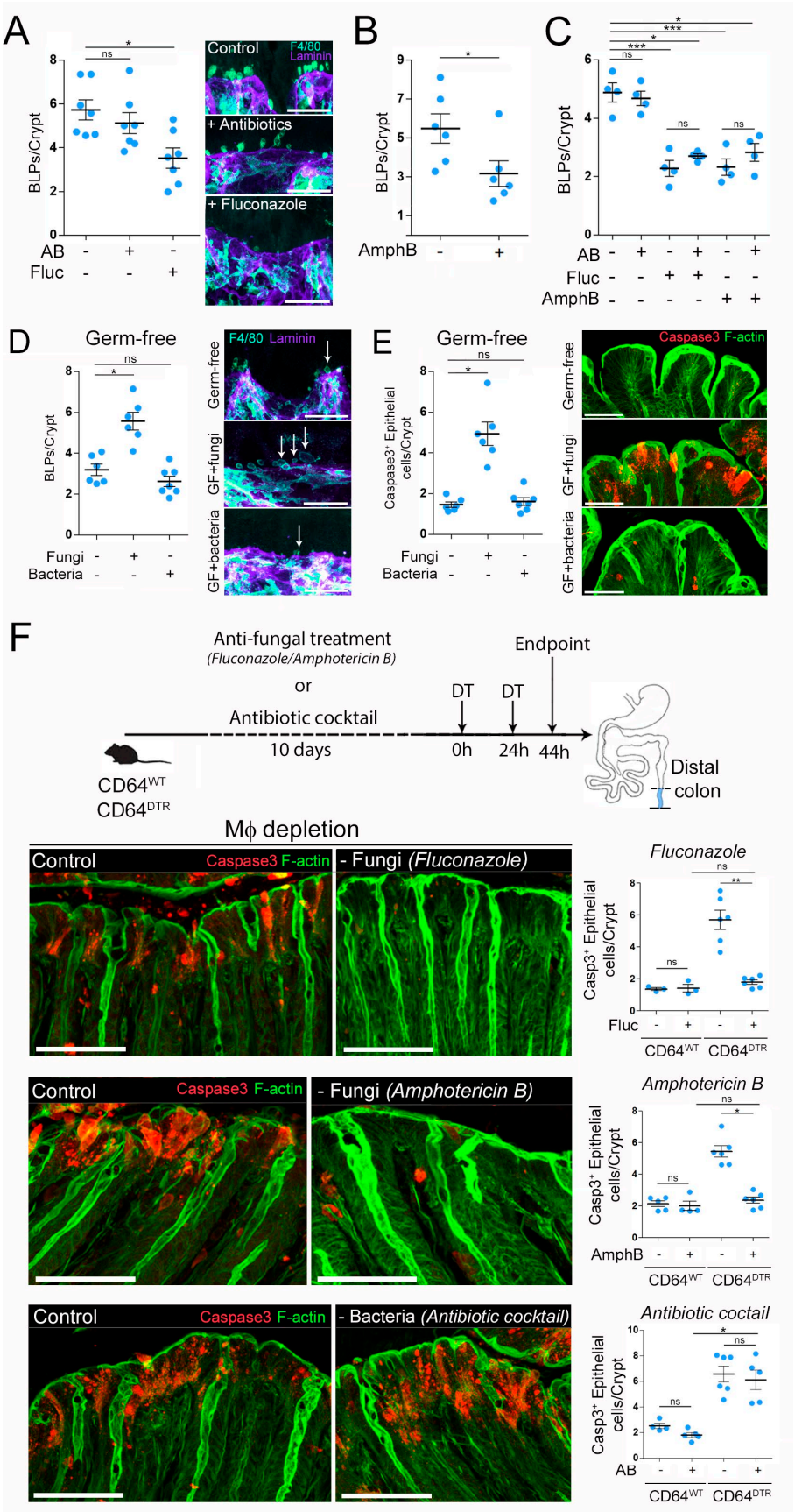


Figure 12.

Intestinal fungi stimulate BLP formation and account for epithelial death in the absence of Mϕ.

Figure 12. Intestinal fungi stimulate BLP formation and account for epithelial death in the absence of Mϕ.(A) Number of BLPs, normalized per crypt in the distal colon of mice treated with antibiotic cocktail (AB) or anti-fungal agent (fluconazole, fluc). Dots represent average number per individual mouse, results are presented as mean ± SEM, multiple comparison Kruskal-Wallis test, *P <0.05. Data pooled from 4 independent experiments. **(B)** Number of BLPs, normalized per crypt in the distal colon of mice treated with anti-fungal agent (amphotericin B, AmphB). Dots represent average number per individual mouse, results are presented as mean ± SEM, Mann-Whitney test, *P <0.05. Data pooled from 2 independent experiments. **(C)** Number of BLPs, normalized per crypt in the distal colon of mice treated with antibiotic cocktail, fluconazole, amphotericin B or in combinations of anti-bacterial and anti-fungal agents (antibiotics + fluconazole, antibiotics + amphotericin B). Dots represent average number per individual mouse, data pooled from 2 independent experiments. Results are presented as mean ± SEM, multiple comparison Holm-Sidak's test, *P <0.05, ***P <0.001. **(D) Number of BLPs, normalized per crypt, in germ-free mice colonized with bacteria (Schaedler flora, ASF) or fungi (*C. albicans*).** Dots represent average number per individual mouse, data pooled from 2 independent experiments, multiple comparison Kruskal-Wallis test, *P <0.05. **(A-D)** Mϕ were visualized by F4/80 staining (cyan) and crypts - with laminin (purple), **maximum z-**projections of 30 µm, scale bars – 10 µm. **(E)** Number of apoptotic (cleaved caspase 3^{+}) epithelial cells per crypt in the distal colon of **germ-free mice colonized with bacteria (Schaedler flora, ASF) or fungi (*C. albicans*).** Dots represent average number per individual mouse, data pooled from 2 independent experiments. **(F)** $CD64^{WT}$ or $CD64^{DTR}$ littermates were treated with anti-fungal agents (fluconazole or amphotericin B in separate sets of experiments) or antibiotic cocktail before Mϕ depletion. 44h after the first DT injection distal colons were processed for IHC staining. All mice received DT injections. **(E-F)** The global architecture of the tissue was visualized with F-actin staining (green) and apoptotic cells were revealed with cleaved caspase 3 staining (red), scale bars – 20 µm. Dots represent average number per individual mouse, data pooled from 3 (fluconazole and antibiotic cocktail treatment) and 2 (amphotericin B treatment) independent experiments. Results are presented as mean ± SEM, multiple comparison Dunn`s test, *P <0.05, **P <0.01.

Figure 13.

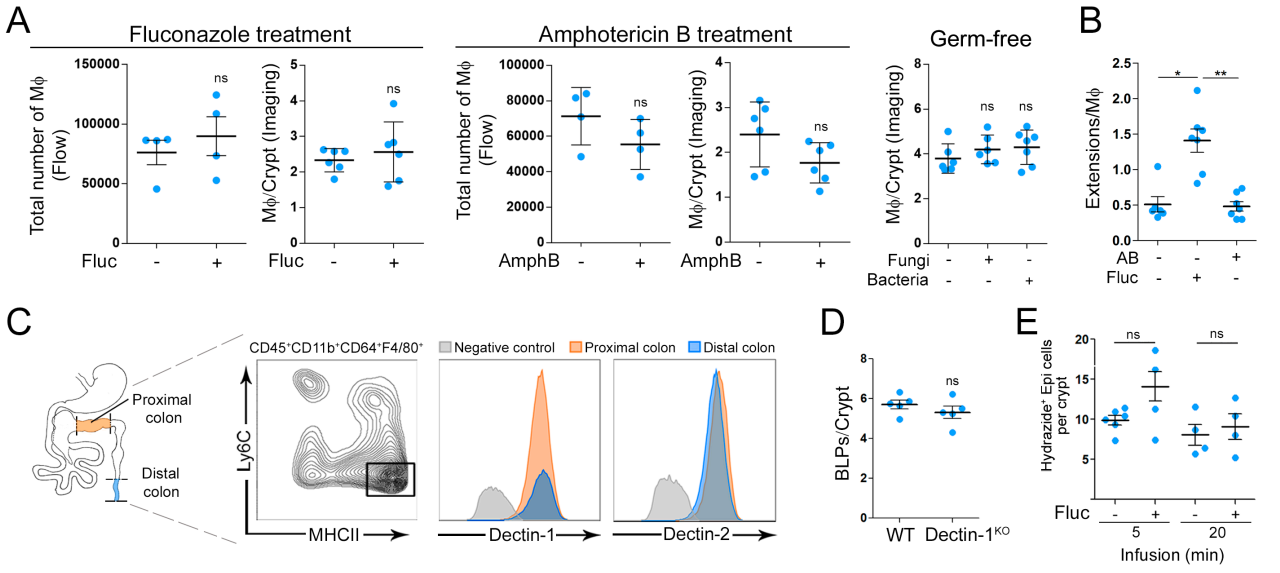


Figure 13. (A) Number of Mϕ in mice treated with anti-fungal agents (fluconazole and amphotericin B), and in germ-free mice, reconstituted with fungi (C. albicans) or bacteria (ASF), analyzed by flow cytometry and imaging. **(B)** Number of extensions normalized per number of Mϕ in mice treated with antibiotic cocktail or fluconazole. Dots represent average number per individual mouse, data pooled from 2 independent experiments. Results are presented as mean ± SEM, Mann-Whitney test, Kruskal-Wallis test was used in germ-free reconstitution experiments and in (B). **(C)** Dectin-1 and Dectin-2 staining of Mϕ isolated from the distal and proximal colon. Gated on Mϕ, gray histogram – negative control (FMO), orange – proximal colon Mϕ, blue – distal colon Mϕ. A representative example from 2 independent experiments, performed with 6 mice in total. **(D)** Number of BLPs analyzed by IHC staining and normalized per crypt of Dectin-1^{WT} and Dectin-1^{KO} mice. Dots represent average number per individual mouse, results are presented as mean ± SEM, Mann-Whitney test. (D) Number of BLPs normalized per crypt in mice pre-treated with anti-fungal agent (fluconazole, fluc) and infused with hypotonic solution. Pooled data from 5 independent experiments. **(E)** Number of $Hydrazide^{+}$ epithelial cells normalized per crypt upon hypotonic solution infusion with hydrazide used as the water tracer. Pooled data from 5 independent experiments. Dots represent average number per individual mouse, results are presented as mean ± SEM, Dunn`s multiple comparison test, *P <0.05.

Intestinal fungi are responsible for epithelial cell death in the distal colon of macrophage-depleted mice

So far, our results suggest that in the distal colon, there is a population of $CD11c^{high}$ Mϕ that form BLPs in response to local fungi. On the other hand, we found that Mϕ depletion was associated with massive epithelial cell apoptosis in the distal colon but not the proximal one (Fig. 5). We, therefore, hypothesized that by forming BLPs, Mϕ might protect epithelial cells from fungi-induced death. Indeed, fungi have been shown to produce many toxic molecules, including toxins and metabolites that can be deleterious for the host [14,296–298]. To test this hypothesis, we pretreated $CD64^{DTR}$ mice with antifungal agents before Mϕ depletion and assessed the impact of such treatment on epithelial cell survival. Strikingly, we found that anti-fungal treatment rescued the epithelial cells from death in Mϕ-depleted animals (Fig. 12F). The number of apoptotic colonocytes in mice treated with either fluconazole or amphotericin B prior to Mϕ depletion was comparable to those observed in Mϕ-containing mice. In contrast, epithelial cell death was not rescued when Mϕ-depleted mice were treated with antibiotics (Fig. 12F). We conclude that fungi are most likely responsible for the death of epithelial cells observed in the distal colon of Mϕ-depleted mice. These results further suggest that Mϕ might protect epithelial cells from fungi-induced cell death.

BLP$^+$ macrophages sample the fluids absorbed through epithelial cells

How do Mϕ detect fungi in the distal colon? Colonic macrophages use C-type lectin receptors such as Dectin-1,Dectin-2 and Mincle to recognize fungi cell-wall constituents and orchestrate antifungal immunity [12,13,208]. However, we did not observe any difference in the level of expression of Dectin-1 and Dectin-2 in Mϕ sorted from the distal and proximal colons (Fig. 13C). In addition, Dectin-1^{KO} Mϕ formed similar numbers of BLPs in the distal colon as compared to wild-type animals (Fig. 13D). These data suggest that BLP$^+$ Mϕ might not respond to intestinal fungi through the recognition of β-glucan by Dectins. Of note, this is consistent with BLPs not reaching the colon lumen and the microorganisms it contains.

BLP characterization showed that they were filled with membranes from epithelial cells and enriched in endo-lysosomal compartments (Fig. 8). We, therefore, hypothesized that BLPs might sample fungal metabolites/toxins indirectly, through the fluids absorbed by the epithelial cells they are in contact with. Indeed, epithelial cells in the distal colon possess specific mechanisms that optimize the absorption of water and facilitate stool dehydration [299]. Such mechanism might allow BLP$^+$ Mϕ to sample the environment in the absence of direct contact with the local microbiota. To assess whether BLP$^+$ Mϕ respond to fluid absorption by epithelial cells, we infused CD11c-Cre/R26^{mTmG} mice intra-rectally with a hypotonic solution. We found that such treatment increased the number of BLPs as fast as 10 min after infusion (Fig. 14A) and returned to steady-state in 30 min. This increase was also observed when fluid absorption was stimulated by aldosterone injection, corticosteroid hormone which increases sodium and thus water absorption specifically in the distal colon (Fig. 14B). To the opposite, when inhibiting water absorption by treating animals with the laxative Bisacodyl, we observed a significant decrease in the number of BLPs (Fig. 14C). Noticeably, this decrease was abrogated when mice were pre-treated with indomethacin, which inhibits the action of Bisacodyl [300]. Strikingly, tracing the fluid absorbed through epithelial cells using Alexa-633-labeled Hydrazide (a 0.5-1.5 kDa low molecular weight compound) showed an important accumulation of the dye inside the BLP$^+$ Mϕ network as fast as 5 min upon infusion (Fig. 14D, F). These results show that the fluid absorbed through the epithelium of the distal colon stimulates the formation of BLPs in associated Mϕ wherein this fluid accumulates. Importantly, we found that the formation of BLPs upon fluid absorption was increased when fungi were present (Fig. 14E) while the efficiency of

epithelial fluid absorption was unchanged (Fig. 13E), supporting our hypothesis that BLPs sample fluids for the presence of fungal products.

Figure 14. BLPs sample fluids absorbed through the epithelium.

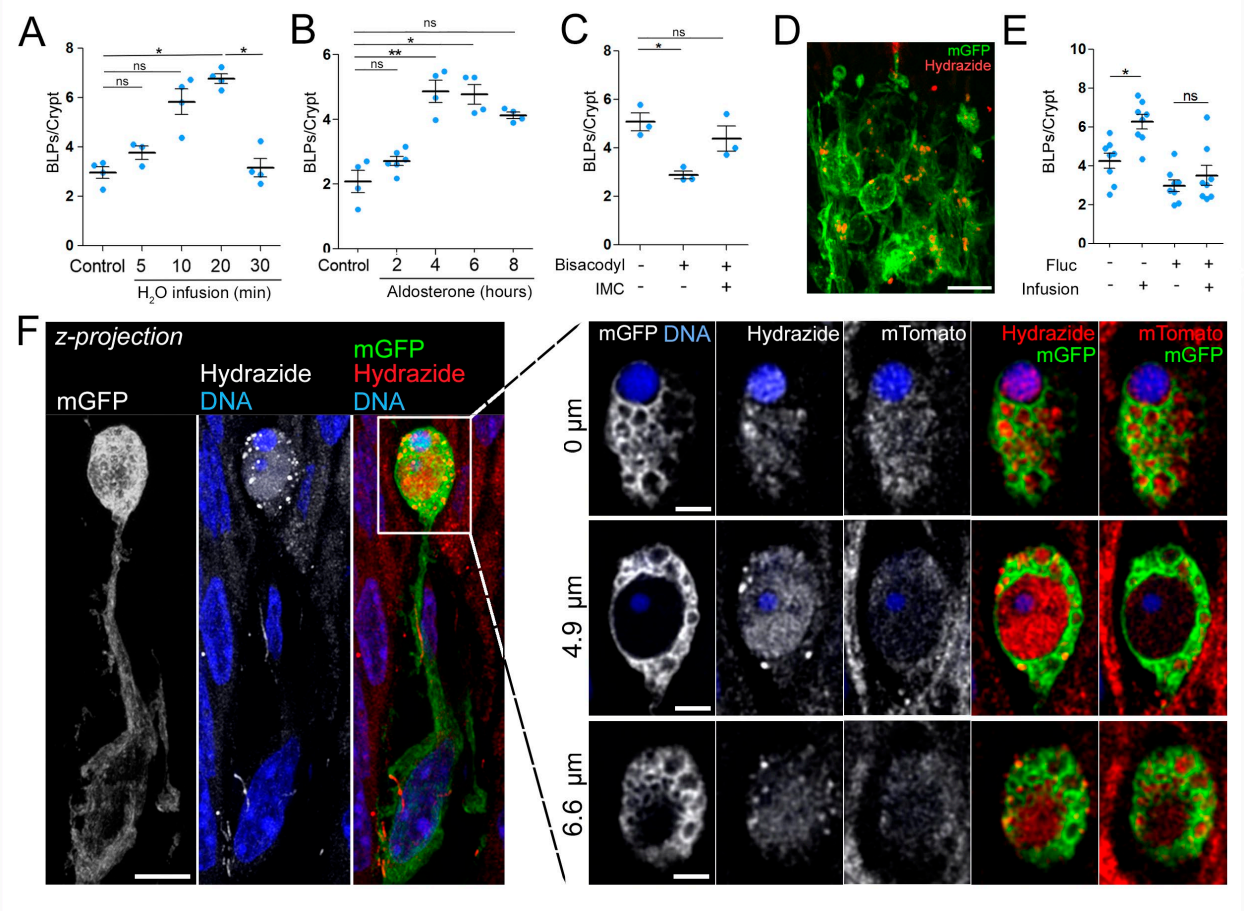


Figure 14. BLPs sample fluids absorbed through the epithelium. (A, B, C) Number of BLPs normalized per crypt upon stimulation/inhibition of intestinal fluid absorption. **(A)** Mice (CD11c: Cre/R26^{mTmG}) received an intra-rectal infusion of hypotonic solution (1:1 H_2O/PBS) and were sacrificed 5, 10, 20 or 30 min later. **(B)** Mice were injected with aldosterone and sacrificed 2, 4, 6 or 8h later. **(C)** Mice (C57BL/6J) were force-fed with a laxative (bisacodyl) and sacrificed 5h later. Indomethacin injection (IMC) 15 min before the gavage was used as an inhibitor of bisacodyl. Dots represent average number per individual mouse, data pooled from 3 (A, B) or 2 (C) independent experiments. Results are presented as mean ± SEM, multiple comparison Kruskal-Wallis test, *P <0.05, **P <0.01. **(D)** Maximal z-projection of distal colonic Mϕ 5 min after intra-rectal infusion of hydrazide in hypotonic solution (1:1 H_2O /PBS + hydrazide), a polar low molecular weight membrane-impermeant dye, coupled with Alexa633, which was used as a water tracer, green – membrane GFP, red – Hydrazide, z projection of 20 µm, scale bar – 10 µm. **(E)** Number of BLPs normalized per crypt in C57BL/6J mice pre-treated with anti-fungal agent (fluconazole, fluc) and infused with hypotonic solution. Dots represent average number per individual mouse, results are presented as mean ± SEM, multiple comparison Kruskal-Wallis test, *P <0.05. Data pooled from 5 independent experiments. **(F)** Maximal z-projection of distal colonic Mϕ forming BLPs, filled with Hydrazide after

intra-rectal infusion. CD11c: Cre/R26^{mTmG} mouse, left - z-projection of 8 µm, scale bar – 2 µm; and individual optical planes at different depths of the same BLP, scale bar – 1 µm.

Mϕ protect epithelial cells from being poisoned by fungal toxins

To directly test this hypothesis, we searched for a molecule to be used as a generic fungal metabolite, toxic for epithelial cells when concentrated. We turned our attention to Gliotoxin. Indeed, this fungi metabolite was shown to induce apoptosis in epithelial cells [14] and to be produced by both pathobionts and food spoilage fungi such as *Penicillium chrysogenum* [301,302], which is abundant in the murine intestinal tract [59]. Of note, Gliotoxin was also found to be produced by *Candida spp.*, including *Candida albicans*, even though there are conflicting reports on this subject [303–308]. To investigate whether Mϕ can sense fungal metabolites present in the fluids absorbed by epithelial cells, we infused fungi-depleted C57BL/6J mice with a hypotonic solution containing or not Gliotoxin (Fig. 15A). We found that Gliotoxin-containing solution stimulated BLP-formation as soon as 5 min after the infusion (Fig. 15B). While the epithelium kept absorbing the Gliotoxin-free hypotonic solution, it stopped the absorption of the one containing Gliotoxin 20 min upon infusion (Fig. 15C). Similar results were obtained when using two additional fungi toxins: Candidalysin from pathobiont *Candida albicans* and T2-toxin from commensal *Fusarium sporotrichoioides* [59,309] (Fig. 15D). These data show that epithelial cells sense and stop absorbing fluids that are poisoned with fungal toxins.

To investigate whether this is an intrinsic capacity of epithelial cells or requires associated BLP^{+} Mϕ, we performed a similar experiment in CD64^{WT} or CD64^{DTR} littermates injected with diphtheria toxin (DT) and infused with the Gliotoxin-containing hypotonic solution (Fig. 15E). Remarkably, we found that while DT-injected CD64^{WT} mice stopped the absorption of the Gliotoxin-containing solution, Mϕ-depleted CD64^{DTR} mice kept absorbing (Fig. 15E). To assess whether this uncontrolled absorption of Gliotoxin had long-term effects on epithelium homeostasis, we infused CD64^{WT} and CD64^{DTR} littermates with the Gliotoxin-containing hypotonic solution and sacrificed them 6h later. In these experiments, distal colon epithelial cells underwent massive apoptosis when Mϕ were depleted, confirming that these phagocytes protect epithelial cells from being poisoned by the fungal toxin (Fig. 15F). We conclude that in the distal colon, Mϕ endow epithelial cells with the ability to recognize toxic fluids and stop absorption, maintaining epithelial integrity and local homeostasis.

Figure 15. Mϕ protect epithelial cells from death by limiting fungal toxin absorption.

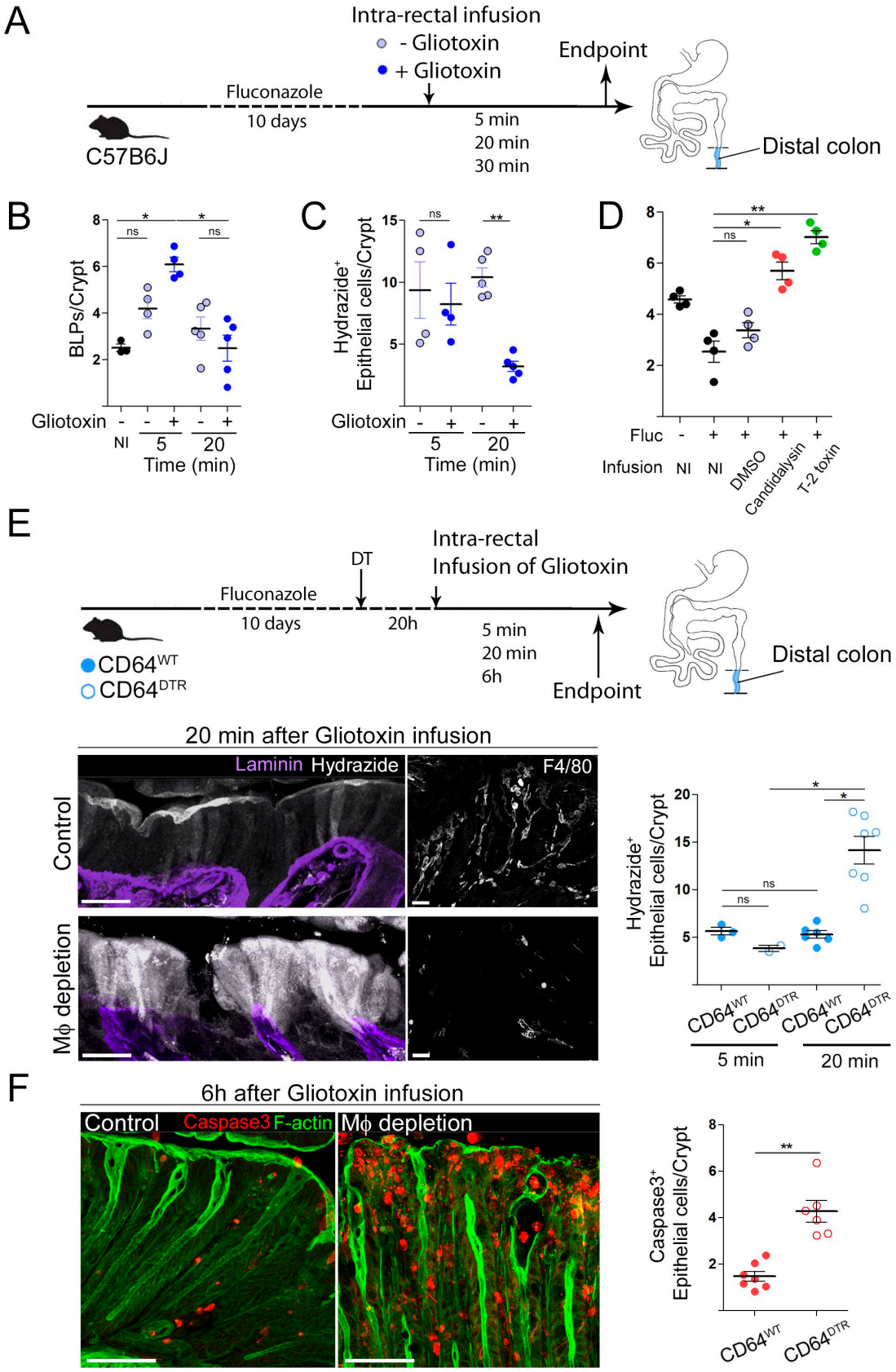


Figure 15. Mϕ protect epithelial cells from death by limiting fungal toxin absorption.

(A) C57BL/6J littermates were treated with anti-fungal agent (fluconazole) and received intra-rectal infusion of hypotonic solution (1:1 H_2O/PBS) with or without gliotoxin and were sacrificed 5 or 20 min later. Hydrazide was used as the water tracer. Distal colons were processed for IHC staining. **(B)** Number of BLPs normalized per crypt in C57BL/6J mice pre-treated with anti-fungal agent and infused with hypotonic solution with or without gliotoxin. Control (non-infused) group is indicated as "NI". **(C)** Number of $Hydrazide^+$ epithelial cells normalized per crypt in C57BL/6J mice pre-treated with anti-fungal agent and infused with hypotonic solution with or without gliotoxin. **(D)** Number of BLPs normalized per crypt in C57BL/6J mice pre-treated with anti-fungal agent (fluconazole, fluc) and infused with hypotonic solution containing DMSO (H_2O-infused control group), Candidalysin or T-2 toxin. Non-infused control groups are indicated as "NI". **(E)** $CD64^{WT}$ or $CD64^{DTR}$ littermates were treated with anti-fungal agent (fluconazole) before Mϕ depletion. 20h after the first DT injection mice received intra-rectal infusion of gliotoxin (in hypotonic solution with hydrazide as the water tracer), and were killed 5 min, 20min or 6h later. All mice were injected with DT. Distal colons were processed for IHC staining. Mϕ depletion was confirmed by F4/80 staining, border between epithelium and stroma was visualized by basement membrane staining (laminin, purple), maximum z-projections of 30 µm. Scale bars – 20 µm. **(C)** Maximum z-projection of distal colon sections of Mϕ-depleted animals 6h after gliotoxin infusion. Global architecture of the tissue was visualized with F-actin staining (green) and apoptotic cells were revealed with cleaved caspase 3 (red) staining. All mice were injected with DT. **(A-F)** Dots represent average number per individual mouse, data pooled from 3 (B-C) or 2 (D-F) independent experiments, results are presented as mean ± SEM. **(B-E)** Multiple comparison Kruskal-Wallis test, **(F)** – Mann- Whithey test, *P<0.05, **P<0.01.

BLPs are needed for Mϕ to prevent epithelium poisoning by fungi toxins

These results highlight the essential role of Mϕ in stopping the absorption of toxin-containing fluids through epithelial cells. Are BLPs required for this process? As shown in Fig. 8, BLPs are enriched for $CD74^{+}$ endo-lysosomal compartments and CD74 expression was slightly increased in cluster 1 (log fold change 0.4). CD74, also known as Invariant Chain, controls MHC class II trafficking to endocytic compartments and its expression typically leads to the expansion of endo-lysosomal compartments (reviewed in [310]). It was also shown to enhance the internalization of extracellular fluid by macropinocytosis [311]. We thus hypothesized that CD74 might help BLP^{+} Mϕ internalizing within endo-lysosomes the fluid and small vesicles released by epithelial cells.

To test this hypothesis, we infused fluconazole-treated $CD74^{WT}$ and $CD74^{KO}$ mice with a hypotonic solution containing Gliotoxin (Fig. 16A). We found that the number of BLPs was equivalent in the two groups of mice at steady state (Fig. 16B). While the number of BLPs increased in wild-type mice 5 min after Gliotoxin infusion, it did not in $CD74^{KO}$ animals, suggesting a decrease in uptake of extracellular fluids. Accordingly, $CD74^{KO}$ subepithelial Mϕ exhibited reduced level of Hydrazide internalization (Fig. 16C). This result suggests that CD74 is required for BLP formation in response to fluid absorption through epithelial cells, indicating that $CD74^{KO}$ mice constitute a valuable model to evaluate the implication of BLPs in fluid sampling by Mϕ. Quantification of fluid absorption showed no difference between $CD74^{WT}$ and $CD74^{KO}$ 5 min after infusion of Gliotoxin (Fig. 16D, graph). This is consistent with a wild-type epithelium absorbing equivalent amounts of toxin-rich fluid at this early time-point (Fig. 15C). Strikingly, while in wild-type mouse absorption of Gliotoxin-containing solution stopped 20 min after infusion, this decrease in absorption was not observed in the epithelium of $CD74^{KO}$ mice (Fig. 16D). In agreement with these results, we found that $CD74^{KO}$ epithelial cells later undergo massive apoptosis (Fig. 16E). These findings strongly suggest that BLPs orchestrate fluid sampling by distal colon Mϕ, which is critical to protect epithelial cells from absorbing fluids enriched in fungi toxins/metabolites.

Figure 16. CD74-dependent BLP formation protects epithelial cells from death by limiting fungal toxin absorption.

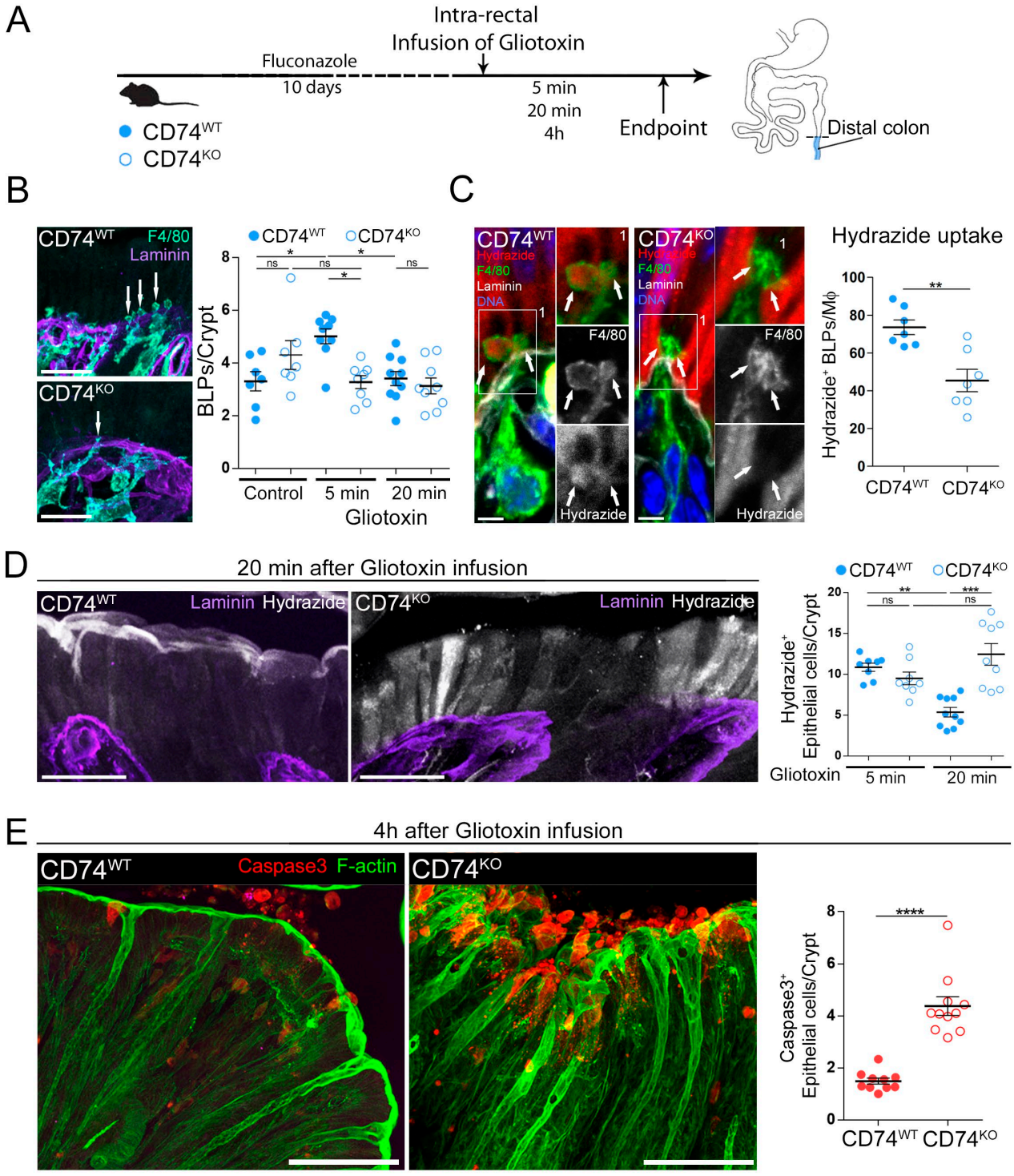


Figure 16. CD74-dependent BLP formation protects epithelial cells from death by limiting fungal toxin absorption.

(A) $CD74^{WT}$ or $CD74^{KO}$ littermates were treated with an anti-fungal agent (fluconazole) and infused intra-rectally with a hypotonic solution containing gliotoxin. Hydrazide was used as the water tracer. Mice were killed 5 min, 20 min or 4h after the infusion and distal colon samples were processed for IHC staining. **(B)** Number of BLPs formed in $CD74^{WT}$ and $CD74^{KO}$ animals upon gliotoxin infusion. Mϕ were visualized with F4/80 staining (cyan), the border between epithelium and stroma - by basement membrane staining (laminin, purple), 5 min after the gliotoxin infusion, scale bar - 20 μm. **(C)** Efficiency of BLP-mediated hydrazide uptake of $CD74^{WT}$ and $CD74^{KO}$ animals upon gliotoxin infusion. Hydrazide was used as water tracer (red), Mϕ were visualized with F4/80 staining (green), basement membrane (laminin) in white on the merge image and DNA is blue (DAPI), scale bars 5 μm. **(D)** Epithelial absorption of fluid in CD74WT and CD74KO animals upon gliotoxin infusion. Hydrazide was used as water tracer and is shown in white, basement membrane (laminin) in purple, maximal z-projections of 30 μm, scale bars 20 μm. **(B, D)** Dots represent average number per individual mouse, data pooled from 5 independent experiments. Results are presented as mean ± SEM, multiple comparison Dunn`s test, *P <0.05, **P<0.01, ***P<0.001. **(E)** Distal colon sections of $CD74^{WT}$ and $CD74^{KO}$ animals 4h after gliotoxin infusion. The global architecture of the tissue was visualized with F-actin staining (green) and apoptotic cells were revealed with cleaved caspase 3 staining (red), z-projections of 30 μm, scale bars – 50 μm. Data pooled from 3 independent experiments, dots represent average number per individual mouse. **(C, E)** Results are presented as mean ± SEM, Mann-Whitney test, **P<0.01, ****P<0.0001.

Discussion

The intestinal barrier separates the gut lumen from the internal milieu. It acts as a selectively permeable filter that allows the absorption of nutrients, electrolytes, and water, which can then reach the blood circulation for organ irrigation. At the same time, because the intestine lumen also contains many toxic substances produced by the microbiota, absorption must be tightly regulated to prevent intoxication and disease. Indeed, dysregulation of intestinal barrier permeability is a leading cause of sepsis-related mortality in critically ill patients and inflammatory bowel diseases (IBD). While mechanisms that regulate intestinal permeability have been widely studied in the small intestine, little is known on how the colon, whose main physiological function is fluid absorption and which contains the highest microorganism burden, protects itself from toxic microbial products.

My PhD thesis describes a mechanism driven by a particular population of CD11c^{high} sub-epithelial macrophages, which ensures rapid quality-check of absorbed fluids to maintain barrier integrity.

Macrophages use "balloon-like protrusions" (BLPs) inserted at the base of the epithelium, to sample the fluids absorbed through epithelial cells.

BLPs are remarkably different from trans-epithelial dendrites (TEDs) described previously in CD11c^{+} cells in the small intestine. CD11c^{+} cells, believed to be dendritic cells, send protrusions that insert between epithelial cells reaching the lumen [279,312]. TEDs were also observed by the live-imaging of small intestinal explants, but had different morphology. They contained balloons at their extremities. CD11c^{+} cells form those balloons on the apical side of the epithelium, contacting the gut lumen directly [313]. The frequency of those trans-epithelial protrusions varies along the crypt-villus axis, with most of them at the villi tips, suggesting that luminal ques drive their formation.

Even though the studies mentioned above claim that the TEDs-forming cells are the dendritic cells, this is not formally proven. Both, dendritic cells and intestinal macrophages express those used markers, CD11c, MHCII, and CX3CR1. Thus, it might be possible that the population of those TEDs-developing cells is macrophages. This might also explain the inconsistencies found in the distribution of TEDs along the small intestine. While using the CX3CR1-GFP model it is shown that CX3CR1^{+} cells develop a maximal number of TEDs in the terminal ileum [312], CD11c-EGFP and MHCII-EGFP models show the maximum of TEDs at the end of jejunum- beginning of ileum [313]. Differences in the shape

of those protrusions, finger-like [279], or balloons-ended [313], might be due fixation procedure which was not ruled out by these studies.

Even though there are multiple inconsistencies in TEDs description, all studies agree on two facts: (1) TEDs are formed in the small intestine; (2) They penetrate the epithelial layer and directly face the gut lumen. This can correspond well to the small intestinal physiology. The epithelium is more permeable, the mucus layer is thin, the microbiota is not numerous and must be maintained at relatively low density. Given this, it seems logical, that immune cells can extend protrusions through the epithelial “leaky” tight-junctions, face the lumen, and contact individual bacteria.

While para-cellular permeability (in between epithelial cells) is elevated in the "leaky" small intestine epithelium, which reflects its physiological role in nutrient absorption and establishment of tolerance to food, the colonic epithelium is rather "tight", i.e. it exhibits limited para-cellular permeability. This helps the colonic epithelium resist local mechanical stress imposed by elevated osmotic pressure and stool solidification, preventing loss of barrier integrity. Thus, in this microenvironment, it seems unlikely that immune cells can penetrate the epithelium without compromising its integrity, and without risking that protrusions will be wiped away by the solid feces. We show that macrophages of the distal and proximal colon, therefore, have developed an alternative sampling strategy in such tightly sealed colonic epithelium. They generate protrusions that reside in the intracellular space of the epithelium without penetrating epithelial junctions.

Thick mucus layer in the distal colon prevents the direct microbiota sampling by TEDs

Interestingly, as the mucus layer progressively thickens towards the distal colon, intra-epithelial protrusions change their shape from simple extensions to balloon-like protrusions (BLPs). In the proximal colon bacteria can physically contact epithelial cells [146]. However, in the distal colon, the mucus layer is as thick as the entire intestinal wall [136,139,147], completely separating the epithelium from the microbiota [134]. We hypothesized that a special microenvironment of the distal colon requires different sampling mechanisms to maintain homeostasis. The local immune cells receive the information from the lumen through the fluids, which are absorbed by the epithelium.

I have shown that CD11c^{high} macrophages indeed engulf absorbed fluids into endo-lysosomal compartments of BLPs. Anti-correlation between the number of simple, thin extensions and BLPs, that macrophages develop, suggests that BLPs originate from the extensions during the sampling process. Accordingly, stimulation of water absorption results in the increase of BLPs as fast as 5 min after the beginning of the infusion. It seems unlikely that macrophages can degrade the basement membrane, form protrusions, and recruit endo-lysosomal compartments during this time course. They most likely form simple extensions, which reside in intra-epithelial space at steady state that can inflate and form BLPs as soon as they are stimulated by the fluid influx.

Do macrophages directly sense the water influx and thus form BLPs, or they respond to the cues derived from the epithelium?

For the TEDs formation in the small intestine, at least two epithelial axes are involved: (1) CX3CR1-CX3CL1 axis, where a contact of epithelial cells with microbes, including Salmonella, stimulates CX3CL1 release and TEDs formation in CX3CR1-dependent manner [312]. CX3CR1 deficiency results in a defect of lamina propria dendritic cells that impair the sampling of bacteria from the intestinal lumen and impedes their ability to take up invasive pathogens in vitro [312]; (2) CCL20 that is released by the epithelium in response to TLRs ligation. In response to TLR2/4/9 ligation by *Salmonella* infection, epithelial cells in the small intestine produce CCL20 [314], which directly stimulates TEDs formation by CD11c^{+}/MHCII^{+} cells [313].

Based on my results that epithelium-derived membranes and hydrazide-traced fluids are found inside BLPs` compartments, both epithelium-mediated and direct sampling mechanisms may operate in the macrophages of the distal colon. In this region, the fluid is absorbed through both trans-cellular (through epithelial cells) and para-cellular (in between epithelial cells) pathways [315], accumulating in the intra-cellular space, exactly where BLPs reside.

BLPs as guardians of epithelial barrier

Because BLPs are located right underneath the epithelial junctional zone, they are in the ideal position to monitor the barrier-breakage events directly. I have performed preliminary experiments, where I perturbed the tight junctions using a low concentration of DSS (0.3% DSS administrated through drinking water). I analyzed the tissue integrity at a very early time point (24h) after the

beginning of treatment. I chose this time point because it was previously shown that under those conditions, the expression of tight-junction protein ZO-1 is 50% decreased without signs of colon mucosa inflammation [316]. This allows uncoupling tight-junction breakage from the inflammation-driven mucosal damage that occurs at later time points. In these experiments, I observed a dramatic increase in the number of BLPs precisely at the time point of decrease of epithelial ZO-1 expression. These results suggest that BLPs engulf products that have not only been absorbed through the epithelium at steady-state but also those that leaked through in case of barrier dysfunction. Thus, we hypothesize that BLP$^+$ macrophages may perform several roles beyond homeostasis: (1) as a buffer system, preventing the leakage of luminal products into the bloodstream in case of occasional epithelial barrier failure; (2) as a "decision-making" cells, that initiate the mucosal inflammation if the amount of leaking products is beyond the certain threshold.

Interestingly, macrophages have been shown to play critical roles in the initiation and progression of IBD [18,258]. The depletion of macrophages results in the increasing severity of colitis [317], whereas newly arrived monocytes differentiate into pro-inflammatory macrophages in mucosal damage[242]. Tissue-resident macrophages are responsible for the recruitment of monocytes upon initiation of intestinal inflammation [318]. Accordingly, the disruption of sub-epithelial macrophages accumulation has been observed in IBD patients [272]. Given the rapid reaction of BLP$^+$ macrophages to the breakage of the epithelial barrier and their sub-epithelial localization, it would be exciting to reveal, which role do they play in the initiation of mucosal inflammatory responses.

BLPs are formed in response to intestinal fungi

While TEDs in the small intestine form in response to bacteria [312–314], we unexpectedly found that distal colon BLP$^+$ macrophages respond to the presence of fungi products. Similar results were observed with two different antifungal agents, fluconazole and amphotericin B, which target distinct fungal species through other mechanisms [293–295]. Additionally, fungal recolonization of germ-free mice increased of BLPs formation. These results are consistent with fungi being particularly enriched in the distal colon [13]. We did not obtain any evidence that bacterial compounds stimulate the formation of BLPs. However, we cannot exclude the possibility that bacteria insensitive to the used antibiotics or absent from the ASF flora used to re-colonize germ-free mice, could still stimulate the formation of BLPs.

How do subepithelial BLP$^+$ macrophages sense fungal products? Our data strongly suggest that Dectins might not be involved in this process in homeostatic conditions as (1) the number of BLPs does not differ between wild-type and Dectin 1^{KO} mice and (2) the level of expression of these receptors are equivalent in macrophages isolated from proximal (a majority are BLP$^-$) and distal colon (a majority are BLP$^+$). This is coherent with previous findings showing that the distal colon contains a thick mucus layer that physically separates the microbiota from the epithelial cells [146]. Therefore, in homeostasis, i.e. in the absence of barrier leakage, there is no contact between sub-epithelial macrophages and the colon lumen, impairing Dectin engagement by their ligands, which are part of the fungal cell wall.

We show that macrophages use BLPs to sample the fluids absorbed through epithelial cells. These fluids carry the whole spectrum of fungal metabolites, providing: (1) a comprehensive picture of local mycobiota composition; (2) the information about living fungi, because ingested or dead fungi do not actively produce metabolites; (3) inform the host immune system about the fungal invasion, as several fungi (such as *C.albicans* or *Aspergillus fumigatus)* start to produce certain metabolites (such as candidalysin or gliotoxin) only upon hyphal transformation when they become invasive.

Importantly, the majority of mycotoxins target the intestinal epithelial barrier [15] as fungi use it as an entry point. Several examples include: Candidalysin that is proven to be crucial for intestinal epithelial damage is required for *C. albicans* further invasion [17]; T-2 toxin, produced by *Fusarium species*, targets intestinal epithelial cells and increases para-cellular permeability, allowing the fungus to grow through [16]; Patulin, known as a fruit-spoilage mycotoxin, produced by *Penicillium*, *Aspergillus,* and *Byssochylamys*, disrupts epithelial barrier integrity by decreasing the expression of tight-junction proteins [319].

Thus, BLP$^+$ macrophages are ideally positioned to sample the products that pass through the epithelium, to capture fungal metabolites. Similar results were obtained when animals were infused with three different fungi toxins (with Gliotoxin, which is produced by both pathobionts and commensals, Candidalysin, from pathobiont *Candida albicans*, and T2-toxin, from commensal *Fusarium sporotrichoioides* [309]). In all cases, the number of BLPs increased upon toxin inoculation in fungi-depleted mice, indicating that BLP$^+$ macrophages recognize all three fungi metabolites. This result suggests that BLPs do not only respond to fungi compounds produced by pathogenic species

but to a broad variety of fungi metabolites. The BLP response may thus be critical not only to sense potentially dangerous fungi species but also to detect the over-growth of commensal fungi, whose metabolites might compromise the survival of epithelial cells if too abundant. Accordingly, we found that commensal fungi are indeed responsible for epithelial cell death in macrophages-depleted mice. Defining the precise nature of the involved commensal fungi requires additional investigations. An interesting candidate is the commensal specie, *Fusarium sporotrichoioides*, as it is targeted by both Fluconazole and Amphothericin B [59] and produces the T2 toxin [309]. Of note, how BLP^+ macrophages themselves resist toxins remains an open question, it could be envisioned that BLPs maintain toxins away from the cell body of these cells.

One question that arises: <u>If fungal metabolites are such a danger to the intestinal barrier, what are the host benefits for maintaining them in the distal colon?</u>

Possible benefits from fungal symbionts

While vaginal *C. albicans* protects the host form urinary tract infections by suppressing the growth of gastro-intestinal *E. coli* on the vulva [320], the host benefits from intestinal fungi in the gastro-intestinal tract remain unclear.

Interestingly, the vast majority of fungal metabolites are immunosuppressive and can lead to the acquisition of anergic phenotype of macrophages *in vitro*. C. albicans metabolites were shown to decrease phagocytic activity [321], as well as nitric oxide production [322] in LPS-stimulated peritoneal macrophages. Additionally, the infusion of fungal metabolites exerts anti-inflammatory effects in murine models of intestinal inflammation [323]. Fungal dysbiosis exacerbates colitis development in several experimental models [59], and is also associated with IBD progression in patients [324]. Thus, it would be very important to understand, whether constant uptake of commensal fungi products, together with the absorbed fluids, participates in creating macrophages anergy and low responsiveness towards microbial stimuli in the distal colon *in vivo* to maintain local homeostasis.

Importantly, in sharp contrast, in response to barrier rupture and fungal invasion, macrophages physically contact fungi through Dectin-1 and mount an effective inflammatory immune response. [12,13].

Do BLP$^+$ macrophages directly sense fungal products absorbed by the epithelium or detect stress compounds released by poisoned epithelial cells? Our data strongly suggest that CD74^{KO} animals cannot detect fungal toxins as efficiently as CD74^{WT} mice. This can be explained by the defect of BLP-mediated fluid sampling in CD74^{KO} animals, or indirectly thought the cross-talk with the epithelium, due to the multiple physiological roles of CD74 [310]. Firstly, high-resolution imaging showed that BLPs are intensely stained for CD74. As is required for the expansion of endo-lysosomal compartments, we thus hypothesized that BLPs of CD74^{KO} macrophages could not sample absorbed fluids efficiently. In favor of this hypothesis, I have observed that while intra-rectally administrated hydrazide accumulated within BLPs 5 min after fluid infusion in CD74^{WT} animals, its accumulation within CD74^{KO} BLPs was significantly reduced.

Secondly, CD74 is also known as a receptor of macrophage-inhibitory-factor (MIF), that is actively released by epithelial cells in response to the inflammatory stimuli [325]. MIF is critical for the function of the intestinal epithelium barrier, as MIF^{KO} animals exhibit elevated colonic permeability due to a decrease in the expression of tight-junction proteins. Thus, it seems equally possible, that after contact with fungal toxins, epithelial cells secrete MIF that is recognized by the macrophages. Since CD74^{KO} macrophages lack the receptor, they fail to respond to this danger signal. It would be very interesting to stimulate MIF^{KO} animals with fungal toxins and evaluate, whether BLP response is preserved. In this case, it is also interesting to know; how do epithelial cells detect the presence of fungal toxins? For epithelium in the oral cavity, the recognition of fungal toxin Candidalysin, a virulence factor of *C. albicans*, secreted during the hyphal invasion, is driven by EGF receptor [211]. Candidalysin directly binds to EGFR, causing its phosphorylation. This initiates the early epithelial response [212], MAPK activation, transcription of c-Fos with the following release of inflammatory cytokines (IL-1α, IL-1β, IL-36γ, IL-6, GM-CSF, G-CSF) and alarmins [213], by epithelial cells that can be also detected by the BLP$^+$ macrophages. Of note, besides the release of inflammatory cytokines, EGFR engagement with following MAPK activation, suppresses epithelial cells shedding and drives a proliferative response [326]. Independently, fungal dysbiosis is known to be present in colon carcinoma patients [327] and fungi have been recently shown to increase cancer cell proliferation in pancreatic tumors [228]. Thus constant EGFR stimulation by excessive fungal toxins might also participate in the cancerogenesis of the distal colon.

Even though it is still unclear whether the fungal toxin sensing by BLP$^+$ macrophages occurs directly or indirectly through epithelial cells, we have shown that the presence of macrophages and BLPs formation is critical to control epithelial absorption. If fluids are over-loaded with fungal metabolites/toxins, macrophages instruct epithelial cells to stop absorption, preventing epithelial cell poisoning and death. In the case of macrophages depletion or BLP formation defects, the epithelium is no longer able to distinguish pure infused solutions from those containing fungal toxins.

How do macrophages signal to the epithelium and decrease the water absorption? This could, for example, occur through the secretion of Prostaglandin 2 (PGE2) by macrophages, which down-regulates Aquaporin 3 localization at the apical membrane of epithelial cells *in vitro* [300]. Aquaporin 3 is one of the major Aquaporins expressed in colonic epithelial cells [299] and whether the BLP$^+$ macrophages can affect its intracellular localization would be an interesting question for the future.

In the absence of macrophages or BLPs, epithelial cells absorb fluids independently of their fungal toxin/metabolite load and undergo apoptosis, compromising barrier integrity. These results suggest that, in homeostasis, the permeability of the intestinal barrier is differentially regulated depending on the local physiological function of the specific intestine segment and on its microbial content. macrophages thus emerge as key players in the orchestration of such regulation.

Independently, by the other group, it has been shown that colonic macrophages spontaneously secrete IL-10, and can efficiently promote Foxp3$^+$ Treg cell conversion *in vitro* in the presence of exogenous TGF-b [29] . Recruitment of Tregs is required for the tolerogenic immune responses to commensal microbiota [328,329]. Interestingly, we have found one to two dendritic cells (F4/80$^-$ CD64$^-$CD103$^+$CD11b$^-$CD11c$^+$MHCII$^+$) below each BLP$^+$ macrophage. Live imaging of colonic explants revealed that while BLP$^+$ macrophages are stable and non-motile, dendritic cells actively migrate on top of them. We hypothesize that macrophages may transmit microbiota-derived products to those dendritic cells to prime T-cell responses in the regional lymphoid structures. Such division of labor between mucosal macrophages and dendritic cells has been shown to orchestrate tolerogenic responses to food in the small intestine [27], the same mechanism might be involved in the distal colon to direct tolerogenic responses towards commensal microbiota. In this case, BLP$^+$ macrophages could act as a “detoxification” platform that first pre-degrade antigens, limiting their possible toxicity and pass it after to the dendritic cells.

High expression of MHCII on BLP$^+$ macrophages suggests that they might also act as an antigen-presenting cells. In line with this I have observed an accumulation of CD3$^+$ CD4$^+$ cells in contact with BLP$^+$ macrophages. One of the genes is upregulated in BLP$^+$ macrophages sequencing is CD9. It forms super complexes with CD74 and CD1d [330] and participates in the CD1d-mediated presentation of lipid antigens to the mucosal iNKT cells [331]. In accordance with this finding, fungal metabolites are mostly hydrophobic and iNKT cells are important for the anti-fungal immunity [332,333]. In this view, BLP$^+$ macrophages might sample, process and present fungal toxins to iNKT cells.

In conclusion, we here highlight a so far uncovered homeostatic function of CD11c^{high} subepithelial macrophages in the distal colon: they help the epithelium maintaining its integrity in an environment subjected to elevated physical and chemical insults that result from osmotic pressure, feces solidification and an important microbial load. How BLP$^+$ macrophages instruct epithelial cells to absorb or not fluids in homeostasis and whether alterations in such mechanisms lead to pathologies such as IBD and cancer shall next be addressed.

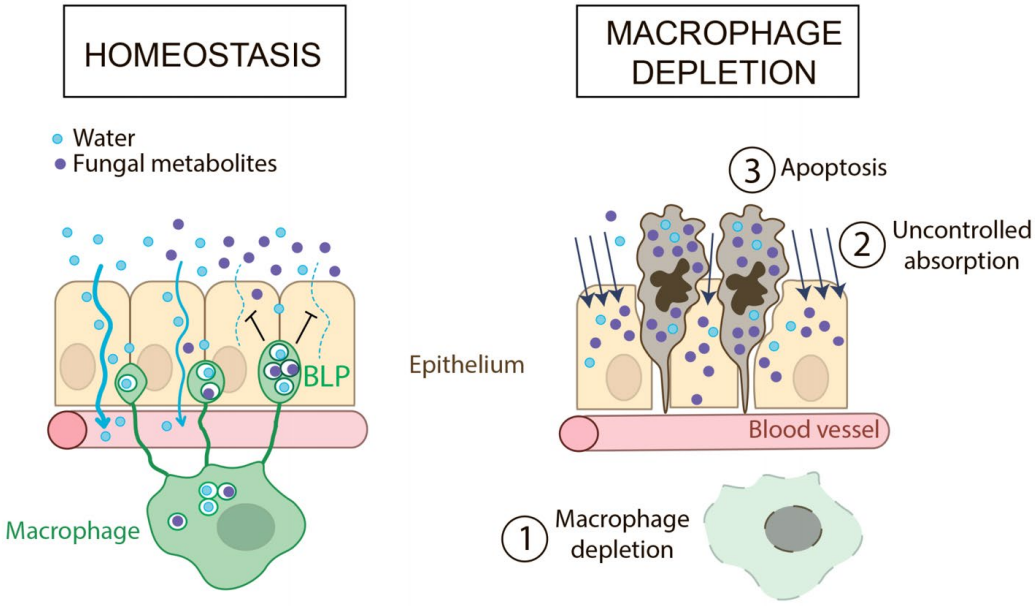


Figure 17. Macrophages regulation of intestinal barrier permeability and integrity.

Distal colonic CD11chigh macrophages are equipped with "balloon-like" protrusions (BLPs) inserted at the base of epithelial cells. BLPs sample the absorbed fluids and stop absorption when fluid is poisoned with fungal metabolites. In the absence of macrophages or BLPs, epithelial cells keep absorbing fungal toxin-containing fluids, leading to their death and subsequent loss of epithelial barrier integrity.

Materials and Methods

Mice

Animal care and use for this study were performed in accordance with the European and French National Regulation for the Protection of Vertebrate Animals used for Experimental and other Scientific Purposes (2010/63/UE) for the care and use of laboratory animals. Experimental procedures were specifically approved by the ethics committee of the Institut Curie CEEA-IC #118 (AuthorizationAPAFiS#26130-2020062023431460-v1 given by National Authority) in compliance with the international guidelines. All mice were maintained in the SPF animal facility of Institut Curie (Paris, France) prior to use. Germ free (GF) mice were bred and maintained within sterile vinyl isolators at Weill Cornell Medical College Mouse Facility. Altered Schaedler flora (ASF) mice were generated from germ-free wild-type C57BL/6 mice upon inoculation with ASF community [208], bred for at least 5 generations for fully immunocompetent progeny and maintained within sterile vinyl isolators. All animal experiments were approved and are in accordance with the Institutional Animal Care and Use Committee guidelines at Weill Cornell Medicine. Experiments were performed on 8 to 16 weeks-old male or female mice. CD11c: Cre/R26^{mTmG} mice were generated by crossing CD11c:Cre$^{+/-}$ mice [278] with the tdTomato/GFP reporter mice, where membrane-targeted green fluorescent protein (GFP) is expressed upon Cre activation [277] and labels CD11c compartment. Villin: Cre/R26^{mTmG} mice were generated by crossing Villin:Cre-ER$^{T2\ +/-}$ mice, bearing tamoxifen-dependent Cre recombinase in intestinal epithelial cells [282] with the tdTomato/GFP reporter mice [277]. Tamoxifen (0215673891, MP Biomedicals™) was prepared as described previously [334] in sunflower seed oil (S5007, Sigma-Aldrich). In order to induce sufficient labeling of intestinal epithelial cells' membrane, mice were i.p. injected with tamoxifen stock solution (50 mg/kg) for 5 consecutive days. C57BL/6J mice (females) were purchased from Charles River. CD64$^{DTR\ +/-}$ mice [273] were a kind gift from Sandrine Henri and Bernard Malissen and used for macrophage depletion experiments. Animals were i.p. injected with unnicked diphtheria toxin from *Corynebacterium diphtheriae* (50µg/kg, solution was prepared in PBS, right before use from 1mg/mL stock solution kept at -80C, 322326, Sigma-Aldrich). Number of injections was dependent on the duration of experiment and on experimental design. For the intestinal barrier integrity experiments, mice received two i.p. injections, 24h apart and sacrificed 20h after the second injection. For infusion

experiments, mice received one i.p. injection 20h prior to infusion. $CD64^{DTR\ -/-}$ littermates injected with DT were used as a control. $CD74^{KO/KO}$ mice [335] were a kind gift from Dr. Hidde Ploegh, $CD74^{WT/WT}$ littermates were used as control. All treatments were done at the same time of the day, to eliminate any variability resulting from the circadian rhythm and its effects on the intestinal physiology.

Tissue preparation

To ensure the same segmentation of the colons across the experiments, colons, including intra-basin part and anus, were removed from the animals, washed with PBS (10010001, ThermoFisher Scientific) at room temperature (RT) and separated onto proximal and distal parts *ex vivo*. Firstly, anus and rectum were cut out (approximately 4 mm from the anus), secondly proximal colon was defined as the first 1/4 of the residual tube, starting from the caecum; distal colon was defined as last 4/4, and segments were separated with the scalpel. Segments were further perpendicularly cut into 3-4 mm pieces and fixed in 4% Paraformaldehyde (PFA) /PBS solution (5 mL per segment) for 1h at RT with mild agitation. PFA 4% solution was prepared on the same day (30525-89-4, Electron Microscopy Sciences) with 10xDPBS (1x final concentration, 14080055, ThermoFisher Scientific) and distilled water (15230001, ThermoFisher Scientific). After fixation, tissue was washed 3 times with PBS (10010056, ThermoFisher Scientific) and processed for the staining.

Immunostaining of colonic tissue sections

Tissue was dehydrated in 15% sucrose (m/v, S8501, Sigma-Aldrich)/PBS solution for 1h and after in 30% sucrose/PBS solution for 2h at RT or overnight (O/N) at 4C (until tissue fragments sunk). After, tissue was embedded with Optimal Cutting Temperature compound (OCT, 4583, Sakura finetek France SAS) in plastic base molds (62352-15, Euromedex), frozen at -20°C and cut on the cryostat using SuperFrost Plus™ Adhesion slides (631-9483, VWR, Menzel Gläser). Tissue sections were left for several minutes to melt and covered in PBS to prevent drying until the permeabilization step. Sections were after permeabilized with 0.2 % Triton x100 (T8787, Sigma-Aldrich)/PBS solution for 1h at RT; blocked with 3% Bovine Serum Albumin (BSA, m/v, IgG-Free, Protease-Free, 001-000-162, Jackson Immuno Research), serum of the host of the secondary antibody (donkey or goat serum, depending on the staining, 1:20 dilution, 017-000-121 and 005-000-121 respectively, Jackson Immuno Research) in 0.05% Triton x100/PBS solution for 1h at RT; and stained with primary antibody

O/N in humidified chambers at RT. Sections were then washed 3 times with 0.05% Tx100/PBS solution for 1h; incubated with secondary antibodies, DAPI and phalloidin, depending on the staining, for 4h at RT; washed 3 times in 0.05% Tx100/PBS solution for 1h and mounted using AquaPolyMount (18606-5, Polysciences). In case the FACS-conjugated antibodies were used (CD11c-APC, CD64-BV421) for co-labeling with other antibodies, they were added after the secondary antibody wash-out and incubated O/N at RT. After samples were later washed 3 additional times with 0.05% Tx100/PBS solution for 1h and mounted. After drying for 1h in the dry incubator at 37C or O/N at the RT, samples were ready for the imaging. All antibodies (references and dilutions) are presented in the Sup. Table 3.

Whole-mount staining of colonic tissue

Fixed tissue was sliced perpendicularly to the intestinal length with the scalpel into 1 mm tissue sections and placed in the Eppendorf tubes filled with PBS (1 tube per staining, 4-6 sections per tube). The staining was performed as described above with slight modifications: permeabilization was performed with 1% Triton X-100 in PBS for 1h at RT (500 uL per Eppendorf tube), all antibody solutions and washing steps were performed using 0.2% Triton X-100 in PBS, under mild shaking conditions (2 mL per Eppendorf tube) and concentration of antibodies was increased (see the supplementary table 3, 150 uL of the final antibody solution per Eppendorf tube). Incubations with antibodies were done without agitation.

Confocal Microscopy

Images were acquired using an inverted confocal microscope (Leica DMi8, SP8 scanning head unit), equipped with HC PL APO CS2 40x/1.30 OIL objective, with a regular pixel size of 284 nm (x, y dimensions), 0,5 -1 um (z dimension) and a resolution of 1024x1024 pixels. For high-resolution BLP structural imaging, deconvolution was used. For these acquisitions we have performed oversampling (pixel size of 36 nm (x, y dimensions) and 0.2 (z dimension)) on the zoomed fragment of the tissue. For all types of acquisition Hybrid Detectors were used. Deconvolution was performed with Huygens Essential Software pack.

Correlative light - transmission electron microscopy (TEM)

Distal colon tissue of CD11c: Cre/R26^{mTmG} mice was fixed in 4% PFA prepared in 0,1M phosphate buffer from 16% aqueous stock (30525-89-4, Electron Microscopy Sciences) and incubated 1h at RT with mild agitation. Tissue was then washed 3 times in the regular PBS without Ca^{2+} and Mg^{2+} and cryoprotected by O/N incubation with 2,3M sucrose at 4°. Freezing of the tissue and cryosectioning was done as described above and sections were mounted in PBS: glycerol (1:1) without additional staining. BLPs were located using the inverted confocal microscope (Leica DMi8, SP8 scanning head unit) and obtained their x, y, z coordinates. Coverslips were then removed and samples were processed for the immunegold staining. The immunolabeling of cryosections was done as described previously [336], with some modifications. In brief, after 30 min in blocking buffer (0,1% gelatin (104070, Merck), 10% Normal goat serum (ab7481, Abcam) and 1% BSA (A9647, Sigma-Aldrich) in PBS), sections were immunolabelled with rabbit anti-GFP antibodies (ab290, Abcam) followed by 1.4 nm Nanogold labeled Fab' anti-rabbit secondary antibody (#2004-5, Nanoprobes). After washing in PBS, sections were fixed in 2% (vol/vol) glutaraldehyde for 5 min, washed in water and silver enhanced (HQ Silver enhancement kit, Nanoprobes, NY). Finally, tissue was processed for osmication, dehydration, Epon embedding and sectioned based on the coordinates obtained previously for the each BLPs. Images were acquired with a digital camera Quemesa (SIS) mounted on a Tecnai Spirit transmission electron microscope (FEI) operated at 80kV. Montage of the EM and fluorescent confocal images was done in AdobePhotoshop.

Isolation of Intestinal Cell Suspensions and flow cytometry

For preparation of single-intestinal-cell suspension colons were opened with scissors along the intestinal length, proximal and distal colons were separated, washed 3 times in different baths of PBS without Ca^{2+} and Mg^{2+}. Next, tissues were incubated on a magnetic stirrer in complete medium (CM, 2% heat-inactivated Fetal Bovine Serum (FBS) in Ca^{2+}–, Mg^{2+}-free Phenol Red 10X HBSS; H4385 Sigma-Aldrich, St. Louis, MO, USA diluted to 1x in filtered H_2O) in the presence of 1 mM DTT (D9779, Sigma-Aldrich, St. Louis, MO, USA) and EDTA (15575-038 from Invitrogen) at 37°C for 30 min and subsequently incubated with 1 mM EDTA in 5% FBS/ PBS at 37°C for 10min. This was followed by incubation with 15mM Hepes (15630-056 from Gibco) in 1% FBS/PBS at RT for 7 min without

agitation. The supernatants containing intestinal epithelial cells were discarded. Isolated tissues were collected and digested using 0.15 mg/mL Liberase^{TM} TL (054010200001, Roche) and 0.1mg/mL DNAse1 (10104159001, Roche) in HBSS at 37°C for 45 min with magnetic agitation. Tissues were then filtered through 100µm cell strainer, and washed in HBSS. Single-cell suspensions were later stained with live-dead stain and Fc-block in a protein-free buffer for 30 min on ice, washed with FACS-buffer (1% BSA, 5% FCS and 2 mM EDTA in PBS), stained with FACS-conjugated antibodies for 20 min on ice, washed and analyzed by flow cytometry. Counting Beads (ACBP-100-10, Spherotech) were used for quantification of cell numbers in the sample and OneComp eBeads™ Compensation Beads (01-1111-42, Thermofisher Scientific, were used as single-color controls for compensation. Dilutions of reagents can be found in Supplemental Table 3. Data was acquired on BD LSRII cytometer and processed with FlowJo vX software. Cell-sorting was performed on BD FACSAria™ sorter.

Single Cell RNA-sequencing using dropseq

RNAseq libraries preparation

Cellular suspension (~5000 cells, with expected recovery of ~3000 cells) of sorted Mϕ from proximal and distal colon of 8 weeks old female C57BL/6J mouse were loaded on the 10X Chromium Controller instrument (10X Genomics) according to the manufacturer's protocol, based on the 10X GEMCode proprietary technology, both samples were processed in one batch. The Chromium Single Cell 3' v2 Reagent kit (10X Genomics) was used to generate the cDNA and prepare the libraries, according to the manufacturer's protocol. The libraries were then equimolarly pooled and sequenced on a Novaseq 6000 (Illumina) in Paired-end 26x91. A coverage of 400M reads per sample was targeted, in order to obtain 100 000 reads per cell. The raw data were then demultiplexed and processed with the Cell Ranger software (10X Genomics) v2.1.1.

Quality check, read alignment, and computation of the UMI counts. FASTQ files are obtained from BCF files using the cellranger mkfastq command from CellRanger v2.1.1. Sequencing quality is assessed using FastQC v11.8. cellranger count command (default parameters) is used to map the reads to the annotated mm10 genome (accession: GCA_000001635.6, gene build: 2016-01), compute UMI counts, and call cellular barcodes.

Processing of the gene-cell expression matrix. The gene-cell expression matrix for each sample is imported in R using Seurat v3.0.0 and normalized as follows: the UMI count of each gene *i* in cell *j* is augmented by 1, divided by the total UMI count for cell *j*, multiplied by 10000, and log-transformed. Cells with less than 200 or more than 4000 detected genes (UMI count ≥ 1) are filtered out. Only the genes detected in ≥ 2 cells in at least one sample are retained. Normalized matrices for the two samples are concatenated to obtain a joint normalized matrix *M* and gene expression is standardized (Z-score) to obtain a scaled matrix *M'*.

Generation of the clustering solution. Feature selection methods and clustering parameters are let vary in order to optimize the definition of the cell populations.

Feature selection is performed on *M* (defined above) using either mean.var.plot or vst method from Seurat. They both model the expression dispersion of each gene in order to detect the candidates that show the highest variability across cells. For mean.var.plot, the average expression is set in [0.1, 0.1] and the scaled dispersion is ≥ *d*, with *d* = 0.5, 1, or 1.5. For vst, the number of top highly variable genes retained is either 500, 1000, or 2000.

A PCA dimensionality reduction is possibly performed on *M'* (defined above) after feature selection. The first 50 principal components (PCs) are calculated using an SVD approximation. The number of PCs to be retained is automatically defined using the approach defined as follows. First, a p-value p_h is computed for each component PC_h using the JackStraw method (Seurat, default parameters). To identify the contribution to the standard deviation that is likely due to noise, we compute the standard deviation σ_{noise} explained on average by PC_{40},…,PC_{50}. The optimal number of top PCs is set to the maximal *h* such that the two conditions $\sigma_h \geq 1.25\sigma_{noise}$ and $p_h \leq 10^{-5}$ simultaneously hold.

Clustering is done using the Waltman and van Eck algorithm, either on the selected features or on the top h PCs, by varying the number of neighbors *k* in {30, 40, 50} and the resolution parameter *r* from 0.1 to 0.5 in steps of 0.1. Overall, 180 clustering solutions are generated: 6 ways to select the features, followed or not by PCA, 3 choices for *k* and 5 choices for *r* in the clustering step.

Selection of the optimal clustering solution and identification of cell populations. Given a clustering solution C, a silhouette width *silh(j)* is computed for each cell *j* using the *n×n* matrix D, where n is the number of cells and D_{jk} is the euclidean distance between cell *j* and cell *k*, computed on the same

space where C is calculated (features or PCs). The average silhouette width across a cluster *c* will be referred to as *silh(c)*.

For each solution, the putative BLP$^+$ Mϕ cluster is defined as the largest whose fraction of cells in the distal colon is greater than in the proximal colon. Among the solutions *C* whose expected fraction of BLP$^+$ Mϕ (based on IHC) is < 0.4 in the proximal colon and comprised between 0.5 and 0.7 in the distal colon, we select the one such that the average between *silh(C)* and *silh(BLP$^+$ Mϕ)* is maximal. The optimal solution contains five clusters (top 1000 variable genes selected with vst, selection of the first 22 PCs, and clustering with parameters $k = 30$ and $r = 0.1$). A tSNE is computed (using default parameters) on the same input used for clustering.

Differential expression analysis and clusters annotation. Differential expression analysis between each cluster and its complementary or between two clusters is performed using the MAST method on the optimal solution defined at the previous step. Genes detected (UMI count > 0) in ≥ 10% cells in one of the two conditions, with $|\log_2 FC| > 0.5$, and adjusted p-value < 0.05 (Bonferroni correction) are defined as differentially expressed. Two clusters expressing higher level of fibroblast markers (Acta2, Dcn, Des, Lamb1, Lama4, Lamc1, Tpm2, Nid1) and of epithelial cell markers (Krt8, Muc2, Krt19, Car1, Krt18, Car4), respectively, and one cluster expressing lower level of the Mϕ marker Itgam (Cd11b) are filtered out, resulting in two remainder clusters for downstream analysis, which will be referred to as BLP$^+$ Mϕ and BLP$^-$ Mϕ, respectively.

Comparison with published colon Mϕ datasets. Processed single-cell RNA-Seq data from monocyte-derived phagocytes in mouse colon are retrieved from (Kang et al.). First, we assess the expression of mature Mϕ signatures (Schridde et al.), namely, the expression of up-regulated genes from P1 (monocytes) to P4 (mature Mϕ), in the seven Mϕ sub-populations identified by Kang *et al*. Second, we compare the two Mϕ sup-populations whose size is decreased in germ-free mice compared to specific pathogen-free mice, corresponding to clusters 4 and 6 in (Kang et al.), to BLP$^+$ Mϕ and BLP$^-$ Mϕ. The genes tested for differential expression between cluster 4 and 6 that are detected in ≥ 10% cells in either cluster 4 or 6, with $|\log_2 FC| > 0.5$, and adjusted p-value < 0.05 (Bonferroni correction) are defined as differentially expressed. We intersect the up-regulated DEGs in BLP$^+$ Mϕ with the up-regulated DEGs in cluster 4 and compute the probability of observing an equal or higher odds-ratio (maximum-likelihood estimate) with a Fisher's exact test (using the R function fisher.test) using the

genes detected in at least 20 cells across BLP^+ Mϕ and BLP^- Mϕ as background. Comparison of the up-regulated DEGs in BLP^- Mϕ and in cluster 6 is evaluated with the same procedure.

Microbiota depletion

Antibiotics cocktail was prepared as described previously [337] and contained Ampicillin A9393 1mg/mL+ Gentamicin sulfate G4918 1mg/mL + Vancomycin 861987 0,5mg/mL+ Metronidazole M1547 1mg/mL+ Neomycin trisulfate salt N1876 1mg/mL (all products purchased at Sigma-Aldrich). For fungi depletion, fluconazole (0,5 mg/mL, F8929, Sigma-Aldrich) and amphotericin B (1 mg/kg, A9528, Sigma-Aldrich) were used. Mice were force-fed for 10 (for fluconazole and antibiotics treatment) or 14 (for amphotericin B treatment) consecutive days by using plastic feeding tubes (FTP-20-38-50, Phymep) greased with Vaseline. Volume of the fed solution was normalized to the weight of an animal (200 uL / 20 g mouse). Solutions were kept at +4C in the dark, and renewed every 5 days.

Bacterial and Fungal colonization of germ-free mice

8-10-week-old germ-free mice were orally either force-fed with Altered Schaedler flora (ASF) or *C. albicans*. After bacterial or fungal colonization, all mice were maintained within sterile vinyl isolators for 3 weeks and then sacrificed to obtain colonic tissues. For bacterial colonization, cecal contents from a ASF mouse were directly diluted with 5 mL sterile PBS to obtain ASF solution. Then each germ-free mouse was fed with 300 □L ASF cecal contents solution. For fungal colonization, *C. albicans* strain (SC 5314, (1 x 10^8 CFU/mouse) were cultured in Sabouraud dextrose broth (SDB) and then washed by sterile PBS twice before oral inoculation.

Intra-rectal infusions

The main driving force for water absorption by colonic epithelium is the osmolarity gradient [299], with the colonic stroma osmolarity of 800-1000 mOsmol/kg [338]. Based on these studies, we have chosen to infuse the solution which is hypotonic to the stroma (DPBS with Ca^{2+} and Mg^{2+} with osmolarity of 290-315 mOsmol/kg, half-diluted in the distilled water). Solutions were prepared 30 min before the infusion at latest and volumes were adjusted to the weight of the individual mice (150uL per 20g mouse). Solutions were pre-heated to 37C just before infusion into the animals.

Hydrazide coupled with Alexa Fluor™ 633 (A30634, Thermo Fisher Scientific) was used to trace fluid absorption. Stock solution (25x, 10 mg/mL) was prepared by diluting 1 mg into 100 uL of sterile distilled water and kept at -20C prior to use. Final infusion solution contained 0,4 mg/mL Hydrazide Alexa Fluor™ 633, DPBS (10x with Ca^{2+} and Mg^{2+}, 1:20 diluted), and sterile distilled water.

Gliotoxin (G9893-5MG, Sigma-Aldrich) solution was prepared and used immediately after the purchase and never kept at -20C or at +4C. Stock solution (383x) was prepared by diluting 5 mg into 1 mL of sterile DMSO. Final infusion solution was prepared on ice and contained 13 µg/mL of Gliotoxin, 0,4 mg/ml Hydrazide-AlexaFluor633, DPBS (10x, 1:20 diluted), and sterile distilled water. Solution was kept on ice in the dark and was heated for 3 min before the infusion.

T-2 (T4887-25MG, Sigma-Aldrich) solution was prepared using DMSO and stored at -80C prior use no longer than 2 weeks. Animals were infused with 1mg/kg of T-2 toxin. Final infusion solution was prepared on ice and contained T-2 toxin, 0,4 mg/ml Hydrazide-AlexaFluor633, DPBS (10x, 1:20 diluted), and sterile distilled water. Solution was kept on ice in the dark and was heated for 3 min before the infusion.

Candidalysin (PCT-4494-v, Peptides International) solution was prepared using DMSO and stored at -80C prior use no longer than 2 weeks. Animals were infused with 75 µg/kg of Candidalysin. Final infusion solution was prepared on ice and contained Candidalysin, 0,4 mg/ml Hydrazide-AlexaFluor633, DPBS (10x, 1:20 diluted), and sterile distilled water. Solution was kept on ice in the dark and was heated for 3 min before the infusion.

To empty the distal colon prior to infusion, mice's stomachs were massaged 5-7 times with 5 min intervals. Animals were then placed under isoflurane gas anesthesia (2.5% v/v), on the heating pad, their breath rate was monitored and percentage of the isoflurane was adjusted based on the breathing rhythm. If mice were showing signs of suffocation, isoflurane dose was decreased. Efficiency of anesthesia was validated prior to the infusion, by the loss of pedal withdrawal reflex. To avoid dehydration animals were subcutaneously injected with warm 0,9% NaCl, 100 uL per animal. After 10 min from the start of anesthesia administration if pedal withdrawal reflex was lost, pre-heated infusion solution was administrated through 1mL syringe with connected plastic feeding tube (FTP-20-38-50, Phymep). Tube's tip was immersed in the infusion solution to facilitate the intra-

rectal insertion. Because the infusion solution was rapidly excreted in the majority of animals, the excreted solution was collected and re-infused every 5 min.

Colonic permeability measurement

To monitor the efficiency of systemic absorption through the colon mucosa, mice were infused with Hydrazide Alexa Fluor™ 633 in hypotonic solution as described above. To measure efficiency of absorption into the blood, 2 min 30 sec prior to the end of the infusion, thorax was cut open and blood was collected by cardiac puncture from the left ventricle. Since absorption of hemoglobin may interact with absorption/emission of Alexa Fluor™ 633, we applied following procedures to avoid hemolysis, such as: (1) use of pre-heated 20G needles with 1mL syringe (2) horizontal positioning of the syringe during the cardiac puncture to decrease the force applied to collect blood (3) slow blood collection and withdrawal into the 2 mL Eppendorf tubes, on average collection was taking 2 min and withdrawal – 30 sec. After the blood collection, Eppendorf tubes were placed in the dark and were left to coagulate for 30 min at RT. After blood was centrifuged at 2200 rcf at 10-15C for 15 min and serum (supernatant) was collected into new 1.5 ml Eppendorf tubes. After the second centrifugation at 2200 rcf at 10-15C for 10 min, serum (supernatant) was placed in 96 well plate, calibration curves were prepared by serial dilutions of Hydrazide Alexa Fluor™ 633, and fluorescence intensity was read on CLARIOstar™ plate reader (BMG LABTECH Inc). To measure the efficiency of epithelial absorption, colon tissues were fixed and stained with phalloidin, DAPI and Laminin antibodies. After z-stacks were acquired for every section and amount of Hydrazide positive epithelial cells were quantified and normalized per number of crypts.

Stimulation of water absorption by aldosterone administration

We used aldosterone injections to stimulate water absorption specifically in distal colon [339–341]. To partially repress endogenous aldosterone production, mice received 0.3% of NaCl in drinking water at least 5 days prior to the injection, as described previously [342,343]. Mice were after i.p. injected with aldosterone (10 mg/kg, in 0.33% ethanol and 0.9% NaCl, A9477, Sigma-Aldrich), sacrificed after 2, 4, 6 and 8 hours and tissue were treated as described above. Control animals were injected with the solvent and sacrificed 2h and 8h after the injection.

Laxative treatment

Bisacodyl, stimulant laxative, which stimulates Cl^- secretion in the colon and not in the small intestine was used to decrease water absorption [300,344]. As described previously [300], bisacodyl was administrated by oral gavage (20 mg/kg, B1390, Sigma-Aldrich) and mice were sacrificed 5h later. In addition, indomethacin (10 mg/kg, I7378, Sigma-Aldrich) was i.p. injected 15 min before oral administration of bisacodyl, to inhibit the bisacodyl activity, other conditions received injection of the solvent.

Anti-CSF1R antibody – mediated macrophage depletion

To produce anti-CSF1R antibody we used the hybridoma cell line AFS98, which was cultured in protein-free hybridome medium (PFHM-II Gibco ref: 12040-077) in disposable reactor cell culture flasks (CELLine 1000 Wheaton ref: WCL1000-1) for 7 days, and antibodies were purified with disposable PD10 desalting columns (GE healthcare ref: 17-0851-01). Mice were i.p. injected with 37.5 mg/kg of antibodies, diluted in PBS every 24h for 3 consecutive days and killed 24h after the 3rd injection.

Quantification And Statistical Analysis

Image analysis and processing

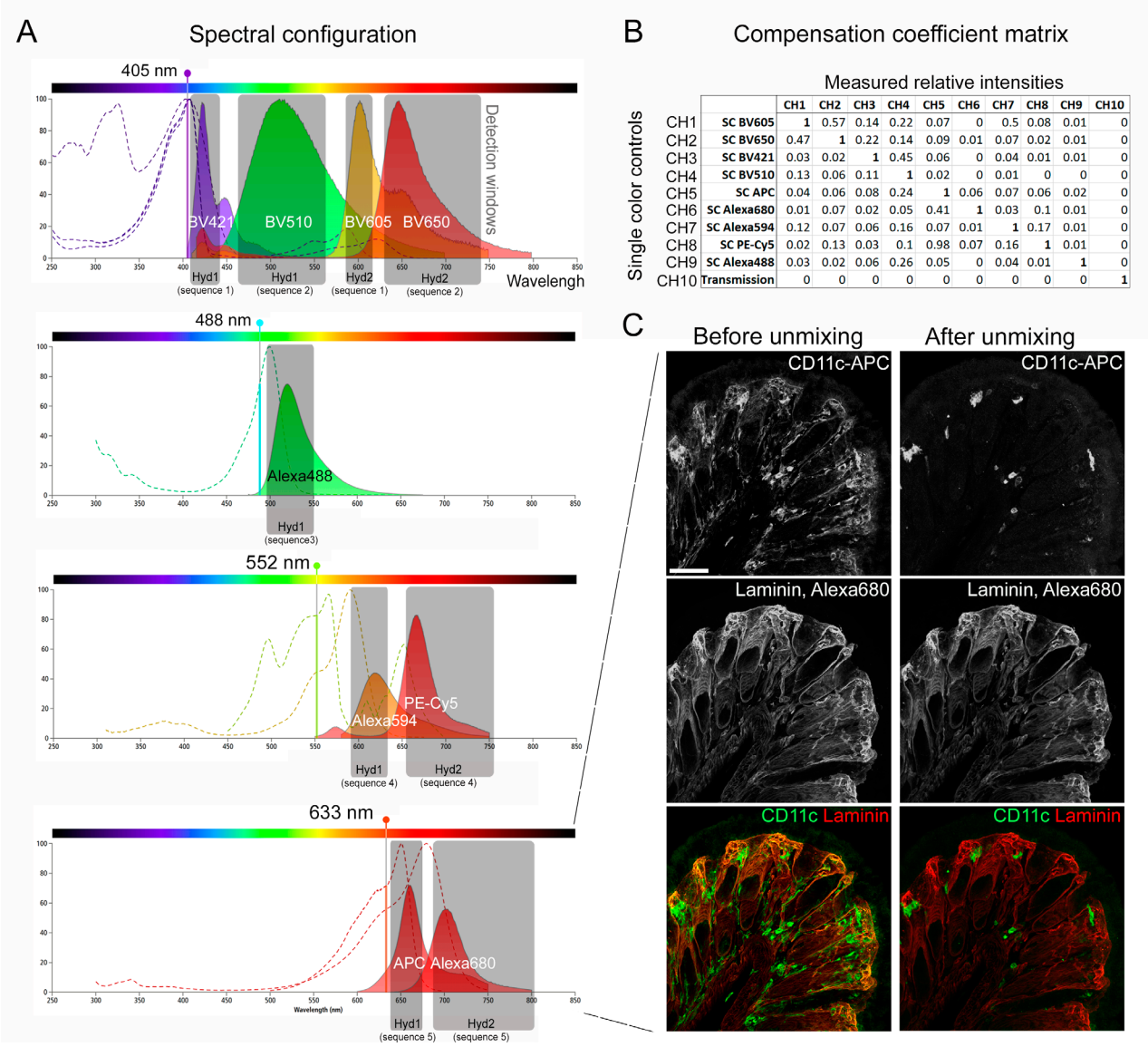
Image analysis and processing was performed using Fiji software [345]. Quantification of BLPs and macrophages were performed using the CellCounter build-in plugin, by manually counting the number of BLPs and crypts on every slide of the acquired z-stack. 3D reconstructions and movies were created using Imaris software.

For experiments with more than 4 colors staining, un-mixing approach was used to remove fluorophores spillover. As described in [346], we used single stain tissues to obtain compensation coefficients that were after applied to perform spectral un-mixing using an homemade Fiji macro.

First, we have chosen the fluorophores combination to minimize crosstalk in between fluorescent emissions when It was impossible to separate the dyes on excitation. A maximum of a 9 colors configuration with 4 lasers set up was used (Fig. 18A). Second, to choose the fluorophore for each particular antigen, we evaluated the staining efficiency. To do so, we performed individual staining

for each particular antigen using the same fluorophore and then we attributed the less efficient staining to the channel that receive less spillover contribution from the other channels. Additionally, staining that label the same cells/structures were put in channels with minimized cross-talk. Third, to obtain compensation coefficients, single stained tissues were imaged with the same microscope settings used for tissues stained with the whole panel of antibodies. Coefficients were calculated as described previously [347] and imported into the matrix (Fig. 18B). After inverse matrix was calculated using Excel and contained compensation coefficients used for spectral un-mixing. Additional details are available on the macro code.

Figure 17. Spectral unmixing



Statistics

Statistical significance was calculated between two groups by Mann-Whitney test. Multiple comparison Kruskal-Wallis, Dunn`s and Holm-Sidak's tests were used to calculate statistical significance between multiple groups. Analyses were performed using GraphPad Prism 8 software. Error bars represent SEM and $p < 0.05$ was considered statistically significant (*$p < 0.05$, **$p < 0.01$, ***$p < 0.001$).

Bibliography

1. Al-Bahrani, A.Z., Darwish, A., Hamza, N., Benson, J., Eddleston, J.M., Snider, R.H., Nylén, E.S., Becker, K.L., Barclay, G.R., and Ammori, B.J. (2010). Gut barrier dysfunction in critically ill surgical patients with abdominal compartment syndrome. Pancreas *39*, 1064–1069.
2. Fishman, J.E., Levy, G., Alli, V., Zheng, X., Mole, D.J., and Deitch, E.A. (2014). The intestinal mucus layer is a critical component of the gut barrier that is damaged during acute pancreatitis. Shock *42*, 264–270.
3. Anbazhagan, A.N., Priyamvada, S., Alrefai, W.A., and Dudeja, P.K. (2018). Pathophysiology of IBD associated diarrhea. Tissue Barriers *6*, 1–21. Available at: https://doi.org/10.1080/21688370.2018.1463897.
4. Michielan, A., and D'Incà, R. (2015). Intestinal Permeability in Inflammatory Bowel Disease: Pathogenesis, Clinical Evaluation, and Therapy of Leaky Gut. Mediators Inflamm. *2015*, 1–10.
5. Yoseph, B.P., Klingensmith, N.J., Liang, Z., Breed, E.R., Burd, E.M., Mittal, R., Dominguez, J.A., Petrie, B., Ford, M.L., and Coopersmith, C.M. (2016). Mechanisms of Intestinal Barrier Dysfunction in Sepsis. Shock *46*, 52–59.
6. de Haan, J.J., Lubbers, T., Derikx, J.P., Relja, B., Henrich, D., Greve, J.W., Marzi, I., and Buurman, W.A. (2009). Rapid development of intestinal cell damage following severe trauma: A prospective observational cohort study. Crit. Care *13*, 1–7.
7. Swank, G.M., and Deitch, E.A. (1996). Role of the gut in multiple organ failure: Bacterial translocation and permeability changes. World J. Surg. *20*, 411–417.
8. Naftalin, R.J. (1994). The dehydrating function of the descending colon in relationship to crypt function. Physiol. Res. *43*, 65–73.
9. Donaldson, G.P., Lee, S.M., and Mazmanian, S.K. (2015). Gut biogeography of the bacterial microbiota. Nat. Rev. Microbiol. *14*, 20–32.
10. Flynn, K.J., Ruffin, M.T., Kim Turgeon, D., and Schloss, P.D. (2018). Spatial variation of the native colon microbiota in healthy adults. Cancer Prev. Res. *11*, 393–401.
11. Scupham, A.J., Presley, L.L., Wei, B., Bent, E., Griffith, N., McPherson, M., Zhu, F., Oluwadara, O., Rao, N., Braun, J., *et al.* (2006). Abundant and diverse fungal microbiota in the murine intestine. Appl. Environ. Microbiol. *72*, 793–801.

12. Leonardi, I., Li, X., Semon, A., Li, D., Doron, I., Putzel, G., Bar, A., Prieto, D., Rescigno, M., McGovern, D.P.B., *et al.* (2018). CX3CR1+, mononuclear phagocytes control immunity to intestinal fungi. Science (80-.). *359*, 232–236.

13. Iliev, I.D., Funari, V.A., Taylor, K.D., Nguyen, Q., Reyes, C.N., Strom, S.P., Brown, J., Becker, C.A., Fleshner, P.R., Dubinsky, M., *et al.* (2012). Interactions between commensal fungi and the C-type lectin receptor dectin-1 influence colitis. Science (80-.). *336*, 1314–1317.

14. Upperman, J.S., Potoka, D.A., Zhang, X.R., Wong, K., Zamora, R., and Ford, H.R. (2003). Mechanism of intestinal-derived fungal sepsis by gliotoxin, a fungal metabolite. J. Pediatr. Surg. *38*, 966–970.

15. Akbari, P., Braber, S., Varasteh, S., Alizadeh, A., Garssen, J., and Fink-Gremmels, J. (2017). The intestinal barrier as an emerging target in the toxicological assessment of mycotoxins. Arch. Toxicol. *91*, 1007–1029.

16. Goossens, J., Pasmans, F., Verbrugghe, E., Vandenbroucke, V., De Baere, S., Meyer, E., Haesebrouck, F., De Backer, P., and Croubels, S. (2012). Porcine intestinal epithelial barrier disruption by the Fusarium mycotoxins deoxynivalenol and T-2 toxin promotes transepithelial passage of doxycycline and paromomycin. BMC Vet. Res. *8*, 1–10.

17. Allert, S., Förster, T.M., Svensson, C.M., Richardson, J.P., Pawlik, T., Hebecker, B., Rudolphi, S., Juraschitz, M., Schaller, M., Blagojevic, M., *et al.* (2018). Candida albicans-induced epithelial damage mediates translocation through intestinal barriers. MBio *9*, 1–20.

18. Smith, P.D., Smythies, L.E., Shen, R., Greenwell-Wild, T., Gliozzi, M., and Wahl, S.M. (2011). Intestinal macrophages and response to microbial encroachment. Mucosal Immunol. *4*, 31–42.

19. Cummings, R.J., Barbet, G., Bongers, G., Hartmann, B.M., Gettler, K., Muniz, L., Furtado, G.C., Cho, J., Lira, S.A., and Blander, J.M. (2016). Different tissue phagocytes sample apoptotic cells to direct distinct homeostasis programs. Nature *539*, 565–569. Available at: http://dx.doi.org/10.1038/nature20138.

20. Sisirak, V., Sally, B., D'Agati, V., Martinez-Ortiz, W., Özçakar, Z.B., David, J., Rashidfarrokhi, A., Yeste, A., Panea, C., Chida, A.S.S., *et al.* (2016). Digestion of Chromatin in Apoptotic Cell Microparticles Prevents Autoimmunity. Cell *166*, 88–101.

21. Pull, S.L., Doherty, J.M., Mills, J.C., Gordon, J.I., and Stappenbeck, T.S. (2005). Activated macrophages are an adaptive element of the colonic epithelial progenitor niche necessary for regenerative responses to injury. Proc. Natl. Acad. Sci. U. S. A. *102*, 99–104.

22. Muller, P.A., Koscsó, B., Rajani, G.M., Stevanovic, K., Berres, M.L., Hashimoto, D., Mortha, A., Leboeuf, M., Li, X.M., Mucida, D., *et al.* (2014). Crosstalk between muscularis macrophages and enteric neurons regulates gastrointestinal motility. Cell *158*, 300–313.

23. Ueda, Y., Kayama, H., Jeon, S.G., Kusu, T., Isaka, Y., Rakugi, H., Yamamoto, M., and Takeda, K. (2010). Commensal microbiota induce LPS hyporesponsiveness in colonic macrophages via the production of IL-10. Int. Immunol. *22*, 953–962.

24. S.Shouval, D., Biswas, A., Goettel, J.A., McCann, K., Conaway, E., Naresh, S.R., Mascanfroni, I.D., Adham, Z. Al, Lavoie, S., Ibourk, M., *et al.* (2017). Interleukin-10 Receptor Signaling in Innate Immune Cells Regulates Mucosal Immune Tolerance and Anti-Inflammatory Macrophage Function. Physiol. Behav. *176*, 139–148.

25. Zigmond, E., Bernshtein, B., Friedlander, G., Walker, C.R., Yona, S., Kim, K.W., Brenner, O., Krauthgamer, R., Varol, C., Müller, W., *et al.* (2014). Macrophage-restricted interleukin-10 receptor deficiency, but not IL-10 deficiency, causes severe spontaneous colitis. Immunity *40*, 720–733.

26. Brockmann, L., Gagliani, N., Steglich, B., Giannou, A.D., Kempski, J., Pelczar, P., Geffken, M., Mfarrej, B., Huber, F., Herkel, J., *et al.* (2017). IL-10 Receptor Signaling Is Essential for T R 1 Cell Function In Vivo . J. Immunol. *198*, 1130–1141.

27. Mazzini, E., Massimiliano, L., Penna, G., and Rescigno, M. (2014). Oral Tolerance Can Be Established via Gap Junction Transfer of Fed Antigens from CX3CR1+ Macrophages to CD103+ Dendritic Cells. Immunity *40*, 248–261. Available at: http://dx.doi.org/10.1016/j.immuni.2013.12.012.

28. Schulthess, J., Pandey, S., Capitani, M., Rue-Albrecht, K.C., Arnold, I., Franchini, F., Chomka, A., Ilott, N.E., Johnston, D.G.W., Pires, E., *et al.* (2019). The Short Chain Fatty Acid Butyrate Imprints an Antimicrobial Program in Macrophages. Immunity *50*, 432-445.e7.

29. Denning, T.L., Norris, B.A., Medina-Contreras, O., Manicassamy, S., Geem, D., Madan, R., Karp, C.L., and Pulendran, B. (2011). Functional Specializations of Intestinal Dendritic Cell and Macrophage Subsets That Control Th17 and Regulatory T Cell Responses Are Dependent on the T Cell/APC Ratio, Source of Mouse Strain, and Regional Localization. J. Immunol. *187*, 733–747.

30. Nagashima, R., Maeda, K., Imai, Y., and Takahashi, T. (1996). Lamina propria macrophages in the human gastrointestinal mucosa: Their distribution, immunohistological phenotype, and function. J. Histochem. Cytochem. *44*, 721–731.

31. Kang, B., Alvarado, L.J., Kim, T., Lehmann, M.L., Cho, H., He, J., Li, P., Kim, B.-H., Larochelle, A., and Kelsall, B.L. (2020). Commensal microbiota drive the functional diversification of colon macrophages. Mucosal Immunol. *13*, 216–229. Available at: http://www.nature.com/articles/s41385-019-0228-3.

32. Nalle, S.C., and Turner, J.R. (2015). Intestinal barrier loss as a critical pathogenic link between inflammatory bowel disease and graft-versus-host disease. Mucosal Immunol. *8*, 720–730.

33. Mescher, A.. (2013). Junqueira`s Basic Histology.

34. Young, B., Woodford, P., and O`Dowd, G. (2014). Wheater`s Functional Histology Available at: http://dx.doi.org/10.1016/j.tws.2012.02.007.

35. Kiela, P.R., and Ghishan, F.K. (2016). Physiology of Intestinal Absorption and Secretion. Best Pr. Res Clin Gastroenterol. *30*, 145–159. Available at: http://www.ncbi.nlm.nih.gov/pubmed/5993931.

36. Kramer, P. (1966). The effect of varying sodium loads on the ileal excreta of human ileostomized subjects. J. Clin. Invest. *45*, 1710–1718.

37. Harris, J., and Shields, R. (1970). Absorption and secretion of water and electrolytes by the intact human colon in diffuse untreated proctocolitis. Gut *11*, 27–33.

38. Gunawardene, A.R., Corfe, B.M., and Staton, C.A. (2011). Classification and functions of enteroendocrine cells of the lower gastrointestinal tract. Int. J. Exp. Pathol. *92*, 219–231.

39. Li, Y., Hao, Y., Fan, F., and Zhang, B. (2018). The Role of Microbiome in Insomnia, Circadian Disturbance and Depression. Front. Psychiatry *9*, 1–11.

40. Rehfeld, J.F. (2014). Gastrointestinal Hormones and Their Targets. In Advances in Experimental Medicine and Biology, pp. 157–175. Available at: http://link.springer.com/10.1007/978-1-4939-0897-4.

41. Moran-Ramos, S., Tovar, A.R., and Torres, N. (2012). Diet: Friend or Foe of Enteroendocrine Cells: How It Interacts with Enteroendocrine Cells. Adv. Nutr. *3*, 8–20. Available at: http://libproxy.usc.edu/login?url=https://search.proquest.com/docview/615271524?accountid=14749%250Ahttps://usc-primo.hosted.exlibrisgroup.com/openurl/01USC/01USC_SP??url_ver=Z39.88-2004&rft_val_fmt=info:ofi/fmt:kev:mtx:journal&genre=article&sid=ProQ:ProQ.

42. Raybould, H.E. (2007). Mechanisms of CCK signaling from gut to brain. Curr. Opin. Pharmacol. *7*, 570–574.

43. Ye, L., Mueller, O., Bagwell, J., Bagnat, M., Liddle, R.A., and Rawls, J.F. (2019). High fat diet induces microbiota-dependent silencing of enteroendocrine cells. Elife *8*, 1–39.

44. Dominguez-Bello, M.G., Costello, E.K., Contreras, M., Magris, M., Hidalgo, G., Fierer, N., and Knight, R. (2010). Delivery mode shapes the acquisition and structure of the initial microbiota across multiple body habitats in newborns. Proc. Natl. Acad. Sci. U. S. A. *107*, 11971–11975.

45. Barile, D., and Rastall, R.A. (2013). Human milk and related oligosaccharides as prebiotics. Curr. Opin. Biotechnol. *24*, 214–219. Available at: http://dx.doi.org/10.1016/j.copbio.2013.01.008.

46. De Vadder, F., Grasset, E., Holm, L.M., Karsenty, G., Macpherson, A.J., Olofsson, L.E., and Bäckhed, F. (2018). Gut microbiota regulates maturation of the adult enteric nervous system via enteric serotonin networks. Proc. Natl. Acad. Sci. U. S. A. *115*, 6458–6463.

47. Sudo, N., Chida, Y., Aiba, Y., Sonoda, J., Oyama, N., Yu, X.N., Kubo, C., and Koga, Y. (2004). Postnatal microbial colonization programs the hypothalamic-pituitary-adrenal system for stress response in mice. J. Physiol. *558*, 263–275.

48. Liang, S., Wu, X., and Jin, F. (2018). Gut-brain psychology: Rethinking psychology from the microbiota–gut–brain axis. Front. Integr. Neurosci. *12*, 1–24.

49. Hulme, H., Meikle, L.M., Strittmatter, N., van der Hooft, J.J.J., Swales, J., Bragg, R.A., Villar, V.H., Ormsby, M.J., Barnes, S., Brown, S.L., *et al.* (2020). Microbiome-derived carnitine

mimics as previously unknown mediators of gut-brain axis communication. Sci. Adv. *6*, 1–11.

50. Strandwitz, P. (2018). Neurotransmitter modulation by the gut microbiota. Brain Res. *1693*, 128–133.

51. Lyte, M. (2004). Microbial endocrinology and infectious disease in the 21st century. Trends Microbiol. *12*, 14–20.

52. Yu, Y., Yang, W., Li, Y., and Cong, Y. (2020). Enteroendocrine Cells: Sensing Gut Microbiota and Regulating Inflammatory Bowel Diseases. Inflamm. Bowel Dis. *26*, 11–20.

53. Kulkarni, S., Ganz, J., Bayrer, J., Becker, L., Bogunovic, M., and Rao, M. (2018). Advances in enteric neurobiology: The "brain" in the gut in health and disease. J. Neurosci. *38*, 9346–9354.

54. Bonaz, B., Bazin, T., and Pellissier, S. (2018). The vagus nerve at the interface of the microbiota-gut-brain axis. Front. Neurosci. *12*, 1–9.

55. Kraft, S.C., Earle, R.H., Roesler, M., and Esterly, J.R. (1976). Unexplained Bronchopulmonary Disease with Inflammatory Bowel Disease. Arch. Intern. Med. *136*, 454–459.

56. Williams, A.E., Edwards, L., and Hussell, T. (2006). Colonic Bacterial Infection Abrogates Eosinophilic Pulmonary Disease. J. Infect. Dis. *193*, 223–230.

57. Verhasselt, V., Milcent, V., Cazareth, J., Kanda, A., Fleury, S., Dombrowicz, D., Glaichenhaus, N., and Julia, V. (2008). Breast milk-mediated transfer of an antigen induces tolerance and protection from allergic asthma. Nat. Med. *14*, 170–175.

58. Skalski, J.H., Limon, J.J., Sharma, P., Gargus, M.D., Nguyen, C., Tang, J., Coelho, A.L., Hogaboam, C.M., Crother, T.R., and Underhill, D.M. (2018). Expansion of commensal fungus Wallemia mellicola in the gastrointestinal mycobiota enhances the severity of allergic airway disease in mice. PLoS Pathog. *14*, 1–24.

59. Wheeler, M.L., Limon, J.J., Bar, A.S., Leal, C.A., Gargus, M., Tang, J., Brown, J., Funari, V.A., Wang, H.L., Crother, T.R., *et al.* (2016). Immunological Consequences of Intestinal Fungal Dysbiosis. Cell Host Microbe *19*, 865–873. Available at: http://dx.doi.org/10.1016/j.chom.2016.05.003.

60. Ruane, D., Brane, L., Reis, B.S., Cheong, C., Poles, J., Do, Y., Zhu, H., Velinzon, K., Choi, J.H., Studt, N., *et al.* (2013). Lung dendritic cells induce migration of protective T cells to the gastrointestinal tract. J. Exp. Med. *210*, 1871–1888.

61. Madan, J.C., Koestle, D.C., Stanton, B.A., Davidson, L., Moulton, L.A., Housman, M.L., Moore, J.H., Guill, M.F., Morrison, H.G., Sogin, M.L., *et al.* (2012). Serial analysis of the gut and respiratory microbiome. MBio *3*, 1–10.

62. Liu, T., Yang, Z., Zhang, X., Han, N., Yuan, J., and Cheng, Y. (2017). 16S rDNA analysis of the effect of fecal microbiota transplantation on pulmonary and intestinal flora. 3 Biotech *7*.

63. Cummings, J.H., and Macfarlane, G.T. (1991). The control and consequences of bacterial fermentation in the human colon. J. Appl. Bacteriol. *70*, 443–459.

64. Trompette, A., Gollwitzer, E.S., Yadava, K., Sichelstiel, A.K., Sprenger, N., Ngom-Bru, C., Blanchard, C., Junt, T., Nicod, L.P., Harris, N.L., *et al.* (2014). Gut microbiota metabolism of dietary fiber influences allergic airway disease and hematopoiesis. Nat. Med. *20*, 159–166.

65. Cait, A., Hughes, M.R., Antignano, F., Cait, J., Dimitriu, P.A., Maas, K.R., Reynolds, L.A., Hacker, L., Mohr, J., Finlay, B.B., *et al.* (2018). Microbiome-driven allergic lung inflammation is ameliorated by short-chain fatty acids. Mucosal Immunol. *11*, 785–795. Available at: http://dx.doi.org/10.1038/mi.2017.75.

66. Dang, A.T., and Marsland, B.J. (2019). Microbes, metabolites, and the gut–lung axis. Mucosal Immunol. *12*, 843–850.

67. Trompette, A., Gollwitzer, E.S., Pattaroni, C., Lopez-Mejia, I.C., Riva, E., Pernot, J., Ubags, N., Fajas, L., Nicod, L.P., and Marsland, B.J. (2018). Dietary Fiber Confers Protection against Flu by Shaping Ly6c− Patrolling Monocyte Hematopoiesis and CD8+ T Cell Metabolism. Immunity *48*, 992-1005.e8.

68. Crowson, A.N., Nuovo, G.J., Mihm, M.C., and Magro, C. (2003). Cutaneous Manifestations of Crohn's Disease, Its Spectrum, and Its Pathogenesis: Intracellular Consensus Bacterial 16S rRNA Is Associated with the Gastrointestinal but Not the Cutaneous Manifestations of Crohn's Disease. Hum. Pathol. *34*, 1185–1192.

69. Shah, K.R., Boland, C.R., Patel, M., Thrash, B., and Menter, A. (2013). Cutaneous manifestations of gastrointestinal disease: Part i. J. Am. Acad. Dermatol. *68*, 189.e1-189.e21. Available at: http://dx.doi.org/10.1016/j.jaad.2012.10.037.

70. Salem, I., Ramser, A., Isham, N., and Ghannoum, M.A. (2018). The gut microbiome as a major regulator of the gut-skin axis. Front. Microbiol. *9*, 1–14.

71. O'Neill, C.A., Monteleone, G., McLaughlin, J.T., and Paus, R. (2016). The gut-skin axis in health and disease: A paradigm with therapeutic implications. BioEssays *38*, 1167–1176.

72. Mowat, A.M., and Agace, W.W. (2014). Regional specialization within the intestinal immune system. Nat. Rev. Immunol. *14*, 667–685.

73. Spencer, J., and Sollid, L.M. (2016). The human intestinal B-cell response. Mucosal Immunol. *9*, 1113–1124.

74. Loktionov, A. (2019). Eosinophils in the gastrointestinal tract and their role in the pathogenesis of major colorectal disorders. World J. Gastroenterol. *25*, 3503–3526.

75. Chu, V.T., Beller, A., Rausch, S., Strandmark, J., Zänker, M., Arbach, O., Kruglov, A., and Berek, C. (2014). Eosinophils promote generation and maintenance of immunoglobulin-A-expressing plasma cells and contribute to gut immune homeostasis. Immunity *40*, 582–593.

76. Groschwitz, K.R., Ahrens, R., Osterfeld, H., Gurish, M.F., Han, X., Åbrink, M., Finkelman, F.D., Pejler, G., and Hogan, S.P. (2009). Mast cells regulate homeostatic intestinal epithelial migration and barrier function by a chymase/Mcpt4-dependent mechanism. Proc. Natl. Acad. Sci. U. S. A. *106*, 22381–22386.

77. Nussbaum, J.C., Van Dyken, S.J., Von Moltke, J., Cheng, L.E., Mohapatra, A., Molofsky, A.B.,

Thornton, E.E., Krummel, M.F., Chawla, A., Liang, H.E., *et al.* (2013). Type 2 innate lymphoid cells control eosinophil homeostasis. Nature *502*, 245–248. Available at: http://dx.doi.org/10.1038/nature12526.

78. Schulz, O., Jaensson, E., Persson, E.K., Liu, X., Worbs, T., Agace, W.W., and Pabst, O. (2009). Intestinal CD103+, but not CX3CR1+, antigen sampling cells migrate in lymph and serve classical dendritic cell functions. J. Exp. Med. *206*, 3101–3114.

79. Hadis, U., Wahl, B., Schulz, O., Hardtke-Wolenski, M., Schippers, A., Wagner, N., Müller, W., Sparwasser, T., Förster, R., and Pabst, O. (2011). Intestinal Tolerance Requires Gut Homing and Expansion of FoxP3+ Regulatory T Cells in the Lamina Propria. Immunity *34*, 237–246.

80. Faria, A.M.C., and Weiner, H.L. (2006). Oral tolerance: Therapeutic implications for autoimmune diseases. Clin. Dev. Immunol. *13*, 143–157.

81. Pabst, O., and Mowat, A.M. (2012). Oral tolerance to food protein. Mucosal Immunol. *5*, 232–239. Available at: http://dx.doi.org/10.1038/mi.2012.4.

82. Carter, B.P.B., and Collins, F.M. (1974). The route of enteric infection in normal mice. *139*, 1189–1202.

83. Ferguson, A. (1977). Intraepithelial lymphocytes of the small intestine. Gut *18*, 921–937.

84. Guy-Grand, D., Cerf-Bensussan, N., Malissen, B., Malassis-Seris, M., Briottet, C., and Vassalli, P. (1991). Two gut intraepithelial CD8+ lymphocyte populations with different T cell receptors: A role for the gut epithelium in T cell differentiation. J. Exp. Med. *173*, 471–481.

85. Manzano, M., Abadía-Molina, A.C., García-Olivares, E., Gil, A., and Rueda, R. (2002). Absolute counts and distribution of lymphocyte subsets in small intestine of BALB/c mice change during weaning. J. Nutr. *132*, 2757–2762.

86. Montalban-Arques, A., Chaparro, M., Gisbert, J.P., and Bernardo, D. (2018). The Innate Immune System in the Gastrointestinal Tract: Role of Intraepithelial Lymphocytes and Lamina Propria Innate Lymphoid Cells in Intestinal Inflammation. Inflamm. Bowel Dis. *24*, 1649–1659.

87. Jensen, K.D.C., Su, X., Shin, S., Li, L., Youssef, S., Yamasaki, S., Steinman, L., Saito, T., Locksley, R.M., Davis, M.M., *et al.* (2008). Thymic Selection Determines γδ T Cell Effector Fate: Antigen-Naive Cells Make Interleukin-17 and Antigen-Experienced Cells Make Interferon γ. Immunity *29*, 90–100.

88. Cheroutre, H., Lambolez, F., and Mucida, D. (2011). The light and dark sides of intestinal intraepithelial lymphocytes. Nat. Rev. Immunol. *11*, 445–456. Available at: http://dx.doi.org/10.1038/nri3007.

89. Sathaliyawala, T., Kubota, M., Yudanin, N., Turner, D., Camp, P., Thome, J.J.C., Bickham, K.L., Lerner, H., Goldstein, M., Sykes, M., *et al.* (2013). Distribution and Compartmentalization of Human Circulating and Tissue-Resident Memory T Cell Subsets. Immunity *38*, 187–197. Available at: http://dx.doi.org/10.1016/j.immuni.2012.09.020.

90. Ivanov, I.I., McKenzie, B.S., Zhou, L., Tadokoro, C.E., Lepelley, A., Lafaille, J.J., Cua, D.J., and

Littman, D.R. (2006). The Orphan Nuclear Receptor RORγt Directs the Differentiation Program of Proinflammatory IL-17+ T Helper Cells. Cell *126*, 1121–1133.

91. Veenbergen, S., and Samsom, J.N. (2012). Maintenance of small intestinal and colonic tolerance by IL-10-producing regulatory T cell subsets. Curr. Opin. Immunol. *24*, 269–276. Available at: http://dx.doi.org/10.1016/j.coi.2012.03.004.

92. Maynard, C.L., Harrington, L.E., Janowski, K.M., Oliver, J.R., Zindl, C.L., Rudensky, A.Y., and Weaver, C.T. (2007). Regulatory T cells expressing interleukin 10 develop from Foxp3+ and Foxp3- precursor cells in the absence of interleukin 10. Nat. Immunol. *8*, 931–941.

93. Le Bourhis, L., Guerri, L., Dusseaux, M., Martin, E., Soudais, C., and Lantz, O. (2011). Mucosal-associated invariant T cells: Unconventional development and function. Trends Immunol. *32*, 212–218. Available at: http://dx.doi.org/10.1016/j.it.2011.02.005.

94. Wittkopf, N., Neurath, M.F., and Becker, C. (2014). Immune-epithelial crosstalk at the intestinal surface. J. Gastroenterol. *49*, 375–387.

95. Knoop, K.A., McDonald, K.G., McCrate, S., McDole, J.R., and Newberry, R.D. (2015). Microbial sensing by goblet cells controls immune surveillance of luminal antigens in the colon. Mucosal Immunol. *8*, 198–210. Available at: http://dx.doi.org/10.1038/mi.2014.58.

96. Allaire, J.M., Crowley, S.M., Law, H.T., Chang, S.Y., Ko, H.J., and Vallance, B.A. (2018). The Intestinal Epithelium: Central Coordinator of Mucosal Immunity. Trends Immunol. *39*, 677–696. Available at: https://doi.org/10.1016/j.it.2018.04.002.

97. Nowarski, R., Jackson, R., and Flavell, R.A. (2017). The Stromal Intervention: Regulation of Immunity and Inflammation at the Epithelial-Mesenchymal Barrier. Cell *168*, 362–375.

98. Owens, B.M.J., and Simmons, A. (2013). Intestinal stromal cells in mucosal immunity and homeostasis. Mucosal Immunol. *6*, 224–234.

99. Cornes, J.S. (1965). Number, size, and distribution of Peyer's patches in the human small intestine: Part I The development of Peyer's patches. Gut *6*, 225–229.

100. Barker, N., Van Es, J.H., Kuipers, J., Kujala, P., Van Den Born, M., Cozijnsen, M., Haegebarth, A., Korving, J., Begthel, H., Peters, P.J., *et al.* (2007). Identification of stem cells in small intestine and colon by marker gene Lgr5. Nature *449*, 1003–1007.

101. Sato, T., Van Es, J.H., Snippert, H.J., Stange, D.E., Vries, R.G., Van Den Born, M., Barker, N., Shroyer, N.F., Van De Wetering, M., and Clevers, H. (2011). Paneth cells constitute the niche for Lgr5 stem cells in intestinal crypts. Nature *469*, 415–418. Available at: http://dx.doi.org/10.1038/nature09637.

102. Gerbe, F., Sidot, E., Smyth, D.J., Ohmoto, M., Matsumoto, I., Dardalhon, V., Cesses, P., Garnier, L., Pouzolles, M., Brulin, B., *et al.* (2016). Intestinal epithelial tuft cells initiate type 2 mucosal immunity to helminth parasites. Nature *529*, 226–230. Available at: http://dx.doi.org/10.1038/nature16527.

103. Gerbe, F., Van Es, J.H., Makrini, L., Brulin, B., Mellitzer, G., Robine, S., Romagnolo, B., Shroyer, N.F., Bourgaux, J.F., Pignodel, C., *et al.* (2011). Distinct ATOH1 and Neurog3

requirements define tuft cells as a new secretory cell type in the intestinal epithelium. J. Cell Biol. *192*, 767–780.

104. Dillon, A., and Lo, D.D. (2019). M cells: Intelligent engineering of mucosal immune surveillance. Front. Immunol. *10*, 1–13.

105. Altmann, G.G., and Enesco, M. (1967). Cell number as a measure of distribution and renewal of epithelial cells in the small intestine of growing and adult rats. Am. J. Anat. *121*, 319–336.

106. Altmann, G.G., and Leblond, C.P. (1970). Factors influencing villus size in the small intestine of adult rats as revealed by transposition of intestinal segments. Am. J. Anat. *127*, 15–36.

107. Clarke, R.M. (1970). Mucosal architecture and epithelial cell production rate in the small intestine of the albino rat. J. Anat. *107*, 519–529.

108. Dowling, R.H., and Booth, C.C. (1966). Functional compensation after small-bowel resection in man. Demonstration by direct measurement. Lancet *2*, 146–147.

109. Berlin, P., Reiner, J., Wobar, J., Bannert, K., Glass, Ä., Walter, M., Bastian, M., Willenberg, H.S., Vollmar, B., Klar, E., *et al.* (2019). Villus Growth, Increased Intestinal Epithelial Sodium Selectivity, and Hyperaldosteronism Are Mechanisms of Adaptation in a Murine Model of Short Bowel Syndrome. Dig. Dis. Sci. *64*, 1158–1170. Available at: https://doi.org/10.1007/s10620-018-5420-x.

110. Hummel, K.P., Richardson, F.L., and Fekete, E. (1966). Anatomy. In Biology of the Laboratory Mouse.

111. Kaiko, G.E., Ryu, S.H., Koues, O.I., Collins, P.L., Solnica-Krezel, L., Pearce, E.J., Pearce, E.L., Oltz, E.M., and Stappenbeck, T.S. (2016). The Colonic Crypt Protects Stem Cells from Microbiota-Derived Metabolites. Cell *165*, 1708–1720.

112. LaPointe, L.C., Dunne, R., Brown, G.S., Worthley, D.L., Molloy, P.L., Wattchow, D., and Young, G.P. (2008). Map of differential transcript expression in the normal human large intestine. Physiol. Genomics *33*, 50–64.

113. Nava, G.M., Friedrichsen, H.J., and Stappenbeck, T.S. (2011). Spatial organization of intestinal microbiota in the mouse ascending colon. ISME J. *5*, 627–638.

114. Neumann, P.A., Koch, S., Hilgarth, R.S., Perez-Chanona, E., Denning, P., Jobin, C., and Nusrat, A. (2014). Gut commensal bacteria and regional Wnt gene expression in the proximal versus distal colon. Am. J. Pathol. *184*, 592–599. Available at: http://dx.doi.org/10.1016/j.ajpath.2013.11.029.

115. Tan, C.W., Hirokawa, Y., Gardiner, B.S., Smith, D.W., and Burgess, A.W. (2013). Colon Cryptogenesis: Asymmetric Budding. PLoS One *8*, 1–18.

116. Finkel, Y., and Larsson, L. (1987). Morphometric and Functional Studies of Proximal and Distal Colon in Young and Adult Rats. J. Pediatr. Gastroenterol. Nutr. *6*, 454–459.

117. Matsuo, K., Ota, H., Akamatsu, T., Sugiyama, A., and Katsuyama, T. (1997). Histochemistry of the surface mucous gel layer of the human colon. Gut *40*, 782–789.

118. Hirsch, D., Pace, P., Binder, H.J., and Hayslett, J.P. (1985). Evidence that aldosterone influences transport in target tissues by dissimilar mechanisms. Am. J. Physiol. - Ren. Fluid Electrolyte Physiol. *17*.

119. BOLL, G., RUDOLPHI, A., SPIEβ, S., and REIMANN, J. (1995). Regional Specialization of Intraepithelial T Cells in the Murine Small and Large Intestine. Scand. J. Immunol. *41*, 103–113.

120. Ibraghimov, A.R., and Lynch, R.G. (1994). Heterogeneity and biased t cell receptor α/β repertoire of mucosal cd8+ cells from murine large intestine: Implications for functional state. J. Exp. Med. *180*, 433–444.

121. Brandtzaeg, P., and Johansen, F.E. (2005). Mucosal B cells: Phenotypic characteristics, transcriptional regulation, and homing properties. Immunol. Rev. *206*, 32–63.

122. Persson, E.K., Scott, C.L., Mowat, A.M., and Agace, W.W. (2013). Dendritic cell subsets in the intestinal lamina propria: Ontogeny and function. Eur. J. Immunol. *43*, 3098–3107.

123. Weber, B., Saurer, L., and Mueller, C. (2009). Intestinal macrophages: Differentiation and involvement in intestinal immunopathologies. Semin. Immunopathol. *31*, 171–184.

124. Koziolek, M., Grimm, M., Becker, D., Iordanov, V., Zou, H., Shimizu, J., Wanke, C., Garbacz, G., and Weitschies, W. (2015). Investigation of pH and Temperature Profiles in the GI Tract of Fasted Human Subjects Using the Intellicap® System. J. Pharm. Sci. *104*, 2855–2863.

125. Ovesen, L., Bendtsen, F., Tage-Jensen, U., Pedersen, N.T., Gram, B.R., and Rune, S.J. (1986). Intraluminal pH in the stomach, duodenum, and proximal jejunum in normal subjects and patients with exocrine pancreatic insufficiency. Gastroenterology *90*, 958–962.

126. Topping, D.L., and Clifton, P.M. (2001). Short-chain fatty acids and human colonic function: Roles of resistant starch and nonstarch polysaccharides. Physiol. Rev. *81*, 1031–1064.

127. Lalezari, D. (2012). Gastrointestinal pH profile in subjects with irritable bowel syndrome. Ann. Gastroenterol. *25*, 333–337.

128. Robinson, C.S., Luckey, H., and Mills, H. (1943). Factors affecting the hydrogen ion concentration of the contents of the small intestine. J. Biol. Chem *147*, 175–181.

129. Hollister, L.E. (1973). Handbook of Pharmacology, ed 5.

130. McNeil, N.I., Ling, K.L.E., and Wager, J. (1987). Mucosal surface pH of the large intestine of the rat and of normal and inflamed large intestine in man. Gut *28*, 707–713.

131. Rechkemmer, G., Wahl, M., Kuschinsky, W., and von Engelhardt, W. (1986). pH-microclimate at the luminal surface of the intestinal mucosa of guinea pig and rat. Pflügers Arch. Eur. J. Physiol. *407*, 33–40.

132. Flemström, G., and Kivilaakso, E. (1983). Demonstration of a pH gradient at the luminal surface of rat duodenum in vivo and its dependence on mucosal alkaline secretion. Gastroenterology *84*, 787–794.

133. Lucas, M.L., Cooper, B.T., Lei, F.H., Johnson, I.T., Holmes, G.K., Blair, J.A., and Cooke, W.T.

(1978). Acid microclimate in coeliac and Crohn's disease: A model for folate malabsorption. Gut *19*, 735–742.

134. Ermund, A., Schütte, A., Johansson, M.E.V., Gustafsson, J.K., and Hansson, G.C. (2013). Studies of mucus in mouse stomach, small intestine, and colon. I. Gastrointestinal mucus layers have different properties depending on location as well as over the Peyer's patches. Am. J. Physiol. - Gastrointest. Liver Physiol. *305*, 341–347.

135. McGuckin, M.A., Lindén, S.K., Sutton, P., and Florin, T.H. (2011). Mucin dynamics and enteric pathogens. Nat. Rev. Microbiol. *9*, 265–278. Available at: http://dx.doi.org/10.1038/nrmicro2538.

136. Johansson, M.E.V., Holmén Larsson, J.M., and Hansson, G.C. (2011). The two mucus layers of colon are organized by the MUC2 mucin, whereas the outer layer is a legislator of host-microbial interactions. Proc. Natl. Acad. Sci. U. S. A. *108*, 4659–4665.

137. Atuma, C., Strugala, V., Allen, A., and Holm, L. (2001). The adherent gastrointestinal mucus gel layer: Thickness and physical state in vivo. Am. J. Physiol. - Gastrointest. Liver Physiol. *280*, 922–929.

138. Elderman, M., Sovran, B., Hugenholtz, F., Graversen, K., Huijskes, M., Houtsma, E., Belzer, C., Boekschoten, M., De Vos, P., Dekker, J., *et al.* (2017). The effect of age on the intestinal mucus thickness, microbiota composition and immunity in relation to sex in mice. PLoS One *12*, 1–22.

139. Johansson, M.E.V., Ambort, D., Pelaseyed, T., Schütte, A., Gustafsson, J.K., Ermund, A., Subramani, D.B., Holmén-Larsson, J.M., Thomsson, K.A., Bergström, J.H., *et al.* (2011). Composition and functional role of the mucus layers in the intestine. Cell. Mol. Life Sci. *68*, 3635–3641.

140. Johansson, M.E.V., Phillipson, M., Petersson, J., Velcich, A., Holm, L., and Hansson, G.C. (2008). The inner of the two Muc2 mucin-dependent mucus layers in colon is devoid of bacteria. PNAS *105*, 15064–15069.

141. Li, H., Limenitakis, J.P., Fuhrer, T., Geuking, M.B., Lawson, M.A., Wyss, M., Brugiroux, S., Keller, I., Macpherson, J.A., Rupp, S., *et al.* (2015). The outer mucus layer hosts a distinct intestinal microbial niche. Nat. Commun. *6*.

142. Johansson, M.E.V., Thomsson, K.A., and Hansson, G.C. (2009). Proteomic analyses of the two mucus layers of the colon barrier reveal that their main component, the Muc2 mucin, is strongly bound to the fcgbp protein. J. Proteome Res. *8*, 3549–3557.

143. Sababi, M., Nilsson, E., and Holm, L. (1995). Mucus and alkali secretion in the rat duodenum: Effects of indomethacin, Nω-Nitro-l-arginine, and luminal acid. Gastroenterology *109*, 1526–1534.

144. Ladinsky, M.S., Araujo, L.P., Zhang, X., Veltri, J., Galan-Diez, M., Soualhi, S., Lee, C., Irie, K., Pinker, E.Y., Narushima, S., *et al.* (2019). Endocytosis of commensal antigens by intestinal epithelial cells regulates mucosal T cell homeostasis. Science (80-.). *363*.

145. Shan, M., Gentile, M., Yeiser, J.R., Walland, A.C., Bornstein, V.U., Chen, K., He, B., Cassis, L., Bigas, A., Comerma, L., *et al.* (2013). Mucus Enhances Gut Homeostasis and Immunoregulatory Signals. Science *342*, 447–453.

146. Kamphuis, J.B.J., Mercier-Bonin, M., Eutamène, H., and Theodorou, V. (2017). Mucus organisation is shaped by colonic content; A new view. Sci. Rep. *7*, 1–13.

147. Hansson, G.C., and Johansson, M.E. V (2010). The inner of the two Muc2 mucin-dependent mucus layers in colon is devoid of bacteria. Gut Microbes *1*, 51–54.

148. Copeman, M., Matuz, J., Leonard, A.J., Pearson, J.P., Dettmar, P.W., and Allen, A. (1994). The gastroduodenal mucus barrier and its role in protection against luminal pepsins: The effect of 16,16 dimethyl prostaglandin E2, carbopol-polyacrylate, sucralfate and bismuth subsalicylate. J. Gastroenterol. Hepatol. *9*, S55–S59.

149. Van der Sluis, M., De Koning, B.A.E., De Bruijn, A.C.J.M., Velcich, A., Meijerink, J.P.P., Van Goudoever, J.B., Büller, H.A., Dekker, J., Van Seuningen, I., Renes, I.B., *et al.* (2006). Muc2-Deficient Mice Spontaneously Develop Colitis, Indicating That MUC2 Is Critical for Colonic Protection. Gastroenterology *131*, 117–129.

150. Bergstrom, K.S.B., Kissoon-Singh, V., Gibson, D.L., Ma, C., Montero, M., Sham, H.P., Ryz, N., Huang, T., Velcich, A., Finlay, B.B., *et al.* (2010). Muc2 protects against lethal infectious colitis by disassociating pathogenic and commensal bacteria from the colonic mucosa. PLoS Pathog. *6*.

151. Furter, M., Sellin, M.E., Hansson, G.C., and Hardt, W.D. (2019). Mucus Architecture and Near-Surface Swimming Affect Distinct Salmonella Typhimurium Infection Patterns along the Murine Intestinal Tract. Cell Rep. *27*, 2665-2678.e3. Available at: https://doi.org/10.1016/j.celrep.2019.04.106.

152. Juge, N. (2012). Microbial adhesins to gastrointestinal mucus. Trends Microbiol. *20*, 30–39. Available at: http://dx.doi.org/10.1016/j.tim.2011.10.001.

153. Kirjavainen, P. V., Ouwehand, A.C., Isolauri, E., and Salminen, S.J. (1998). The ability of probiotic bacteria to bind to human intestinal mucus. FEMS Microbiol. Lett. *167*, 185–189.

154. van Tassell, M.L., and Miller, M.J. (2011). Lactobacillus adhesion to mucus. Nutrients *3*, 613–636.

155. Sicard, J.F., Bihan, G. Le, Vogeleer, P., Jacques, M., and Harel, J. (2017). Interactions of intestinal bacteria with components of the intestinal mucus. Front. Cell. Infect. Microbiol. *7*.

156. Johansson, M.E.V., Sjövall, H., and Hansson, G.C. (2013). The gastrointestinal mucus system in health and disease. Nat. Rev. Gastroenterol. Hepatol. *10*, 352–361.

157. Desai, M.S., Seekatz, A.M., Koropatkin, N.M., Kamada, N., Hickey, C.A., Wolter, M., Pudlo, N.A., Kitamoto, S., Terrapon, N., Muller, A., *et al.* (2016). A Dietary Fiber-Deprived Gut Microbiota Degrades the Colonic Mucus Barrier and Enhances Pathogen Susceptibility. Cell *167*, 1339-1353.e21.

158. Marcobal, A., Southwick, A.M., Earle, K.A., and Sonnenburg, J.L. (2013). A refined palate:

Bacterial consumption of host glycans in the gut. Glycobiology *23*, 1038–1046.

159. Sommer, F., Adam, N., Johansson, M.E.V., Xia, L., Hansson, G.C., and Bäckhed, F. (2014). Altered mucus glycosylation in core 1 O-glycan-deficient mice affects microbiota composition and intestinal architecture. PLoS One *9*.

160. Birchenough, G.M.H., Nystrom, E.E.L., Johansson, M.E.V., and Hansson, G.C. (2016). A sentinel goblet cell guards the colonic crypt by triggering Nlrp6-dependent Muc2 secretion. Science (80-.). *352*, 1535–1542.

161. Knoop, K.A., and Newberry, R.D. (2018). Goblet cells: multifaceted players in immunity at mucosal surfaces. Mucosal Immunol. *11*, 1551–1557. Available at: http://dx.doi.org/10.1038/s41385-018-0039-y.

162. Albenberg, L., Esipova, T. V., Judge, C.P., Bittinger, K., Chen, J., Laughlin, A., Grunberg, S., Baldassano, R.N., Lewis, J.D., Li, H., *et al.* (2014). Correlation between intraluminal oxygen gradient and radial partitioning of intestinal microbiota. Gastroenterology *147*, 1055-1063.e8. Available at: http://dx.doi.org/10.1053/j.gastro.2014.07.020.

163. Glover, L.E., Lee, J.S., and Colgan, S.P. (2016). Oxygen metabolism and barrier regulation in the intestinal mucosa. J. Clin. Invest. *126*, 3680–3688.

164. Bond, J.H., Prentiss, R.A., and Michael, D.L. (1979). The effects of feeding on blood flow to the stomach, small bowel, and colon of the conscious dog. J Lab Clin Med *93*, 594–599.

165. Mortensen, F.V., Nielsen, H., Mulvany, M.J., and Hessov, I. (1990). Short chain fatty acids dilate isolated human colonic resistance arteries. Gut *31*, 1391–1394.

166. Friedman, E.S., Bittinger, K., Esipova, T. V., Hou, L., Chau, L., Jiang, J., Mesaros, C., Lund, P.J., Liang, X., FitzGerald, G.A., *et al.* (2018). Microbes vs. chemistry in the origin of the anaerobic gut lumen. Proc. Natl. Acad. Sci. U. S. A. *115*, 4170–4175.

167. Zheng, L., Kelly, C.J., and Colgan, S.P. (2015). Physiologic hypoxia and oxygen homeostasis in the healthy intestine. A review in the theme: Cellular responses to hypoxia. Am. J. Physiol. - Cell Physiol. *309*, C350–C360.

168. Fanaro, S., Chierici, R., Guerrini, P., and Vigi, V. (2003). Intestinal microflora in early infancy. Acta Paediatr Suppl *91*, 48–55.

169. Favier, C.F., Vaughan, E.E., De Vos, W.M., and Akkermans, A.D.L. (2002). Molecular monitoring of succession of bacterial communities in human neonates. Appl. Environ. Microbiol. *68*, 219–226.

170. Sonnenburg, J.L., Xu, J., Leip, D.D., Chen, C.H., Westover, B.P., Weatherford, J., Buhler, J.D., and Gordon, J.I. (2005). Glycan foraging in vivo by an intestine-adapted bacterial symbiont. Science (80-.). *307*, 1955–1959.

171. Byndloss, M.X., Pernitzsch, S.R., and Bäumler, A.J. (2018). Healthy hosts rule within: ecological forces shaping the gut microbiota. Mucosal Immunol. *11*, 1299–1305. Available at: http://dx.doi.org/10.1038/s41385-018-0010-y.

172. Kelly, C.J., Zheng, L., Campbell, E.L., Saeedi, B., Scholz, C.C., Bayless, A.J., Wilson, K.E., Glover, L.E., Kominsky, D.J., Magnuson, A., *et al.* (2015). Crosstalk between microbiota-derived short-chain fatty acids and intestinal epithelial HIF augments tissue barrier function. Cell Host Microbe *17*, 662–671. Available at: http://dx.doi.org/10.1016/j.chom.2015.03.005.

173. Donohoe, D.R., Garge, N., Zhang, X., Sun, W., O'Connell, T.M., Bunger, M.K., and Bultman, S.J. (2011). The microbiome and butyrate regulate energy metabolism and autophagy in the mammalian colon. Cell Metab. *13*, 517–526. Available at: http://dx.doi.org/10.1016/j.cmet.2011.02.018.

174. Litvak, Y., Byndloss, M.X., and Bäumler, A.J. (2018). Colonocyte metabolism shapes the gut microbiota. Science (80-.). *362*.

175. Rivera-Chávez, F., Zhang, L.F., Faber, F., Lopez, C.A., Byndloss, M.X., Olsan, E.E., Xu, G., Velazquez, E.M., Lebrilla, C.B., Winter, S.E., *et al.* (2016). Depletion of Butyrate-Producing Clostridia from the Gut Microbiota Drives an Aerobic Luminal Expansion of Salmonella. Cell Host Microbe *19*, 443–454.

176. Saeedi, B.J., Kao, D.J., Kitzenberg, D.A., Dobrinskikh, E., Schwisow, K.D., Masterson, J.C., Kendrick, A.A., Kelly, C.J., Bayless, A.J., Kominsky, D.J., *et al.* (2015). HIF-dependent regulation of claudin-1 is central to intestinal epithelial tight junction integrity. Mol. Biol. Cell *26*, 2252–2262.

177. Shin, N.R., Whon, T.W., and Bae, J.W. (2015). Proteobacteria: Microbial signature of dysbiosis in gut microbiota. Trends Biotechnol. *33*, 496–503. Available at: http://dx.doi.org/10.1016/j.tibtech.2015.06.011.

178. Byndloss, M.X., Olsan, E.E., Rivera-Chávez, F., Tiffany, C.R., Cevallos, S.A., Lokken, K.L., Torres, T.P., Byndloss, A.J., Faber, F., Gao, Y., *et al.* (2017). Microbiota-activated PPAR-γ signaling inhibits dysbiotic Enterobacteriaceae expansion. Science (80-.). *357*, 570–575.

179. Ravel, J., Gajer, P., Abdo, Z., Schneider, G.M., Koenig, S.S.K., McCulle, S.L., Karlebach, S., Gorle, R., Russell, J., Tacket, C.O., *et al.* (2011). Vaginal microbiome of reproductive-age women. Proc. Natl. Acad. Sci. U. S. A. *108*, 4680–4687.

180. Qin, J., Li, R., Raes, J., Arumugam, M., Burgdorf, K.S., Manichanh, C., Nielsen, T., Pons, N., Levenez, F., Yamada, T., *et al.* (2010). A human gut microbial gene catalogue established by metagenomic sequencing. Nature *464*, 59–65.

181. Hornung, B., Martins dos Santos, V.A.P., Smidt, H., and Schaap, P.J. (2018). Studying microbial functionality within the gut ecosystem by systems biology. Genes Nutr. *13*, 1–19.

182. Stzepourginski, I., Nigro, G., Jacob, J.M., Dulauroy, S., Sansonetti, P.J., Eberl, G., and Peduto, L. (2017). CD34+ mesenchymal cells are a major component of the intestinal stem cells niche at homeostasis and after injury. Proc. Natl. Acad. Sci. U. S. A. *114*, E506–E513.

183. Martinez-Guryn, K., Hubert, N., Frazier, K., Urlass, S., Musch, M.W., Ojeda, P., Pierre, J.F., Miyoshi, J., Sontag, T.J., Cham, C.M., *et al.* (2018). Small Intestine Microbiota Regulate Host Digestive and Absorptive Adaptive Responses to Dietary Lipids. Cell Host Microbe *23*, 458-469.e5. Available at: https://doi.org/10.1016/j.chom.2018.03.011.

184. Flint, H.J., Scott, K.P., Duncan, S.H., Louis, P., and Forano, E. (2012). Microbial degradation of complex carbohydrates in the gut. Gut Microbes, 289–306.

185. Gilbert, M.S., Ijssennagger, N., Kies, A.K., and van Mil, S.W.C. (2018). Protein fermentation in the gut; implications for intestinal dysfunction in humans, pigs, and poultry. Am. J. Physiol. - Gastrointest. Liver Physiol. *315*, G159–G170.

186. Weckx, S., Roy, D., and Vuyst, L. De (2015). Mutual Cross-Feeding Interactions between Bifidobacterium longum subsp . longum NCC2705 and Eubacterium rectale ATCC 33656. Appl. Environ. Microbiol. *81y*, 7767–7781.

187. He, X., McLean, J.S., Edlund, A., Yooseph, S., Hall, A.P., Liu, S.Y., Dorrestein, P.C., Esquenazi, E., Hunter, R.C., Cheng, G., *et al.* (2015). Cultivation of a human-associated TM7 phylotype reveals a reduced genome and epibiotic parasitic lifestyle. Proc. Natl. Acad. Sci. U. S. A. *112*, 244–249.

188. Dwidar, M., Monnappa, A.K., and Mitchell, R.J. (2012). The dual probiotic and antibiotic nature of Bdellovibrio bacteriovorus. BMB Rep. *45*, 71–78.

189. Salzman, N.H., Hung, K., Haribhai, D., Chu, H., Karlsson-Sjöberg, J., Amir, E., Teggatz, P., Barman, M., Hayward, M., Eastwood, D., *et al.* (2010). Enteric defensins are essential regulators of intestinal microbial ecology. Nat. Immunol. *11*, 76–83. Available at: http://dx.doi.org/10.1038/ni.1825.

190. Islam, K.B.M.S., Fukiya, S., Hagio, M., Fujii, N., Ishizuka, S., Ooka, T., Ogura, Y., Hayashi, T., and Yokota, A. (2011). Bile acid is a host factor that regulates the composition of the cecal microbiota in rats. Gastroenterology *141*, 1773–1781. Available at: http://dx.doi.org/10.1053/j.gastro.2011.07.046.

191. Schluter, J., and Foster, K.R. (2012). The Evolution of Mutualism in Gut Microbiota Via Host Epithelial Selection. PLoS Biol. *10*.

192. Bures, J., Cyrany, J., Kohoutova, D., Förstl, M., Rejchrt, S., Kvetina, J., Vorisek, V., and Kopacova, M. (2010). Small intestinal bacterial overgrowth syndrome. World J. Gastroenterol. *16*, 2978–2990.

193. Pédron, T., Mulet, C., Dauga, C., Frangeul, L., Chervaux, C., Grompone, G., and Sansonettia, P.J. (2012). A crypt-specific core microbiota resides in the mouse colon. MBio *3*, 1–7.

194. Swidsinski, A., Sydora, B.C., Doerffel, Y., Loening-Baucke, V., Vaneechoutte, M., Lupicki, M., Scholze, J., Lochs, H., and Dieleman, L.A. (2007). Viscosity gradient within the mucus layer determines the mucosal barrier function and the spatial organization of the intestinal microbiota. Inflamm. Bowel Dis. *13*, 963–970.

195. Smith, H.F., Fisher, R.E., Everett, M.L., Thomas, A.D., Randal Bollinger, R., and Parker, W. (2009). Comparative anatomy and phylogenetic distribution of the mammalian cecal appendix. J. Evol. Biol. *22*, 1984–1999.

196. Vidyasagar, S., and Ramakrishna, B.S. (2002). Effects of butyrate on active sodium and chloride transport in rat and rabbit distal colon. J. Physiol. *539*, 163–173.

197. Sandle, G.I. (1998). Salt and water absorption in the human colon: A modern appraisal. Gut *43*, 294–299.

198. Legoux, F., Bellet, D., Daviaud, C., El Morr, Y., Darbois, A., Niort, K., Procopio, E., Salou, M., Gilet, J., Ryffel, B., *et al.* (2019). Microbial metabolites control the thymic development of mucosal-associated invariant T cells. Science (80-.). *366*, 494–499.

199. Gorbach, S.L., Plaut, A.G., Nahas, L., Weinstein, L., Spanknebel, G., and Levitan, R. (1967). Studies of intestinal microflora. II. Microorganisms of the small intestine and their relations to oral and fecal flora. Gastroenterology *53*, 856–867.

200. Kumamoto, C.A. (2016). The Fungal Mycobiota: Small Numbers, Large Impacts. Cell Host Microbe *19*, 750–751. Available at: http://dx.doi.org/10.1016/j.chom.2016.05.018.

201. Milo, R., Phillips, R., and Orme, N. (2016). Cell Biology by the numbers.

202. Hoffmann, C., Dollive, S., Grunberg, S., Chen, J., Li, H., Wu, G.D., Lewis, J.D., and Bushman, F.D. (2013). Archaea and Fungi of the Human Gut Microbiome: Correlations with Diet and Bacterial Residents. PLoS One *8*.

203. Kapitan, M., Niemiec, M.J., Steimle, A., Frick, J.S., and Jacobsen, I.D. (2019). Fungi as Part of the Microbiota and Interactions with Intestinal Bacteria. Curr Top Microbiol Immunol *422*, 265–301.

204. Auchtung, T.A., Fofanova, T.Y., Stewart, C.J., Nash, A.K., Wong, M.C., Gesell, J.R., Auchtung, J.M., Ajami, N.J., and Petrosino, J.F. (2018). Investigating Colonization of the Healthy Adult Gastrointestinal Tract by Fungi. mSphere *3*, 1–16.

205. Mukaremera, L., Lee, K.K., Mora-Montes, H.M., and Gow, N.A.R. (2017). Candida albicans yeast, pseudohyphal, and hyphal morphogenesis differentially affects immune recognition. Front. Immunol. *8*, 1–12.

206. Moyes, D.L., Runglall, M., Murciano, C., Shen, C., Nayar, D., Thavaraj, S., Kohli, A., Islam, A., Mora-Montes, H., Challacombe, S.J., *et al.* (2010). A biphasic innate immune MAPK response discriminates between the yeast and hyphal forms of candida albicans in epithelial cells. Cell Host Microbe *8*, 225–235. Available at: http://dx.doi.org/10.1016/j.chom.2010.08.002.

207. Templeton, S.P., Rivera, A., Hube, B., and Jacobsen, I.D. (2018). Editorial: Immunity to human fungal pathogens: Mechanisms of host recognition, protection, pathology, and fungal interference. Front. Immunol. *9*, 1–4.

208. Li, X., Leonardi, I., Semon, A., Doron, I., Gao, I.H., Putzel, G.G., Kim, Y., Kabata, H., Artis, D., Fiers, W.D., *et al.* (2018). Response to Fungal Dysbiosis by Gut-Resident CX3CR1 + Mononuclear Phagocytes Aggravates Allergic Airway Disease. Cell Host Microbe *24*, 847-856.e4.

209. Han, K.H., Park, S.J., Choi, S.J., Park, J.Y., and Lee, K.H. (2013). Immunological features of macrophages induced by various morphological structures of candida albicans. J. Microbiol. Biotechnol. *23*, 1031–1040.

210. Bondy, G.S., and Pestka, J.J. (2000). Immunomodulation by fungal toxins. J. Toxicol. Environ.

Heal. - Part B Crit. Rev. *3*, 109–143.

211. Moyes, D.L., Wilson, D., Richardson, J.P., Mogavero, S., Tang, S.X., Wernecke, J., Höfs, S., Gratacap, R.L., Robbins, J., Runglall, M., *et al.* (2016). Candidalysin is a fungal peptide toxin critical for mucosal infection. Nature *532*, 64–68. Available at: http://dx.doi.org/10.1038/nature17625.

212. Ho, J., Yang, X., Nikou, S.A., Kichik, N., Donkin, A., Ponde, N.O., Richardson, J.P., Gratacap, R.L., Archambault, L.S., Zwirner, C.P., *et al.* (2019). Candidalysin activates innate epithelial immune responses via epidermal growth factor receptor. Nat. Commun. *10*. Available at: http://dx.doi.org/10.1038/s41467-019-09915-2.

213. Ho, J., Wickramasinghe, D.N., Nikou, S.-A., Hube, B., Richardson, J.P., and Naglik, J.R. (2020). Candidalysin Is a Potent Trigger of Alarmin and Antimicrobial Peptide Release in Epithelial Cells. Cells *9*, 699.

214. Kasper, L., König, A., Koenig, P.A., Gresnigt, M.S., Westman, J., Drummond, R.A., Lionakis, M.S., Groß, O., Ruland, J., Naglik, J.R., *et al.* (2018). The fungal peptide toxin Candidalysin activates the NLRP3 inflammasome and causes cytolysis in mononuclear phagocytes. Nat. Commun. *9*. Available at: http://dx.doi.org/10.1038/s41467-018-06607-1.

215. Mura, E., Edwards, J., Kittelmann, S., Kaerger, K., Voigt, K., Mrázek, J., Moniello, G., and Fliegerova, K. (2019). Anaerobic fungal communities differ along the horse digestive tract. Fungal Biol. *123*, 240–246.

216. Iwasaki, T. (2004). Recent advances in the treatment of graft-versus-host disease. Clin. Med. Res. *2*, 243–252.

217. Tang, C., Kamiya, T., Liu, Y., Kadoki, M., Kakuta, S., Oshima, K., Hattori, M., Takeshita, K., Kanai, T., Saijo, S., *et al.* (2015). Inhibition of dectin-1 signaling ameliorates colitis by inducing lactobacillus-mediated regulatory T cell expansion in the intestine. Cell Host Microbe *18*, 183–197. Available at: http://dx.doi.org/10.1016/j.chom.2015.07.003.

218. Karimi, K., Inman, M.D., Bienenstock, J., and Forsythe, P. (2009). Lactobacillus reuteri-induced regulatory T cells protect against an allergic airway response in mice. Am. J. Respir. Crit. Care Med. *179*, 186–193.

219. Lyons, A., O'Mahony, D., O'Brien, F., MacSharry, J., Sheil, B., Ceddia, M., Russell, W.M., Forsythe, P., Bienenstock, J., Kiely, B., *et al.* (2010). Bacterial strain-specific induction of Foxp3+ T regulatory cells is protective in murine allergy models. Clin. Exp. Allergy *40*, 811–819.

220. Roger, L.C., Costabile, A., Holland, D.T., Hoyles, L., and McCartney, A.L. (2010). Examination of faecal Bifidobacterium populations in breast- and formula-fed infants during the first 18 months of life. Microbiology *156*, 3329–3341.

221. Tap, J., Mondot, S., Levenez, F., Pelletier, E., Caron, C., Furet, J.P., Ugarte, E., Muñoz-Tamayo, R., Paslier, D.L.E., Nalin, R., *et al.* (2009). Towards the human intestinal microbiota phylogenetic core. Environ. Microbiol. *11*, 2574–2584.

222. Turnbaugh, P.J., Ridaura, V.K., Faith, J.J., Rey, F.E., Knight, R., and Gordon, J.I. (2009). The effect of diet on the human gut microbiome: A metagenomic analysis in humanized gnotobiotic mice. Sci. Transl. Med. *1*.

223. Turnbaugh, P.J., Ley, R.E., Mahowald, M.A., Magrini, V., Mardis, E.R., and Gordon, J.I. (2006). An obesity-associated gut microbiome with increased capacity for energy harvest. Nature *444*, 1027–1031.

224. Ternes, D., Karta, J., Tsenkova, M., Wilmes, P., Haan, S., and Letellier, E. (2020). Microbiome in Colorectal Cancer: How to Get from Meta-omics to Mechanism? Trends Microbiol. *28*, 401–423. Available at: https://doi.org/10.1016/j.tim.2020.01.001.

225. Repass, J. (2018). Replication Study: Fusobacterium nucleatum infection is prevalent in human colorectal carcinoma. 1–12.

226. Bhatt, A.P., Redinbo, M.R., and Bultman, S.J. (2017). The role of the microbiome in cancer development and therapy. CA. Cancer J. Clin. *67*, 326–344.

227. Bullman, S., Pedamallu, C.S., Sicinska, E., Clancy, T.E., Zhang, X., Cai, D., Neuberg, D., Huang, K., Guevara, F., Nelson, T., *et al.* (2017). Analysis of Fusobacterium persistence and antibiotic response in colorectal cancer. Science (80-.). *358*, 1443–1448.

228. Aykut, B., Pushalkar, S., Chen, R., Li, Q., Abengozar, R., Kim, J.I., Shadaloey, S.A., Wu, D., Preiss, P., Verma, N., *et al.* (2019). The fungal mycobiome promotes pancreatic oncogenesis via activation of MBL. Nature *574*, 264–267. Available at: http://dx.doi.org/10.1038/s41586-019-1608-2.

229. Xavier, J.B., Young, V.B., Skufca, J., Ginty, F., Testerman, T., Pearson, A.T., Macklin, P., Mitchell, A., Shmulevich, I., Xie, L., *et al.* (2020). The Cancer Microbiome: Distinguishing Direct and Indirect Effects Requires a Systemic View. Trends in Cancer *6*, 192–204.

230. Bachem, A., Makhlouf, C., Binger, K.J., de Souza, D.P., Tull, D., Hochheiser, K., Whitney, P.G., Fernandez-Ruiz, D., Dähling, S., Kastenmüller, W., *et al.* (2019). Microbiota-Derived Short-Chain Fatty Acids Promote the Memory Potential of Antigen-Activated CD8+ T Cells. Immunity *51*, 285-297.e5.

231. Hume, D.A., Loutit, J.F., and Gordon, S. (1984). The mononuclear phagocyte system of the mouse defined by immunohistochemical localization of antigen F4/80: Macrophages of bone and associated connective tissue. J. Cell Sci. *VOL. 66*, 189–194.

232. Bain, C.C., and Mowat, A.M. (2011). Intestinal macrophages - specialised adaptation to a unique environment. Eur. J. Immunol. *41*, 2494–2498.

233. Zigmond, E., and Jung, S. (2013). Intestinal macrophages: Well educated exceptions from the rule. Trends Immunol. *34*, 162–168. Available at: http://dx.doi.org/10.1016/j.it.2013.02.001.

234. Gross-Vered, M., Trzebanski, S., Shemer, A., Bernshtein, B., Curato, C., Stelzer, G., Salame, T.M., David, E., Boura-Halfon, S., Chappell-Maor, L., *et al.* (2020). Defining murine monocyte differentiation into colonic and ileal macrophages. Elife *9*, 1–19.

235. Roberts, A.W., Lee, B.L., Deguine, J., John, S., Shlomchik, M.J., and Barton, G.M. (2017).

Tissue-Resident Macrophages Are Locally Programmed for Silent Clearance of Apoptotic Cells. Immunity *47*, 913-927.e6. Available at: https://doi.org/10.1016/j.immuni.2017.10.006.

236. Smythies, L.E., Sellers, M., Clements, R.H., Mosteller-Barnum, M., Meng, G., Benjamin, W.H., Orenstein, J.M., and Smith, P.D. (2015). Human intestinal macrophages display profound inflammatory anergy despite avid phagocytic and bacteriocidal activity. J. Clin. Invest *115*, 66–75.

237. Maheshwari, A., Kelly, D.R., Nicola, T., Ambalavanan, N., Jain, S.K., Murphyullrich, J., Athar, M., Shimamura, M., Bhandari, V., Aprahamian, C., *et al.* (2011). TGF-β2 suppresses macrophage cytokine production and mucosal inflammatory responses in the developing intestine. Gastroenterology *140*, 242–253. Available at: http://dx.doi.org/10.1053/j.gastro.2010.09.043.

238. Rich, B.S., and Dolgin, S.E. (2017). Necrotizing enterocolitis. Pediatr. Rev. *38*, 552–559.

239. Denning, N.L., and Prince, J.M. (2018). Neonatal intestinal dysbiosis in necrotizing enterocolitis. Mol. Med. *24*, 1–10.

240. Liu, Z., Gu, Y., Chakarov, S., Bleriot, C., Kwok, I., Chen, X., Shin, A., Huang, W., Dress, R.J., Dutertre, C.A., *et al.* (2019). Fate Mapping via Ms4a3-Expression History Traces Monocyte-Derived Cells. Cell *178*, 1509-1525.e19. Available at: http://dx.doi.org/10.1016/j.cell.2019.08.009.

241. Yona, S., Kim, K.-W., Wolf, Y., Mildner, A., Varol, D., Breker, M., Strauss-Ayali, Dalit , Viukov, S., Guilliams, Martin , Misharin, A., Hume, D.A., Perlman, H., *et al.* (2013). Fate mapping reveals origins and dynamics of monocytes and tissue macrophages under homeostasis. Immunity *38*, 79–91.

242. Bain, C.C., Scott, C.L., Uronen-Hansson, H., Gudjonsson, S., Jansson, O., Grip, O., Guilliams, M., Malissen, B., Agace, W.W., and Mowat, A.M.I. (2013). Resident and pro-inflammatory macrophages in the colon represent alternative context-dependent fates of the same Ly6C hi monocyte precursors. Mucosal Immunol. *6*, 498–510.

243. Caprara, G., Allavena, P., and Erreni, M. (2020). Intestinal macrophages at the crossroad between diet, inflammation, and cancer. Int. J. Mol. Sci. *21*, 1–31.

244. Serbina, N. V., and Pamer, E.G. (2006). Monocyte emigration from bone marrow during bacterial infection requires signals mediated by chemokine receptor CCR2. Nat. Immunol. *7*, 311–317.

245. Schridde, A., Bain, C.C., Mayer, J.U., Montgomery, J., Pollet, E., Denecke, B., Milling, S.W.F., Jenkins, S.J., Dalod, M., Henri, S., *et al.* (2017). Tissue-specific differentiation of colonic macrophages requires TGFβ receptor-mediated signaling. Mucosal Immunol. *10*, 1387–1399. Available at: http://dx.doi.org/10.1038/mi.2016.142.

246. Lavin, Y., Winter, D., Blecher-Gonen, R., David, E., Keren-Shaul, H., Merad, M., Jung, S., and Amit, I. (2014). Tissue-resident macrophage enhancer landscapes are shaped by the local microenvironment. Cell *159*, 1312–1326. Available at: http://dx.doi.org/10.1016/j.cell.2014.11.018.

247. Schridde, A., Bain, C.C., Mayer, J.U., Montgomery, J., Pollet, E., Denecke, B., Milling, S.W.F., Jenkins, S.J., Dalod, M., Henri, S., *et al.* (2017). Tissue-specific differentiation of colonic macrophages requires TGFβ receptor-mediated signaling. Mucosal Immunol. *10*, 1387–1399. Available at: http://dx.doi.org/10.1038/mi.2016.142.

248. Ishifune, C., Maruyama, S., Sasaki, Y., Yagita, H., Hozumi, K., Tomita, T., Kishihara, K., and Yasutomo, K. (2014). Differentiation of CD11c+CX3CR1+ cells in the small intestine requires Notch signaling. Proc. Natl. Acad. Sci. U. S. A. *111*, 5986–5991.

249. De Schepper, S., Verheijden, S., Aguilera-Lizarraga, J., Viola, M.F., Boesmans, W., Stakenborg, N., Voytyuk, I., Smidt, I., Boeckx, B., Dierckx de Casterlé, I., *et al.* (2018). Self-Maintaining Gut Macrophages Are Essential for Intestinal Homeostasis. Cell *175*, 400-415.e13.

250. Sehgal, A., Donaldson, D.S., Pridans, C., Sauter, K.A., Hume, D.A., and Mabbott, N.A. (2018). The role of CSF1R-dependent macrophages in control of the intestinal stem-cell niche. Nat. Commun. *9*, 1–17. Available at: http://dx.doi.org/10.1038/s41467-018-03638-6.

251. Marelli, G., Belgiovine, C., Mantovani, A., Erreni, M., and Allavena, P. (2017). Non-redundant role of the chemokine receptor CX3CR1 in the anti-inflammatory function of gut macrophages. Immunobiology *222*, 463–472. Available at: http://dx.doi.org/10.1016/j.imbio.2016.07.013.

252. Medina-Contreras, O., Geem, D., Laur, O., Williams, I.R., Lira, S.A., Nusrat, A., Parkos, C.A., and Denning, T.L. (2011). CX3CR1 regulates intestinal macrophage homeostasis, bacterial translocation, and colitogenic Th17 responses in mice. J. Clin. Invest. *121*, 4787–4795.

253. Kapoor, N., Liang, W., Marbán, E., Cho, H.C., Schridde, A., Bain, C.C., Mayer, J.U., Montgomery, J., Pollet, E., Denecke, B., *et al.* (1951). Tissue-specific differentiation of colonic macrophages requires TGFβ receptor-mediated signaling. Mucosal Immunol. *10*, 1387–1399. Available at: http://dx.doi.org/10.1038/mi.2016.142.

254. Chang, P. V., Hao, L., Offermanns, S., and Medzhitov, R. (2014). The microbial metabolite butyrate regulates intestinal macrophage function via histone deacetylase inhibition. Proc. Natl. Acad. Sci. U. S. A. *111*, 2247–2252.

255. Mortha, A., Chudnovskiy, A., Hashimoto, D., Bogunovic, M., Spencer, S.P., Belkaid, Y., and Merad, M. (2014). Microbiota-dependent crosstalk between macrophages and ILC3 promotes intestinal homeostasis. Science (80-.). *343*.

256. Shaw, T.N., Houston, S.A., Wemyss, K., Bridgeman, H.M., Barbera, T.A., Zangerle-Murray, T., Strangward, P., Ridley, A.J.L., Wang, P., Tamoutounour, S., *et al.* (2018). Tissue-resident macrophages in the intestine are long lived and defined by Tim-4 and CD4 expression. J. Exp. Med. *215*, 1507–1518.

257. Bujko, A., Atlasy, N., Landsverk, O.J.B., Richter, L., Yaqub, S., Horneland, R., Øyen, O., Aandahl, E.M., Aabakken, L., Stunnenberg, H.G., *et al.* (2018). Transcriptional and functional profiling defines human small intestinal macrophage subsets. J. Exp. Med. *215*, 441–458.

258. Bernshtein, B., Curato, C., Ioannou, M., Thaiss, C.A., Gross-Vered, M., Kolesnikov, M., Wang, Q., David, E., Chappell-Maor, L., Harmelin, A., *et al.* (2019). IL-23-producing IL-10Rα-deficient

gut macrophages elicit an IL-22-driven proinflammatory epithelial cell response. Sci. Immunol. *4*, 1–15.

259. Glocker, E.O., Kotlarz, D., Boztug, K., Gertz, E.M., Schäffer, A.A., Noyan, F., Perro, M., Diestelhorst, J., Allroth, A., Murugan, D., *et al.* (2009). Inflammatory bowel disease and mutations affecting the interleukin-10 receptor. N. Engl. J. Med. *361*, 2033–2045.

260. Huynh, D., Dai, X.M., Nandi, S., Lightowler, S., Trivett, M., Chan, C.K., Bertoncello, I., Ramsay, R.G., and Stanley, E.R. (2009). Colony Stimulating Factor-1 Dependence of Paneth Cell Development in the Mouse Small Intestine. Gastroenterology *137*, 136-144.e3. Available at: http://dx.doi.org/10.1053/j.gastro.2009.03.004.

261. Akcora, D., Huynh, D., Lightowler, S., Germann, M., Robine, S., de May, J.R., Pollard, J.W., Stanley, E.R., Malaterre, J., and Ramsay, R.G. (2013). The CSF-1 receptor fashions the intestinal stem cell niche. Stem Cell Res. *10*, 203–212. Available at: http://dx.doi.org/10.1016/j.scr.2012.12.001.

262. Smythies, L.E., Orenstein, J.M., and Phillip, D.S. (2005). Human intestinal macrophages display profound inflammatory anergy despite avid phagocytic and bacteriocidal activity. J. Clin. Invest. *115*, 66–75.

263. Conti, H.R., Shen, F., Nayyar, N., Stocum, E., Sun, J.N., Lindemann, M.J., Ho, A.W., Hai, J.H., Yu, J.J., Jung, J.W., *et al.* (2009). Th17 cells and IL-17 receptor signaling are essential for mucosal host defense against oral candidiasis. J. Exp. Med. *206*, 299–311.

264. Leonardi, I., Li, X., Semon, A., Li, D., Doron, I., Putzel, G., Bar, A., Prieto, D., Rescigno, M., Mcgovern, D.P.B., *et al.* (2018). CX3CR1+ mononuclear phagocytes control immunity to intestinal fungi. 1–6.

265. Smythies, L.E., Shen, R., Bimczok, D., Novak, L., Clements, R.H., Eckhoff, D.E., Bouchard, P., George, M.D., Hu, W.K., Dandekar, S., *et al.* (2010). Inflammation anergy in human intestinal macrophages is due to Smad-induced IκBα expression and NF-κB inactivation. J. Biol. Chem. *285*, 19593–19604.

266. Mahida, Y.R., Wu, K.C., and Jewell, D.P. (1989). Respiratory burst activity of intestinal macrophages in normal and inflammatory bowel disease. Gut *30*, 1362–1370.

267. Kankuri, E., Asmawi, M.Z., Korpela, R., Vapaatalo, H., and Moilanen, E. (1999). Induction of iNOS in a rat model of acute colitis. Inflammation *23*, 141–152.

268. J., R., G., H., A.K., H., A., B., P., B., H., S., Rugtveit, J., Haraldsen, G., Høgåsen, A.K., Bakka, A., *et al.* (1995). Respiratory burst of intestinal macrophages in inflammatory bowel disease is mainly caused by CD14+L1+ monocyte derived cells. Gut *37*, 367–373. Available at: http://www.pubmedcentral.nih.gov/articlerender.fcgi?artid=1382817&tool=pmcentrez&rendertype=abstract%5Cnhttp://www.embase.com/search/results?subaction=viewrecord&from=export&id=L25264280%5Cnhttp://sfx.library.uu.nl/utrecht?sid=EMBASE&issn=00175749&id=doi:

269. Roberts, P.J., Riley, G.P., Morgan, K., Miller, R., Hunter, J.O., and Middleton, S.J. (2001). The physiological expression of inducible nitric oxide synthase (iNOS) in the human colon. J. Clin.

Pathol. *54*, 293–297.

270. Winer, D.A., Luck, H., Tsai, S., and Winer, S. (2016). The intestinal immune system in obesity and insulin resistance. Cell Metab. *23*, 413–426. Available at: http://dx.doi.org/10.1016/j.cmet.2016.01.003.

271. Kawano, Y., Nakae, J., Watanabe, N., Kikuchi, T., Tateya, S., Tamori, Y., Kaneko, M., Abe, T., Onodera, M., and Itoh, H. (2016). Colonic Pro-inflammatory Macrophages Cause Insulin Resistance in an Intestinal Ccl2/Ccr2-Dependent Manner. Cell Metab. *24*, 295–310. Available at: http://dx.doi.org/10.1016/j.cmet.2016.07.009.

272. Rubio, C.A., Cord, L., and Schmidt, T.P. (2018). Partial to complete abrogation of the sub-epithelial macrophage barrier against the gut- microbiota in patients with ulcerative colitis and Crohn´s colitis. Int. J. Lab. Hematol. *72*, 580–587.

273. Baranska, A., Shawket, A., Jouve, M., Baratin, M., Malosse, C., Voluzan, O., Manh, T.P.V., Fiore, F., Bajénoff, M., Benaroch, P., *et al.* (2018). Unveiling skin macrophage dynamics explains both tattoo persistence and strenuous removal. J. Exp. Med. *215*, 1115–1133.

274. Foster, E.S., Budinger, M.E., Hayslett, J.P., and Binder, H.J. (1986). Ion transport in proximal colon of the rat. Sodium depletion stimulates neutral sodium chloride absorption. J. Clin. Invest. *77*, 228–235.

275. Dolman, D., and Edmonds, C.. (1975). The effect of aldosterone and the renin-angiotensis system on sodium, potassium and chloride transport by proximal and distal rat colon in vivo. J. Physiol., 597–611.

276. Hardin, J.A., Kimm, M.H., Wirasinghe, M., and Gall, D.G. (1999). Macromolecular transport across the rabbit proximal and distal colon. Gut *44*, 218–225.

277. Muzumdar, M.D., Tasic, B., Kazunari, M., Ling, L., and Luo, L. (2007). A Global Double-Fluorescent Cre Reporter Mouse. Genesis *45*, 593–605.

278. Caton, M.L., Smith-Raska, M.R., and Reizis, B. (2007). Notch-RBP-J signaling controls the homeostasis of CD8- dendritic cells in the spleen. J. Exp. Med. *204*, 1653–1664.

279. Rescigno, M., Urbano, M., Valzasina, B., Francolini, M., Rotta, G., Bonasio, R., Granucci, F., Kraehenbuhl, J.P., and Ricciardi-Castagnoli, P. (2001). Dendritic cells express tight junction proteins and penetrate gut epithelial monolayers to sample bacteria. Nat. Immunol. *2*, 361–367.

280. Vallon-Eberhard, A., Landsman, L., Yogev, N., Verrier, B., and Jung, S. (2006). Transepithelial Pathogen Uptake into the Small Intestinal Lamina Propria. J. Immunol. *176*, 2465–2469.

281. Mowat, A.M., and Bain, C.C. (2011). Mucosal macrophages in intestinal homeostasis and inflammation. J. Innate Immun. *3*, 550–564.

282. El Marjou, F., Janssen, K.P., Chang, B.H.J., Li, M., Hindie, V., Chan, L., Louvard, D., Chambon, P., Metzger, D., and Robine, S. (2004). Tissue-specific and inducible Cre-mediated recombination in the gut epithelium. Genesis *39*, 186–193.

283. Zheng, G.X.Y., Terry, J.M., Belgrader, P., Ryvkin, P., Bent, Z.W., Wilson, R., Ziraldo, S.B., Wheeler, T.D., McDermott, G.P., Zhu, J., *et al.* (2017). Massively parallel digital transcriptional profiling of single cells. Nat. Commun. *8*, 1–12.

284. Satija, R., Farrell, J.A., Gennert, D., Schier, A.F., and Regev, A. (2015). Spatial reconstruction of single-cell gene expression data. Nat. Biotechnol. *33*, 495–502.

285. Kohatsu, L., Hsu, D.K., Jegalian, A.G., Liu, F.-T., and Baum, L.G. (2006). Galectin-3 Induces Death of Candida Species Expressing Specific β-1,2-Linked Mannans . J. Immunol. *177*, 4718–4726.

286. Linden, J.R., De Paepe, M.E., Laforce-Nesbitt, S.S., and Bliss, J.M. (2013). Galectin-3 plays an important role in protection against disseminated candidiasis. Med. Mycol. *51*, 641–651.

287. Esteban, A., Popp, M.W., Vyas, V.K., Strijbis, K., Ploegh, H.L., and Fink, G.R. (2011). Fungal recognition is mediated by the association of dectin-1 and galectin-3 in macrophages. Proc. Natl. Acad. Sci. U. S. A. *108*, 14270–14275.

288. Genua, M., D'Alessio, S., Cibella, J., Gandelli, A., Sala, E., Correale, C., Spinelli, A., Arena, V., Malesci, A., Rutella, S., *et al.* (2015). The urokinase plasminogen activator receptor (uPAR) controls macrophage phagocytosis in intestinal inflammation. Gut *64*, 589–600.

289. Wiersinga, W.J., Kager, L.M., Hovius, J.W.R., van der Windt, G.J.W., de Vos, A.F., Meijers, J.C.M., Roelofs, J.J., Dondorp, A., Levi, M., Day, N.P., *et al.* (2010). Urokinase Receptor Is Necessary for Bacterial Defense against Pneumonia-Derived Septic Melioidosis by Facilitating Phagocytosis. J. Immunol. *184*, 3079–3086.

290. Sang-Uk Seo, Nobuhiko Kamada, Raúl Muñoz-Planillo, Yun-Gi Kim, Donghyun Kim, Yukiko Koizumi, Mizuho Hasegawa, Stephanie D. Himpsl, Hilary P. Browne, Trevor D. Lawley, Harry L. T. Mobley, Naohiro Inohara, and G.N. (2015). Distinct commensals induce interleukin-1β via NLRP3 inflammasome in inflammatory monocytes to promote intestinal inflammation in response to injury. Immunity *42*, 744–755.

291. Rogier, R., Ederveen, T.H.A., Boekhorst, J., Wopereis, H., Scher, J.U., Manasson, J., Frambach, S.J.C.M., Knol, J., Garssen, J., van der Kraan, P.M., *et al.* (2017). Aberrant intestinal microbiota due to IL-1 receptor antagonist deficiency promotes IL-17- and TLR4-dependent arthritis. Microbiome *5*, 63.

292. Suzuki, M., Tachibana, I., Takeda, Y., He, P., Minami, S., Iwasaki, T., Kida, H., Goya, S., Kijima, T., Yoshida, M., *et al.* (2009). Tetraspanin CD9 Negatively Regulates Lipopolysaccharide-Induced Macrophage Activation and Lung Inflammation. J. Immunol. *182*, 6485–6493.

293. Morrow, J.D. (1991). Fluconazole: A New Triazole Antifungal Agent.pdf. Am. J. Med. Sci. *302*, 129–132.

294. Anderson, T.M., Clay, M.C., Cioffi, A.G., Diaz, K.A., Hisao, G.S., Tuttle, M.D., Nieuwkoop, A.J., Comellas, G., Maryum, N., Wang, S., *et al.* (2014). Amphotericin forms an extramembranous and fungicidal sterol sponge. Nat. Chem. Biol. *10*, 400–406. Available at: http://dx.doi.org/10.1038/nchembio.1496.

295. Bolard, J., Joly, V., and Yeni, P. (1993). Mechanism of action of Amphotericin B at the cellular level. Its modulation by delivery systems. J. Liposome Res. *3*, 409–427.

296. Bukelskien, V. (2006). Study of health risks associated with Aspergillus amstelodami and its mycotoxic effects. Ekologija, 42–47.

297. Weber, K., Sohr, R., Schulz, B., Fleischhacker, M., and Ruhnke, M. (2008). Secretion of E,E-farnesol and biofilm formation in eight different Candida species. Antimicrob. Agents Chemother. *52*, 1859–1861.

298. Egbuta, M.A., Mwanza, M., and Babalola, O.O. (2017). Health risks associated with exposure to filamentous fungi. Int. J. Environ. Res. Public Health *14*, 14–17.

299. Masyuk, A.I., Marinelli, R.A., and LaRusso, N.F. (2002). Water transport by epithelia of the digestive tract. Gastroenterology *122*, 545–562.

300. Ikarashi, N., Baba, K., Ushiki, T., Kon, R., Mimura, A., Toda, T., Ishii, M., Ochiai, W., and Sugiyama, K. (2011). The laxative effect of bisacodyl is attributable to decreased aquaporin-3 expression in the colon induced by increased PGE 2 secretion from macrophages. Am. J. Physiol. - Gastrointest. Liver Physiol. *301*, 887–895.

301. Ismaiel, A.A., and Papenbrock, J. (2015). Mycotoxins: Producing fungi and mechanisms of phytotoxicity. Agriculture *5*, 493–537.

302. Lewis, R.E., Wiederhold, N.P., Lionakis, M.S., Prince, R.A., and Kontoyiannis, D.P. (2005). Frequency and species distribution of gliotoxin-producing Aspergillus isolates recovered from patients at a tertiary-care cancer center. J. Clin. Microbiol. *43*, 6120–6122.

303. Kupfahl, C., Ruppert, T., Dietz, A., Geginat, G., and Hof, H. (2007). Candida species fail to produce the immunosuppressive secondary metabolite gliotoxin in vitro. FEMS Yeast Res. *7*, 986–992.

304. Tshabalala, N., Mrudula, P., and Dutton, M.F. (2016). Examination of Candida albicans strains from South Africa for the production of gliotoxin and other cytotoxic secondary metabolites. J. Yeast Fungal Res. *7*, 19–27.

305. Kosalec, I., Puel, O., Delaforge, M., Kopjar, N., Antolovic, R., Jelic, D., Matica, B., Galtier, P., and Pepeljnjak, S. (2008). Isolation and cytotoxicity of low-molecular-weight metabolites of Candida albicans. Front. Biosci. *13*, 6893–6904.

306. Bertling, A., Niemann, S., Uekötter, A., Fegeler, W., Lass-Flörl, C., Von Eiff, C., and Kehrel, B.E. (2010). Candida albicans and its metabolite gliotoxin inhibit platelet function via interaction with thiols. Thromb. Haemost. *104*, 270–278.

307. Shah, D.T., Glover, D.D., and Larsen, B. (1995). In situ Mycotoxin Production by Candida albicans in Women with Vaginitis. Gynecol Obs. Invest *39*, 67–69.

308. Shah, D.T., and Larsen, B. (1991). Clinical isolates of yeast produce a gliotoxin-like substance. Mycopathologia *116*, 203–208.

309. Marasas, W.F.O., Yagen, B., Sydenham, E., Combrinck, S., and Thiel, P.G. (1987).

Comparative yields of T-2 toxin and related trichothecenes from five toxicologically important strains of Fusarium sporotrichioides. Appl. Environ. Microbiol. *53*, 693–696.

310. Schröder, B. (2016). The multifaceted roles of the invariant chain CD74 - More than just a chaperone. Biochim. Biophys. Acta - Mol. Cell Res., 1269–1281.

311. Chabaud, M., Heuze, M.L., Bretou, M., Vargas, P., Maiuri, P., Solanes, P., Maurin, M., Terriac, E., Le Berre, M., Lankar, D., *et al.* (2015). Cell migration and antigen capture are antagonistic processes coupled by myosin II in dendritic cells. Nat. Commun. *6*, 1–16.

312. Niess, J.H., Brand, S., Gu, X., Landsman, L., Jung, S., McCormick, B.A., Vyas, J.M., Boes, M., Ploegh, H.L., Fox, J.G., *et al.* (2005). CX3CR1-mediated dendritic cell access to the intestinal lumen and bacterial clearance. Science (80-.). *307*, 254–258.

313. Chieppa, M., Rescigno, M., Huang, A.Y.C., and Germain, R.N. (2006). Dynamic imaging of dendritic cell extension into the small bowel lumen in response to epithelial cell TLR engagement. J. Exp. Med. *203*, 2841–2852.

314. Izadpanah, A., Dwinell, M.B., Eckmann, L., Varki, N.M., and Kagnoff, M.F. (2001). Regulated MIP-3α/CCL20 production by human intestinal epithelium: Mechanism for modulating mucosal immunity. Am. J. Physiol. - Gastrointest. Liver Physiol. *280*, 710–719.

315. Gitter, A.H., Bendfeldt, K., Schulzke, J.D., and Fromm, M. (2000). Trans/paracellular, surface/crypt, and epithelial/subepithelial resistances of mammalian colonic epithelia. Eur J Physiol *439*, 477–482.

316. Poritz, L.S., Garver, K.I., Green, C., Fitzpatrick, L., Ruggiero, F., and Koltun, W.A. (2007). Loss of the Tight Junction Protein ZO-1 in Dextran Sulfate Sodium Induced Colitis. J. Surg. Res. *140*, 12–19.

317. Qualls, J.E., Kaplan, A.M., Rooijen, N. Van, and Cohen, D. a (2006). Suppression of experimental colitis by intestinal mononuclear phagocytes. J. Leukoc. Biol. *80*, 802–815.

318. Jones, G.R., Bain, C.C., Fenton, T.M., Kelly, A., Brown, S.L., Ivens, A.C., Travis, M.A., Cook, P.C., and MacDonald, A.S. (2018). Dynamics of colon monocyte and macrophage activation during colitis. Front. Immunol. *9*.

319. McLaughlin, J., Lambert, D., Padfield, P.J., Burt, J.P.H., and O'Neill, C.A. (2009). The mycotoxin patulin, modulates tight junctions in caco-2 cells. Toxicol. Vitr. *23*, 83–89. Available at: http://dx.doi.org/10.1016/j.tiv.2008.10.009.

320. Hall, R.A., and Noverr, M.C. (2017). Fungal interactions with the human host: exploring the spectrum of symbiosis. Curr. Opin. Microbiol. *40*, 58–64. Available at: http://dx.doi.org/10.1016/j.mib.2017.10.020.

321. Schindler, B., and Segal, E. (2008). Candida albicans metabolite affects the cytoskeleton and phagocytic activity of murine macrophages. Med. Mycol. *46*, 251–258.

322. Chinen, T., Qureshi, M.H., Koguchi, Y., and Kawakami, K. (1999). Candida albicans suppresses nitric oxide (NO) production by interferon- gamma (IFN-γ) and lipopolysaccharide (LPS)-stimulated murine peritoneal macrophages. Clin. Exp. Immunol. *115*, 491–497.

323. Schreiber, D., Marx, L., Felix, S., Clasohm, J., Weyland, M., Schäfer, M., Klotz, M., Lilischkis, R., Erkel, G., and Schäfer, K.H. (2017). Anti-inflammatory effects of fungal metabolites in mouse intestine as revealed by in vitro models. Front. Physiol. *8*, 1–15.

324. Liguori, G., Lamas, B., Richard, M.L., Brandi, G., da Costa, G., Hoffmann, T.W., Di Simone, M.P., Calabrese, C., Poggioli, G., Langella, P., *et al.* (2016). Fungal dysbiosis in mucosa-associated microbiota of Crohn's disease patients. J. Crohn's Colitis *10*, 296–305.

325. Vujicic, M., Saksida, T., Despotovic, S., Bajic, S.S., Lalić, I., Koprivica, I., Gajic, D., Golic, N., Tolinacki, M., and Stojanovic, I. (2018). The Role of Macrophage Migration Inhibitory Factor in the Function of Intestinal Barrier. Sci. Rep. *8*, 1–12.

326. Miguel, J.C., Adrienne, A.M., Hsieh, J.J., Harnisch, L.C., Alam, D. Al, Polk, D.B., Lien, C.-L., Watson, A.J.M., and Frey, M.R. (2016). Epidermal growth factor suppresses intestinal epithelial cell shedding via a MAPK dependent pathway. JCS.

327. Coker, O.O., Nakatsu, G., Dai, R.Z., Wu, W.K.K., Wong, S.H., Ng, S.C., Chan, F.K.L., Sung, J.J.Y., and Yu, J. (2019). Enteric fungal microbiota dysbiosis and ecological alterations in colorectal cancer. Gut *68*, 654–662.

328. Cebula, A., Seweryn, M., Rempala, G.A., Pabla, S.S., McIndoe, R.A., Denning, T.L., Bry, L., Kraj, P., Kisielow, P., and Ignatowicz, L. (2013). Thymus-derived regulatory T cells contribute to tolerance to commensal microbiota. Nature *497*, 258–262.

329. Lathrop, S.K., Bloom, S.M., Rao, S.M., Nutsch, K., Lio, C.W., Santacruz, N., Peterson, D.A., Stappenbeck, T.S., and Hsieh, C.S. (2011). Peripheral education of the immune system by colonic commensal microbiota. Nature *478*, 250–254. Available at: http://dx.doi.org/10.1038/nature10434.

330. Sloma, I., Zilber, M.-T., Vasselon, T., Setterblad, N., Cavallari, M., Mori, L., De Libero, G., Charron, D., Mooney, N., and Gelin, C. (2008). Regulation of CD1a Surface Expression and Antigen Presentation by Invariant Chain and Lipid Rafts. J. Immunol. *180*, 980–987.

331. De Libero, G., Collmann, A., and Mori, L. (2009). The cellular and biochemical rules of lipid antigen presentation. Eur. J. Immunol. *39*, 2648–2656.

332. Induces, R., and Disease, A. (2014). A Fungal Glycosphingolipid Directly Activates Natural Killer T Cells and Rapidly Induces Airways Disease. Nat. Med. *19*, 1297–1304.

333. Cohen, N.R., Tatituri, R.V.V., Rivera, A., Watts, G.F.M., Kim, E.Y., Chiba, A., Fuchs, B.B., Mylonakis, E., Besra, G.S., Levitz, S.M., *et al.* (2011). Innate recognition of cell wall β-Glucans drives invariant natural killer T cell responses against fungi. Cell Host Microbe *10*, 437–450. Available at: http://dx.doi.org/10.1016/j.chom.2011.09.011.

334. Metzger, D., and Chambon, P. (2001). Site- and time-specific gene targeting in the mouse. Methods *24*, 71–80.

335. Viville, S., Neefjes, J., Lotteau, V., Dierich, A., Lemeur, M., Ploegh, H., Benoist, C., and Mathis, D. (1993). Mice lacking the MHC class II-associated invariant chain. Cell *72*, 635–648.

336. Melo, R.C.N., Morgan, E., Monahan-Earley, R., Dvorak, A.M., and Weller, P.F. (2014). Pre-

embedding immunogold labeling to optimize protein localization at subcellular compartments and membrane microdomains of leukocytes. Nat. Protoc. *9*, 2382–2394. Available at: http://dx.doi.org/10.1038/nprot.2014.163.

337. Qiu, X., Zhang, F., Yang, X., Wu, N., Jiang, W., Li, X., Li, X., and Liu, Y. (2015). Changes in the composition of intestinal fungi and their role in mice with dextran sulfate sodium-induced colitis. Sci. Rep. *5*, 1–12.

338. Thiagarajah, J.R., Jayaraman, S., Naftalin, R.J., and Verkman, A.S. (2001). In vivo fluorescence measurement of Na+ concentration in the pericryptal space of mouse descending colon. Am. J. Physiol. - Cell Physiol. *281*.

339. Garty, H. (2000). Regulation of the epithelial Na+ channel by aldosterone: Open questions and emerging answers. Kidney Int. *57*, 1270–1276.

340. Goldschmidt, I., Grahammer, F., Warth, R., Schulz-Baldes, A., Garty, H., Greger, R., and Bleich, M. (2004). Kidney and Colon Electrolyte Transport in CHIF Knockout Mice. Cell. Physiol. Biochem. *14*, 113–120.

341. Greig, E.R., Baker, E.H., Mathialahan, T., Boot-Handford, R.P., and Sandle, G.I. (2002). Segmental variability of ENaC subunit expression in rat colon during dietary sodium depletion. Pflugers Arch. Eur. J. Physiol. *444*, 476–483.

342. Fakitsas, P., Adam, G., Daidié, D., Van Bemmelen, M.X., Fouladkou, F., Patrignani, A., Wagner, U., Warth, R., Camargo, S.M.R., Staub, O., *et al.* (2007). Early aldosterone-induced gene product regulates the epithelial sodium channel by deubiquitylation. J. Am. Soc. Nephrol. *18*, 1084–1092.

343. Turchin, A., Guo, C.Z., Adler, G.K., Ricchiuti, V., Kohane, I.S., and Williams, G.H. (2006). Effect of acute aldosterone administration on gene expression profile in the heart. Endocrinology *147*, 3183–3189.

344. Engelhorn, R., Seeger, E., Zwaving, J.H., and Eberlin, M. (2014). Laxatives. In Ullmann`s Encyclopedia of industrial Chemistry, pp. 1–9.

345. Schindelin, J., Arganda-Carreras, I., Frise, E., Kaynig, V., Longair, M., Pietzsch, T., Preibisch, S., Rueden, C., Saalfeld, S., Schmid, B., *et al.* (2012). Fiji: An open-source platform for biological-image analysis. Nat. Methods *9*, 676–682.

346. Gerner, M.Y., Kastenmuller, W., Ifrim, I., Kabat, J., and Germain, R.N. (2012). Histo-cytometry: A method for highly multiplex quantitative tissue imaging analysis applied to dendritic cell subset microanatomy in lymph nodes. Immunity *37*, 364–376.

347. Roederer, M. (2002). Compensation in Flow Cytometry. Curr. Protoc. Cytom. *22*, 1–20.